

# The Development of MESHNOTE Code for Radionuclide Migration in the Near Field

December, 1999

JAPAN NUCLEAR CYCLE  
DEVELOPMENT INSTITUTE

本資料の全部または一部を複写・複製・転写する場合は、下記にお問い合わせください。

〒319-1194 茨城県那珂郡東海村大字村松4-33  
核燃料サイクル開発機構 東海事業所  
運営管理部 技術情報室

Inquiries about copyright and reproduction should be addressed to :  
Technical Information Section,  
Administration Division,  
Tokai Works,  
Japan Nuclear Cycle Development Institute  
4-33 Muramatsu, Tokai-mura, Naka-gun, Ibaraki-ken, 319-1194  
Japan

© 核燃料サイクル開発機構 (Japan Nuclear Cycle Development Institute)  
1999

## ニアフィールド中核種移行解析コード MESHNOTE の開発

(研究報告)

若杉 圭一郎\* 牧野 仁史\* Peter Robinson\*\*

### 要旨

ニアフィールド中核種移行解析コード MESHNOTE は、人工バリア中での核種移行に係わるガラスの溶解、緩衝材中の核種の移行、周辺岩盤への核種の放出を解析するために、QuantiSci 社との共同で開発したコードである。MESHNOTE は一次元円筒座標系において有限差分法を用いることにより、物質の拡散移行問題を数値的に解く。

MESHNOTE は以下の特徴を有している。

- 複数崩壊連鎖、緩衝材への線形・非線形収着、溶解度による核種濃度の制限を考慮して、核種が緩衝材中を拡散により移行する過程を解析できる。
- 複数崩壊連鎖については、崩壊系列において同一の親核種からの複数の娘核種の生成（崩壊分岐）、ならびに複数の親核種からの同一の娘核種の生成（崩壊合流）を考慮することができる。
- 緩衝材中の拡散による移行の境界条件となる、ガラス固化体からの核種の溶出と緩衝材からの周辺岩盤への核種の放出を現象に即して取り扱うことができる。
- 溶解度、収着定数、拡散係数など核種移行特性を支配する主要パラメータの時間・空間依存性を考慮した解析が可能である。
- ユーザーの指定した許容誤差範囲に基づき、各時間ステップにおける解の精度を監視しながら時間ステップを自動的に増加させ、効率的に解析を実施することが可能である。

本報告書では、MESHNOTE の概念モデル、数学モデル、数値解法について示すとともに、解析解や他のコードとの比較により、MESHNOTE が有する種々の機能について検証する。

---

\* 東海事業所 環境保全・研究開発センター 処分研究部 システム解析グループ

\*\* QuantiSci

## The Development of MESHNOTE Code for Radionuclide Migration in the Near Field

Keiichiro Wakasugi\* Hitoshi Makino\* Peter Robinson\*\*

### Abstract

MESHNOTE code was developed to evaluate the engineered barrier system in collaboration with QuantiSci. This code is used to simulate glass dissolution, diffusive transport of nuclides in the buffer material and release to surrounding host rock. MESHNOTE is a one-dimensional finite difference code, which uses cylindrical co-ordinates for the solution of a radially symmetric diffusion problem.

MESHNOTE has the following characteristics:

- MESHNOTE can solve for diffusive transport of nuclides through an annulus shaped buffer region while accounting for multiple decay chains, linear and non-linear sorption onto the buffer materials and elemental solubility limits;
- MESHNOTE can solve for ingrowth of plural daughter nuclides from a singular parent nuclide (branching), and the ingrowth of a singular daughter nuclide from plural parent nuclides (rejoining);
- MESHNOTE can treat the leaching of nuclide from the vitrified waste and the release of nuclide from buffer to surrounding rock, which are boundary conditions for migration in the buffer, basing on the phenomena;
- MESHNOTE can treat principal parameters ( e.g. solubility and distribution coefficient) relevant to nuclide migration as time and space-dependence parameters;
- The time stepping scheme in MESHNOTE is controlled by tolerance defined by the user. The time stepping will increase automatically while checking the accuracy of the numerical solution.

The conceptual model, the mathematical model and the numerical implementation of the MESHNOTE code are described in this report and the characteristic functions of MESHNOTE are verified by comparing with analytical solutions or simulations produced with other calculation codes.

---

\* Repository System Analysis Group Waste Isolation Research Division  
Waste Management and Fuel Cycle Research Center Tokai Works

\*\* QuantiSci



# CONTENTS

|       |   |    |
|-------|---|----|
| 1     | Introduction                                      | 1  |
| 2     | Conceptual and Mathematical Model                 | 4  |
| 2.1   | Outline   | 4  |
| 2.2   | Conceptual model                                  | 4  |
| 2.3   | Mathematical model                                | 5  |
| 2.3.1 | Mass partitioning                                 | 7  |
| 2.3.2 | Governing equation (migration in the buffer)      | 9  |
| 2.3.3 | Glass dissolution                                 | 13 |
| 2.3.4 | Release to host rock                              | 15 |
| 2.3.5 | Time and space-dependence of principal parameter  | 17 |
| 3     | Numerical Implementation                          | 18 |
| 3.1   | Spatial discretization                            | 18 |
| 3.2   | Solution algorithm                                | 20 |
| 4     | Verification                                      | 22 |
| 4.1   | Fundamental functions                             | 24 |
| 4.1.1 | Single nuclide migration                          | 24 |
| 4.1.2 | Depletion of nuclide inventory                    | 28 |
| 4.1.3 | Non-linear sorption                               | 30 |
| 4.2   | Decay chain                                       | 32 |
| 4.2.1 | Single chain decay                                | 32 |
| 4.2.2 | Multiple chains decay                             | 34 |
| 4.2.3 | Branching and rejoining chains decay              | 40 |
| 4.3   | Glass dissolution model                           | 44 |
| 4.3.1 | First-order reaction model                        | 44 |
| 4.3.2 | Hydration reaction model                          | 47 |
| 4.4   | Time dependent parameter                          | 50 |
| 4.4.1 | Solubility  | 50 |
| 4.4.2 | Sorption constant                                 | 52 |
| 4.4.3 | Diffusion coefficient                             | 54 |
| 4.4.4 | Volume flow rate of water through the mixing cell | 56 |
| 4.5   | Space dependent parameter                         | 59 |
| 4.5.1 | Solubility  | 59 |
| 4.5.2 | Sorption constant                                 | 62 |
| 4.5.3 | Diffusion coefficient                             | 64 |
| 5     | Conclusions                                       | 67 |
| 6     | Acknowledgment                                    | 68 |

|                   |     |
|-------------------|-----|
| 7 Reference ..... | 69  |
| Appendix A .....  | A-1 |
| Appendix B .....  | B-1 |

## LIST OF FIGURES

- Figure 1-1 The basic concept of geological disposal in Japan
- Figure 2-1 Geometry of the engineered barrier system
- Figure 2-2 Nuclide migration processes in the engineered barrier system
- Figure 3-1 Spatial grid in the radial coordinate of the buffer material
- Figure 3-2 Solution algorithm
- Figure 4-1 Comparison of release rate from the EBS for single nuclide migration (Tc-99)
- Figure 4-2 Comparison of concentration profile in the buffer materials for single nuclide migration (Tc-99)
- Figure 4-3 Comparison of release rate from the EBS for the depletion process of nuclide inventory (Tc-99)
- Figure 4-4 Comparison of the relation between the concentration of dissolved nuclide and the concentration of sorbed nuclide for the non-linear sorption model (Tc-99)
- Figure 4-5 Comparison of release rate from the EBS in verification of single chain decay
- Figure 4-6 Comparison of release rate from the EBS in verification of multiple chains decay
- Figure 4-7 Branching and rejoining
- Figure 4-8 Comparison of nuclide amount in the EBS for the branching case
- Figure 4-9 Comparison of nuclides amount in the EBS for the rejoining case
- Figure 4-10 Comparison of dissolution rate of Silicon from the vitrified waste(verification of initial dissolution rate)
- Figure 4-11 Comparison of dissolution rate of Silicon from the vitrified waste (verification of hydration rate)
- Figure 4-12 Comparison of release rate from the EBS for time dependent solubility
- Figure 4-13 Comparison of release rate from the EBS for time dependent distribution coefficient
- Figure 4-14 Comparison of release rate from the EBS for time dependent diffusion coefficient
- Figure 4-15 Comparison of release rate from the EBS for time dependent volume flow rate of water through the mixing cell
- Figure 4-16 Effect of volume flow rate of water through the mixing cell on release rate of Tc-99 from the EBS
- Figure 4-17 Geometry of the EBS for verification case of space dependent parameter
- Figure 4-18 Comparison of release rate from the EBS for space dependent solubility
- Figure 4-19 Concentration profile in the buffer material for space dependent solubility (this profile is at  $1 \times 10^4$  years)
- Figure 4-20 Comparison of release rate from the EBS for space dependent distribution coefficient
- Figure 4-21 Comparison of release rate from the EBS for space dependent diffusion coefficient
- Figure 4-22 Concentration profile in the buffer material for space dependent diffusion coefficient (this profile is at  $1 \times 10^5$  years)

## LIST OF TABLES

|            |  |
|------------|--|
| Table 2-1  | Parameters for processes   |
| Table 2-2  | Parameters for features  |
| Table 2-3  | List of subscript  |
| Table 2-4  | Parameter with time and space-dependent  |
|            |  |
| Table 4-1  | Summary of verification analysis   |
| Table 4-2  | Relative error of release rate from the EBS for single nuclide (Tc-99) migration case                                |
| Table 4-3  | Relative error of release rate from the EBS for the effect of depletion of nuclide (Tc-99) inventory                 |
| Table 4-4  | Relative error of the concentration of sorbed nuclide (Tc-99)  |
| Table 4-5  | Nuclide migration data for verification of single decay chain  |
| Table 4-6  | Relative error of the maximum release rate in verification of single chain decay                                     |
| Table 4-7  | Half lives and inventories of nuclides in verification of multiple chains decay                                      |
| Table 4-8  | Solubilities and distribution coefficients in verification of multiple chains decay                                  |
| Table 4-9  | Relative error of the maximum release rate in verification of multiple chains decay                                  |
| Table 4-10 | Half lives and inventories (branching)   |
| Table 4-11 | Half lives and inventories (rejoining)   |
| Table 4-12 | Relative error of the amount of nuclide  |
| Table 4-13 | Initial dissolution rate data  |
| Table 4-14 | Relative error of the dissolution rate of Silicon (verification of initial dissolution rate)                         |
| Table 4-15 | Hydration reaction rate data   |
| Table 4-16 | Relative error of the dissolution rate of Silicon(verification of hydration reaction rate)                           |
| Table 4-17 | Time-dependence of solubility (Tc)   |
| Table 4-18 | Relative error of the release rate from the EBS for time dependent solubility  |
| Table 4-19 | Time-dependence of distribution coefficient (Tc)   |
| Table 4-20 | Relative error of the release rate from the EBS for time dependent distribution coefficient                          |
| Table 4-21 | Time-dependence of diffusion coefficient (Tc)  |
| Table 4-22 | Relative error of the release rate from the EBS for time dependent diffusion coefficient                             |
| Table 4-23 | Time-dependence of volume flow rate of water through the mixing cell   |
| Table 4-24 | Relative error of the release rate from the EBS for time dependent volume flow rate of water through the mixing cell |
| Table 4-25 | Space-dependence of solubility (Tc)  |
| Table 4-26 | Relative error of the release rate from the EBS for space dependent solubility                                       |
| Table 4-27 | Space-dependence of distribution coefficient (Tc)  |
| Table 4-28 | Relative error of the release rate from the EBS for space dependent distribution coefficient                         |
| Table 4-29 | Space-dependence of diffusion coefficient in porewater (Tc)  |

Table 4-30 Relative error of the release rate from the EBS for space dependent diffusion coefficient

## 1 Introduction

The Power Reactor and Nuclear Fuel Development Corporation (PNC) published the first progress report (H3) on the feasibility of geological disposal of high-level radioactive waste in Japan based on the results of their R & D program (PNC, 1992). According to H3, the multi-barrier system was the most appropriate system for geological disposal. The key aspect of the multi-barrier system considered was the engineered barrier system (EBS) component consisting of glass waste form, overpack and buffer material (Figure 1-1).



Figure 1-1 The basic concept of geological disposal in Japan

The various scenarios in which nuclides are transported from the repository to the biosphere are considered in performance assessment of the geological disposal. The AEC Guidelines (AEC, 1997) states that scenarios should be classified as follows:

- Scenarios in which the human environment may be affected due to the physical isolation of the waste being compromised (*isolation failure scenarios*);
- Scenarios in which radionuclides may be transported from vitrified waste to the biosphere through the buffer materials and host rock with flowing groundwater (*groundwater scenarios*).

MESHNOTE was developed as the code for nuclide migration in engineered barrier to simulate the groundwater scenarios in collaboration with QuantiSci (Robinson et al, 1992).

MESHNOTE is a one-dimensional finite difference code, which uses cylindrical co-ordinates for the solution of a radially symmetric diffusion problem. MESHNOTE is based on the

calculation code RELEASE (Ohi et al, 1992) for nuclide migration in the engineered barrier system used in H3.

MESHONTE code has the following characteristics:

- **Diffusion, sorption, precipitation and multiple decay chains,**  
MESHNOTE solves for diffusive migration of nuclides through an annulus shaped buffer region including transport processes such as multiple decay chains, linear and non-linear sorption onto the buffer materials and each elemental solubility limits;
- **Mass partitioning of total amount to aqueous, sorbed and precipitate concentration,**  
The governing equation representing diffusion is solved for total amount (mass) of the nuclide per unit volume, which is the sum of aqueous concentration, sorbed concentration and precipitate concentration. The derived total mass is distributed in the three distinct forms;
- **Decay of nuclides treated accounting to the analytical Bateman equation,**  
The decay term in the governing equation is solved through the analytical Bateman equation in advance. This numerical solution scheme allows reduction of the run time;
- **Branching and rejoining of decay chains,**  
MESHNOTE can solve the ingrowth of plural daughter nuclides from a singular parent nuclide (branching), and the ingrowth of a singular daughter nuclide from plural parent nuclides (rejoining);
- **Glass dissolution,**  
MESHNOTE can solve glass dissolution, which coupled a first-order reaction, hydration reaction and diffusion/dissipation of soluble Silicon in the buffer materials. This model can be applied mathematically to the simple constant glass dissolution model. The time dependence of glass surface area with glass dissolution can be also considered;
- **Release of nuclide from the buffer to the host rock**  
MESHNOTE can treat the release of nuclide from buffer to surrounding host rock, which are boundary conditions for migration in the buffer, by introducing the mixing cell with hypothetical mixing volume.
- **Time and space-dependence of principal parameters,**  
MESHNOTE can treat the change of nuclide migration parameters (e.g. solubility and distribution coefficient) with time and space.;
- **Automatic time stepping scheme to reduce the run time,**  
The time stepping scheme in MESHNOTE is controlled by a tolerance value defined by the user. The time stepping will increase automatically while maintaining the accuracy of the solution.

The conceptual model, the mathematical model, the numerical implementation of the

MESHNOTE code and the verification by comparison of analytical solution or simulations produced with other calculation codes are described in this report.



## 2 Conceptual and Mathematical Model

### 2.1 Outline

MESHNOTE code is developed to calculate leaching of nuclide from vitrified waste, migration in the buffer materials including retardation, solubility limit and radionuclide decay and release to the surrounding host rock. In this section, primary assumptions for nuclide migration in the engineered barrier system and the corresponding conceptual/mathematical models applied to MESHNOTE are described. The following assumptions are considered as premises for development of the conceptual model:

- The excavation disturbed zone (EDZ) exists outside the engineered barrier system. Nuclides which are released from the buffer materials are transported to the host rock through the EDZ;
- Nuclide migration in the engineered barrier system (EBS) for a single vitrified waste package is studied.

### 2.2 Conceptual model

The leaching of nuclides from the vitrified waste to the porewater and migration in the EBS is controlled by several physical and chemical characteristics of the EBS and the radioelements themselves. These characteristics set important limitations on the subsequent release of the nuclide from the EBS to the host rock. These characteristics include the following processes and factors:

- Leaching of nuclides from the vitrified waste to the porewater;
- Retardation properties of the EBS;
- Limitation of nuclides concentration by elemental solubilities;
- Migration of nuclides by diffusion in the buffer;
- Release of nuclides from the EBS to host rock;
- Decay and ingrowth of nuclides.

Based on the above processes and factors, the conceptual models have been developed taking into consideration a group of phenomena related to nuclide migration in the EBS. The following specific assumptions are made:

- After overpack failure, the porewater in the buffer materials will come into contact with the vitrified waste. This will cause release of nuclides, which is affected by dissolution of the glass matrix and hydration reaction. Diffusion/dissipation of soluble Silicon in the buffer materials will also contribute to the long-term glass dissolution. Nuclides will be

leached from vitrified waste as the glass dissolves. The rate of glass dissolution will define the release rate of nuclides (congruent dissolution), which are mixed homogeneously in the vitrified glass;

- Nuclide migration in the EBS will be retarded by sorption processes, which are assumed to be instantaneous and reversible. The linear sorption model and non-linear sorption model, which is applied a Langmuir adsorption isotherm to consider the limitation of sorption capacity, are assumed. The resistance for nuclide migration in cracks in the vitrified waste is ignored;
- The nuclide concentration in the vicinity of the vitrified waste and in the buffer materials will be limited by solubility which is partitioned among stable and radioactive isotopes. Precipitation and dissolution are assumed to be instantaneous and reversible reactions. Precipitated solid phases may redissolve later to maintain saturation. Dilution by isotopes derived from the groundwater or the buffer materials is ignored;
- Nuclide migration in the buffer materials will occur by diffusion;
- Nuclides reaching the boundary between the buffer and host rock mix instantaneously with the groundwater flow in the outer region of the buffer, and release to the host rock;
- Nuclide decay/ingrowth, which a number of decay chains and/or the branching and rejoining of decay chains are included, is considered in the analysis of nuclide migration in all regions of the EBS.

### 2.3 Mathematical model

The mathematical models are developed based on the above conceptual model. The following additional assumptions and simplifications have been added for mathematical modeling:

- A hypothetical water-filled volume, called the 'Reservoir' surrounding the vitrified waste, is assumed for modeling the glass dissolution. It is assumed that nuclides in the vitrified waste leach in this hypothetical volume homogeneously and are then migrate to the buffer materials;
- It is assumed that nuclides reaching the boundary between the buffer material and host rock are mixed instantaneously with the groundwater flowing through the EDZ. In other words, the EDZ is treated as a hypothetical mixing volume (called 'Mixing cell' in MESHNOTE). The nuclide concentration derived from this mixing is taken as the outer boundary condition;
- Migration of nuclides in the buffer material by diffusion is modeled using a cylindrical radial co-ordinate system. The nuclide concentrations in the buffer materials are assumed not to have any axial nor circumferential gradient, but to have a radial gradient only;

- A number of decay chains are considered simultaneously to treat solubility partitioning among isotopes belonging to different decay chain.

The geometry of the EBS assumed in the analysis is based on the design geometry, but a cylindrical radial co-ordinates system is used for simplification (see Figure 2-1).

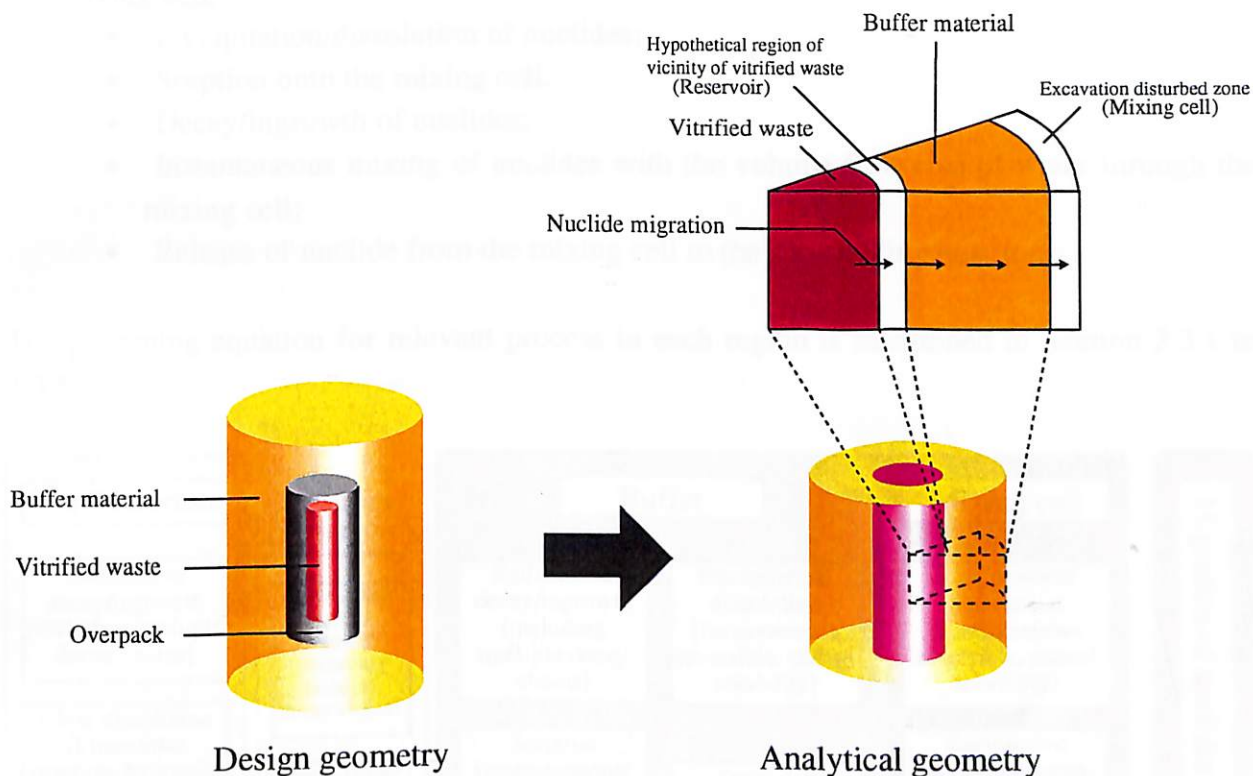


**Figure 2-1 Geometry of the engineered barrier system**

Based on the above conceptual model and additional assumptions for mathematical model, the processes of nuclide migration in the EBS related to the mathematical model in each region are summarized below (see Figure 2-2):

- Vitrified waste.
  - Glass dissolution;
  - Leaching of nuclides to reservoir with dissolution of vitrified waste;
  - Decay/ingrowth of nuclides;
- Reservoir.
  - Precipitation/dissolution of nuclides;
  - Decay/ingrowth of nuclides;
  - Release to the buffer material;
- Buffer.
  - Nuclide diffusion in the buffer material;

- Precipitation/dissolution of nuclides;
- Sorption onto the buffer;
- Decay/ingrowth of nuclides;
- Release of nuclides to the mixing cell;

● Mixing cell,

- Precipitation/dissolution of nuclides;
- Sorption onto the mixing cell;
- Decay/ingrowth of nuclides;
- Instantaneous mixing of nuclides with the volume flow rate of water through the mixing cell;
- Release of nuclide from the mixing cell to the surrounding host rock.

The governing equation for relevant process in each region is mentioned in Section 2.3.1 to 2.3.5.

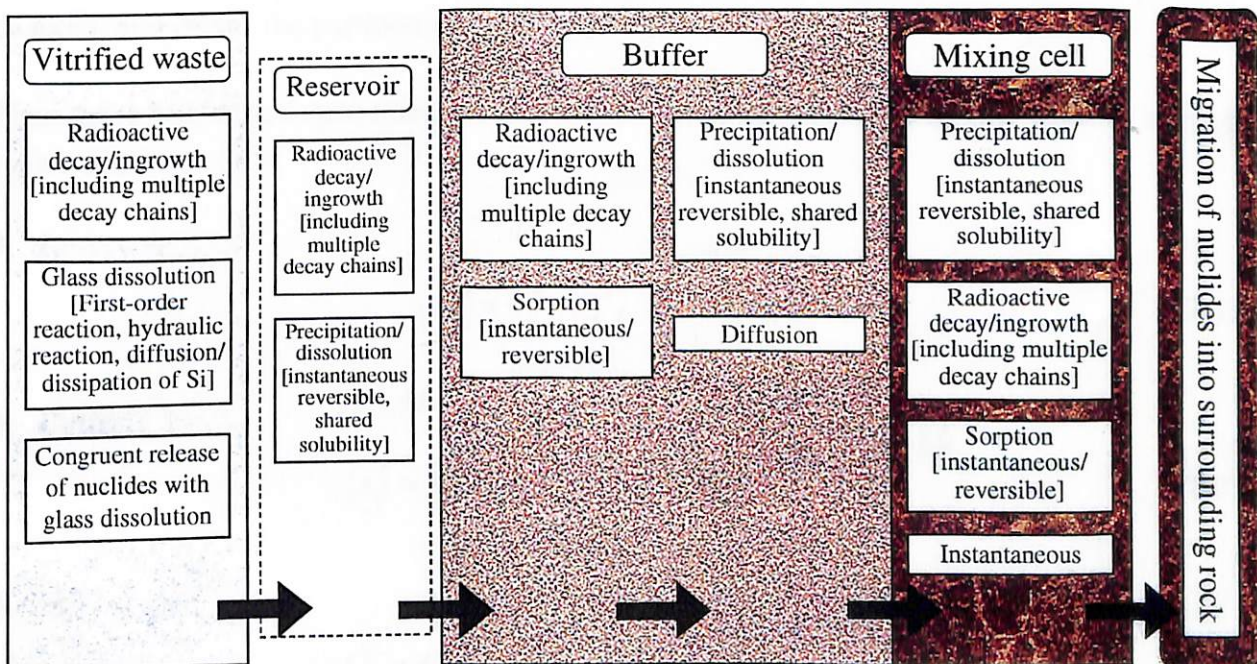


**Figure 2-2 Nuclide migration processes in the engineered barrier system**

### 2.3.1 Mass partitioning

MESHNOTE considers the partitioning of the total amount (mass) per unit volume of a nuclide into 3 types, concentration of dissolved nuclides, concentration of sorbed nuclides and concentration of precipitate. This partitioning is modeled throughout the buffer region and the mixing cell. For reservoir only dissolved nuclides and precipitate have been modeled explicitly.



For example, we consider mass partitioning of nuclide in the buffer. The total amount of nuclide in unit volume of the buffer which includes the buffer material and the porewater ( $A$  [mol m<sup>3</sup> of the buffer]) is distributed to the concentration of dissolved nuclides in unit volume of the porewater ( $C_{ij}$  [mol m<sup>3</sup> of the porewater]), concentration of sorbed nuclides in unit volume of the buffer material ( $S_{ij}$  [mol m<sup>3</sup> of the buffer material]) and concentration of precipitate in unit volume of the buffer ( $P_{ij}$  [mol m<sup>3</sup> of the buffer]). Then the governing equations are formulated considering relevant processes using above parameter and the parameters used in the equations are defined in Tables 2-1 to 2-3.

Where, the subscripts of *Glass*, *R*, *B* and *M* are used to distinguish the equations and parameters for four regions (vitrified waste, reservoir, buffer material and mixing cell) respectively. The subscripts of *ij* (isotope *j* element *i*) and *IJ* (isotope *J* element *I*) are used to distinguish the nuclide and its parent nuclide respectively.

In order to deal with the migration of nuclides which can form these three distinct forms, it is convenient to consider the total amount (mass) per unit volume of the nuclides as the primary quantity, and derive the partitioning when required.

Thus these partitioned quantities are related via the totals amount per unit volume in each region (in moles m<sup>3</sup>):

- Reservoir,

$$A_{ij}^R = C_{ij}^R + P_{ij}^R, \quad (2-1)$$

- Buffer,

$$A_{ij}^B = \epsilon^B C_{ij}^B + (1 - \epsilon^B) S_{ij}^B + P_{ij}^B, \quad (2-2)$$

- Mixing cell,

$$A_{ij}^M = \epsilon^M C_{ij}^M + (1 - \epsilon^M) S_{ij}^M + P_{ij}^M, \quad (2-3)$$

where to consider the limitation of sorption capacity, the concentration of sorbed nuclides,  $S_{ij}$ , is applied as a non-linear Langmuir adsorption isotherm for each element:

$$S_i(C_i) = \frac{\alpha_i C_i}{1 + \beta_i C_i}, \quad (2-4)$$

where  $\alpha_i$  and  $\beta_i$  are dimensionless quantities for element *i* and nuclide *j* is an isotope. For linear equilibrium sorption to be modeled,  $\beta_i$  can be set to zero and then  $\alpha_i$  is represented by the usual distribution coefficients ( $Kd_i$ ) and true density ( $\rho$ ) as follows:

$$S_i(C_i) = \rho K d_i C_i. \quad (2-5)$$

To evaluate the precipitate, the total elemental capacity of element  $i$  ( $\Gamma_i$ ), which is related to the elemental solubility ( $C_i^*$ ) and indicate maximum value of the total elemental amount without precipitate, is:

$$\Gamma_i = \varepsilon C_i^* + (1 - \varepsilon) S_i(C_i^*), \quad (2-6)$$

and if this capacity is exceeded by the total elemental amount, precipitate will be formed. That is if:

$$\sum_j A_{ij} \geq \Gamma_i, \quad (2-7)$$

then we must set:

$$C_{ij} = C_i^* \frac{A_{ij}}{\sum_j A_{ij}}, \quad (2-8)$$

$$S_{ij} = S_i(C_i^*) \frac{A_{ij}}{\sum_j A_{ij}}, \quad (2-9)$$

therefore the amount of precipitate is derived by using the equation (2-10):

$$P_{ij} = A_{ij} - \Gamma_i \frac{A_{ij}}{\sum_j (A_{ij})}. \quad (2-10)$$

### 2.3.2 Governing equation (migration in the buffer)

The governing nuclide transport equation in the buffer is expressed by equation (2-11) which represents nuclide diffusion, sorption, precipitation/dissolution and decay.  $A_{ij}^B(r, t)$  is the total amount per unit volume (in moles  $\text{m}^{-3}$ ) of isotope  $j$  of element  $i$ , at position  $r$  and time  $t$  in the buffer. It is noted that by solving multiple decay chains simultaneously, detailed evaluations can be carried out for phenomena such as precipitation in the buffer materials and the sharing of elemental solubility limits among isotopes.

$$\frac{\partial A_{ij}^B(r,t)}{\partial t} = \varepsilon^B Dp_i \frac{1}{r} \frac{\partial}{\partial r} \left( r \frac{\partial C_{ij}^B(r,t)}{\partial r} \right) - \lambda_{ij} A_{ij}^B(r,t) + \lambda_{ij} A_{ij}^B(r,t). \quad (2-11)$$

- $Dp_i$  : Diffusion coefficient in porewater [ $\text{m}^2 \text{y}^{-1}$ ]  
 $\varepsilon^B$  : Porosity of the buffer material [-]  
 $r$  : Distance from the center of vitrified waste [m]  
 $t$  : Time [y]  
 $\lambda_{ij}$  : Decay constant [ $\text{y}^{-1}$ ]

The boundary conditions which are applied to  $C_{ij}^B$  are as follows. At the inner boundary ( $r = r_{in}$ ), a reservoir volume exists into which the nuclides are supplied from the glass. Within this reservoir the aqueous concentration of radioelements are subject to their elemental solubility limits, that is:

If

$$\sum_j A_{ij}^R(t) < C_i^*, \quad (2-12)$$

then,

$$C_{ij}^B(r_{in}, t) = A_{ij}^R(t), \quad (2-13)$$

where  $C_i^*$  is the solubility limit of element  $i$ . If however

$$\sum_j A_{ij}^R(t) \geq C_i^*, \quad (2-14)$$

then we must set

$$C_{ij}^B(r_{in}, t) = C_i^* \frac{A_{ij}^R(t)}{\sum_j A_{ij}^R(t)}. \quad (2-15)$$

The release from the reservoir to the buffer is used as inner boundary condition to the equation (2-10). The quantity of  $A_{ij}^R(t)$  is the total amount per unit volume of isotope  $j$  of element  $i$ , in the reservoir (which has volume  $V^R$ ). This amount is governed by the following equation of mass balance:

$$V^R \frac{\partial A_{ij}^R}{\partial t} = 2\pi r_{in} L \varepsilon^B Dp_i \left. \frac{\partial C_{ij}^B}{\partial r} \right|_{r=r_{in}} + M_{ij}^{Glass} g_{Si} - V^R \lambda_{ij} A_{ij}^R + V^R \lambda_{ij} A_{ij}^R, \quad (2-16)$$

- $M_{ij}^{Glass}$  : Inventory of isotope  $j$  of element  $i$  in vitrified waste [mol]  
 $g_{Si}$  : Fractional rate of decrease of the glass volume [ $y^{-1}$ ] (see Section 2.3.3)  
 $L$  : Buffer length [m]  
 $r_{in}$  : Inner radius of the buffer material [m]

Thus the inner boundary condition is a function of time and naturally reduces the mass in the reservoir through radioactive decay and transport away through the buffer.

At the outer boundary of the buffer, a mixing cell model is applied. This cell represents EDZ and has its own physical and chemical properties. This boundary condition is stated as follows:

$$V^M \frac{\partial A_{ij}^M}{\partial t} = -2\pi r_{out} L \epsilon^B D p_i \left. \frac{\partial C_{ij}^B}{\partial r} \right|_{r=r_{out}} - V^M \lambda_{ij} A_{ij}^M + V^M \lambda_{II} A_{II}^M - Q C_{ij}^M, \quad (2-17)$$

- $V^M$  : Volume of mixing cell [ $m^3$ ]  
 $Q$  : volume flow rate of water through the cell [ $m^3 y^{-1}$ ] (see 2.3.4)  
 $r_{out}$  : Outer radius of the buffer material [m]

where  $C_{ij}^M(t) \equiv C_{ij}^B(r_{out}, t)$  is the concentration of isotope  $j$  of element  $i$  in the mixing cell.

These equation are solved for the following initial condition:

$$C_{ij}^B(r, 0) = 0. \quad (r_{in} \leq r \leq r_{out}) \quad (2-18)$$

In order to evaluate the concentration of dissolved nuclide, sorbed nuclide and precipitate nuclide from the total amount of nuclide, it is convenient at this point to introduce two new quantities  $\gamma_i(r, t)$  and  $\sigma_i(r, t)$  which are define as:

$$\gamma_i(r, t) = \frac{C_i^B(r, t)}{A_i^B(r, t)}, \quad (2-19)$$

$$\sigma_i(r, t) = \frac{S_i^B(r, t)}{A_i^B(r, t)}. \quad (2-20)$$

From the isotherm relation (see equation (2-4)), these are related together by:

$$\sigma_i(r, t) = \frac{\alpha_i \gamma_i(r, t)}{1 + \beta_i \gamma_i(r, t) A_i^B(r, t)}. \quad (2-21)$$



To derive  $\gamma_i$  and  $\sigma_i$ , we must deal with two cases,  $A_i^B > \Gamma_i^B$  and  $A_i^B \leq \Gamma_i^B$ .

(1)  $A_i^B > \Gamma_i^B$

Now if the precipitate occurs,  $A_i^B > \Gamma_i^B$ , we observe from equation (2-8) that:

$$\gamma_i(r, t) = \frac{C_i^*}{A_i^B(r, t)}, \quad (2-22)$$

for all nuclides which are isotopes of element  $i$ . Thus we derive  $\sigma_i$ , using equation (2-20).

(2)  $A_i^B \leq \Gamma_i^B$ .

On the other hand, if the total amount dose not exceed the capacity for the element ( $A_i^B \leq \Gamma_i^B$  which also means  $P_i^B = 0$ ), then we must subdivide into two more cases.

(a)  $A_i^B = 0$

If the total amount equals zero (due to decay and transport), we must set the variable  $\gamma_i$  to avoid numerical instability of the solution, then we set:

$$\gamma_i = \frac{1}{\epsilon^B + (1 - \epsilon^B)\alpha_i}, \quad (2-23)$$

for all nuclides which are isotopes of element  $i$ . This result follows from equations (2-19), (2-2) and (2-5) with  $P_i^B \equiv 0$ .

(b)  $A_i^B \neq 0$

If the total amount does not equal zero with the non-linear isotherm, we must solve two unknown quantities,  $\gamma_i$  and  $\sigma_i$ . At first we can obtain  $\gamma_i$  solving the following quadratic equation:

$$p\gamma_i^2 + q\gamma_i - 1 = 0, \quad (2-24)$$

which arises from the definitions of the mass partitioning (equation (2-2)) with equations (2-19) to (2-21). The coefficients are given by:

$$p = \beta_i A_i^B \epsilon^B, \quad (2-25)$$

$$q = \varepsilon^B + (1 - \varepsilon^B)\alpha_i - \beta_i A_i^B. \quad (2-26)$$

Hence if  $p=0$  (assuming the linear equilibrium sorption for  $S_i$  ( $\because \beta_i=0$ )), we have  $\gamma_i = q^{-1}$ , or else we take  $\gamma_i$  as the positive root of the quadratic ( $\gamma_i = (-q + (q^2 - 4pq)^{1/2})/(2p)^{-1}$ ). There is only a single positive root since  $\gamma_i$  is positive.

Therefore we can use equation (2-21) to derive  $\sigma_i$  for the buffer once the  $\gamma_i$  are known.

Finally once  $A_{ij}^B$  is computed, we may derive the partitioned amount per unit volume as following at any time of point in space:

$$C_{ij}^B = \gamma_i A_{ij}, \quad (2-27)$$

$$S_{ij}^B = \sigma_i A_{ij}, \quad (2-28)$$

$$P_{ij}^B = A_{ij} - \varepsilon^B C_{ij}^B - (1 - \varepsilon^B) S_{ij}^B \quad (2-29)$$

### 2.3.3 Glass dissolution

In MESHNOTE code, glass dissolution could be represented by first-order reaction law with diffusion/dissipation of soluble Silicon in the buffer materials and hydration reaction of cause by constant dissolution. The equations governing this process are coupled to the migration process of the dissolved Silicon in the buffer material. Furthermore, glass dissolution is connected to nuclides migration process by congruent release of nuclides from glass as shown equation (2-16).

We define  $g_{Si}$  to be the fractional rate of decrease of the glass volume. This is calculated as:

$$g_{Si}(t) = \left[ k^+ \left( 1 - \frac{C_{Si}^R(t)}{C_{Si}^*} \right) + k_r \right] \frac{a^{Glass}(t)}{\rho^{Glass} V^{Glass}(t)}. \quad (2-30)$$

- $a^{Glass}(t)$  : Surface area of vitrified waste at time  $t$  [ $m^2$ ]
- $\rho^{Glass}(t)$  : Density of vitrified waste at time  $t$  [ $kg\ m^{-3}$ ]
- $V^{Glass}(t)$  : Volume of vitrified waste at time  $t$  [ $m^3$ ]
- $C_{Si}^*$  : Solubility of Silicon [ $mol\ m^{-3}$ ]
- $k^+$  : Initial dissolution rate [ $kg\ m^{-2}\ y^{-1}$ ]
- $k_r$  : Hydration rate [ $kg\ m^{-2}\ y^{-1}$ ]

The glass volume at a time can be calculated by the following equation:

$$V^{Glass}(t) = V^{Glass}(0) \frac{A_{Si}^{Glass}(t)}{A_{Si}^{Glass}(0)}, \quad (2-31)$$

where  $A_{Si}^{Glass}$  is the total amount of Silicon in the glass and  $V^{glass}(t)$  is the volume of glass at time  $t$ . The surface area of the glass is given by:

$$a^{Glass}(t) = a^{Glass}(0) \left( \frac{V^{Glass}(t)}{V^{Glass}(0)} \right)^\beta, \quad (2-32)$$

where  $\beta$  can be set to  $2/3$  if a geometric interpretation is appropriate or to zero if the decrease of the glass surface area with time due to glass dissolution is conservatively neglected.

The time-dependence amounts of nuclides in the vitrified waste are given by equation (2-33):

$$\frac{d M_{ij}^{Glass}(t)}{d t} = -M_{ij}^{Glass}(t) g_{Si} - \lambda_{ij} M_{ij}^{Glass}(t) + \lambda_{II} M_{II}^{Glass}(t), \quad (2-33)$$

where  $M_{ij}^{Glass}$  represents the total amount of each nuclide in the vitrified waste.

The release and migration behavior of the Silicon itself is modeled using precisely the same equations as for the nuclides (see equation (2-16)). Two additional features are included for the Silicon:

- An initial concentration in the buffer;
- Non-zero concentration in the water entering the mixing cell.

The first of these sets an initial condition for the Silicon migration in the EBS. The latter adds an additional term ( $QC_{Si}^{GW}$ ) to the mixing cell equation (2-17) when it is applied to Silicon and it is given by:

$$V^M \frac{\partial A_{Si}^M}{\partial t} = -2\pi r_{out} L \epsilon^B D p_i \left. \frac{\partial C_{Si}^B}{\partial r} \right|_{r=r_{out}} - V^M A_{Si}^M + V^M A_{Si}^M - QC_{Si}^M + QC_{Si}^{GW}, \quad (2-34)$$

where  $C_{Si}^{GW}$  is concentration of Silicon in the groundwater entering the mixing cell from surrounding host rock.

### 2.3.4 Release to Host rock

Nuclide migration in the EBS is evaluated by solving the governing equation (2-11) with the nuclide concentrations at the buffer/rock boundary described by equation (2-17). We assume instantaneous mixing with nuclide released from the buffer materials into the mixing cell and the volume flow rate of water through the mixing cell.

Finally the release rate of nuclides from the mixing cell into to the surrounding host rock is derived as output of MESHNOTE. This release rate can be simply defined as:

$$f_{ij}^{Buffer \rightarrow Hostrock} = QC_{ij}^M. \quad (2-35)$$

**Table 2-1 Parameters for processes**

| Processes                                   | Parameters                             | Units                             | Descriptions  |
|---|--|-----------------------------------|---|
| Time  | $t$                                    | y                                 | Time after overpack failure                             |
| Radioactive decay                           | $\lambda_{ij}$                         | y <sup>-1</sup>                   | Decay constant of isotope $j$ of element $i$            |
| Glass dissolution                           | $k^+$                                  | g m <sup>-2</sup> y <sup>-1</sup> | Initial dissolution rate                                |
|   | $k_r$                                  | g m <sup>-2</sup> y <sup>-1</sup> | Hydration rate  |
|   | $g_{Si}$                               | y <sup>-1</sup>                   | Fractional rate of decrease of the glass volume         |
| Precipitation/dissolution of element        | $C_i^*$                                | mol m <sup>-3</sup>               | Solubility of element $i$                               |
|   | $C_{Si}^*$                             | mol m <sup>-3</sup>               | Solubility of Silicon                                   |
| Diffusion in buffer                         | $Dp_i$                                 | m <sup>2</sup> y <sup>-1</sup>    | Diffusion in porewater of element $i$                   |
| Sorption to buffer                          | $\alpha_i$                             | -                                 | Langmuir isotherm parameter of element $i$              |
|   | $\beta_i$                              | -                                 | Langmuir isotherm parameter of element $i$              |
|   | $Kd_i$                                 | m <sup>3</sup> kg <sup>-1</sup>   | Distribution coefficient of element $i$                 |
| Groundwater flow rate at the outer boundary | $Q$                                    | m <sup>3</sup> y <sup>-1</sup>    | Volume flow rate of water through the mixing cell (EDZ) |
| Migration to host rock                      | $f_{ij}^{Buffer \rightarrow Hostrock}$ | mol y <sup>-1</sup>               | Release rate to host rock                               |

Table 2-2 Parameters for features

| Region               | Parameters          |                     |   |
|----------------------|---------------------|---------------------|---|
| Vitrified waste form | $M_{ij}^{Glass}$    | mol                 | Inventory of isotope $j$ of element $i$ in the glass  |
|                      | $a^{Glass}$         | m <sup>2</sup>      | Surface area of the glass   |
|                      | $V^{Glass}(t)$      | m <sup>3</sup>      | Volume of the glass at time $t$   |
|                      | $\rho^{Glass}$      | g m <sup>-3</sup>   | Density of the glass  |
|                      | $A_{Si}^{Glass}(t)$ | mol                 | Total amount of Silicon at time $t$   |
| Reservoir            | $A_{ij}^R$          | mol m <sup>-3</sup> | Total amount of isotope $j$ of element $i$ per unit volume in the reservoir                           |
|                      | $C_{ij}^R$          | mol m <sup>-3</sup> | Concentration of dissolved isotope $j$ of element $i$ in the reservoir                                |
|                      | $P_{ij}^R$          | mol m <sup>-3</sup> | Concentration of precipitated isotope $j$ of element $i$ in the reservoir                             |
|                      | $V^R$               | m <sup>3</sup>      | Volume of reservoir for the glass dissolution model   |
|                      | $C_{Si}^R$          | mol m <sup>-3</sup> | Concentration of dissolved Silicon in the reservoir   |
| Buffer               | $r_{in}$            | m                   | Inner radius of the buffer  |
|                      | $r_{out}$           | m                   | Outer radius of the buffer  |
|                      | $L$                 | m                   | Length of buffer  |
|                      | $\varepsilon^B$     | -                   | Porosity of the buffer  |
|                      | $A_{ij}^B$          | mol m <sup>-3</sup> | Total amount of isotope $j$ of element $i$ per unit volume of the buffer                              |
|                      | $C_{ij}^B$          | mol m <sup>-3</sup> | Concentration of dissolved isotope $j$ of element $i$ per unit volume of porewater                    |
|                      | $S_{ij}^B$          | mol m <sup>-3</sup> | Concentration of sorbed isotope $j$ of element $i$ per unit volume of the buffer material             |
|                      | $P_{ij}^B$          | mol m <sup>-3</sup> | Concentration of precipitated isotope $j$ of element $i$ per unit volume of the buffer                |
| Mixing cell          | $\rho^B$            | kg m <sup>-3</sup>  | True density at the buffer  |
|                      | $V^M$               | m <sup>3</sup>      | Volume of mixing cell   |
|                      | $\varepsilon^M$     | -                   | Porosity of mixing cell   |
|                      | $A_{ij}^M$          | mol m <sup>-3</sup> | Total amount of isotope $j$ of element $i$ per unit volume of the mixing cell                         |
|                      | $C_{ij}^M$          | mol m <sup>-3</sup> | Concentration of isotope $j$ of element $i$ per unit volume of water in the mixing cell               |
|                      | $S_{ij}^M$          | mol m <sup>-3</sup> | Concentration of sorbed isotope $j$ of element $i$ per unit volume of sorbed media in the mixing cell |
|                      | $P_{ij}^M$          | mol m <sup>-3</sup> | Concentration of precipitated isotope $j$ of element $i$ per unit volume of the mixing cell           |

Table 2-3 List of subscript

| Subscript | Description                                 |
|-----------|---|
| $ij$      | Nuclide : isotope $j$ of element $i$        |
| $IJ$      | Parent nuclide : isotope $J$ of element $I$ |
| $Glass$   | Vitrified waste (waste glass)               |
| $R$       | Reservoir                                   |

### 2.3.5 Time and space-dependence of principal parameter

MESHNOTE code can treat the evolution of principal nuclide migration parameter (solubility distribution coefficient and diffusion coefficient etc.) with time. Furthermore the buffer region can be subdivided into 2 layer (inner layer and outer layer) which have different migration characteristic and, the position of the boundary of the two layer can be change with time. These functions are summarized in the Table 2-4.

The treatment for time and space-dependent parameter dose not depend on the governing equation or solution algorithm, but can be dealt with the control of parameter change used in the program.

**Table 2-4 Capability of parameter evolution with time and space-dependent in NESHNOTE**

|   | Reservoir | Buffer material* |             | Mixing cell |
|---|-----------|------------------|-------------|-------------|
|   |           | Inner layer      | Outer layer |             |
| Solubility  | ○         | ○                | ○           | ○           |
| Distribution coefficient                          | —         | ○                | ○           | ○           |
| Diffusion coefficient                             | —         | ○                | ○           |             |
| Volume flow rate of water through the mixing cell | —         | —                | —           | ○           |

○ : Parameter which can be change with time.

\* : The difference data in inner layer and outer layer of the buffer can be defined. The position of the boundary of inner and outer layer can be also change with time.

### 3 Numerical Implementation

In the following description of the numerical schemes used in MESHNOTE, it is clear to represent the quantities of interest at given time of point in space if we drop the nuclide and element subscripts, and the region superscript on the quantities of interest.

#### 3.1 Spatial discretisation

We consider the discretisation of the governing equation in Section 2.3.2 based on the finite difference method. Figure 3-1 shows the spatial grid in the radial coordinate considered in the MESHNOTE code. If we use the number of cell as  $N$ , the buffer region is divided equally into  $N-2$  cells.

The width of a cell ( $\delta r$ ) and the length from center of vitrified waste to center of each cell ( $r_k$ ) are given by:

$$\delta r = \frac{r_{out} - r_{in}}{N - 1}, \quad (3-1)$$

$$r_k = r_{in} + (k - 1)\delta r, \quad k=2, \dots, N-1 \quad (3-2)$$

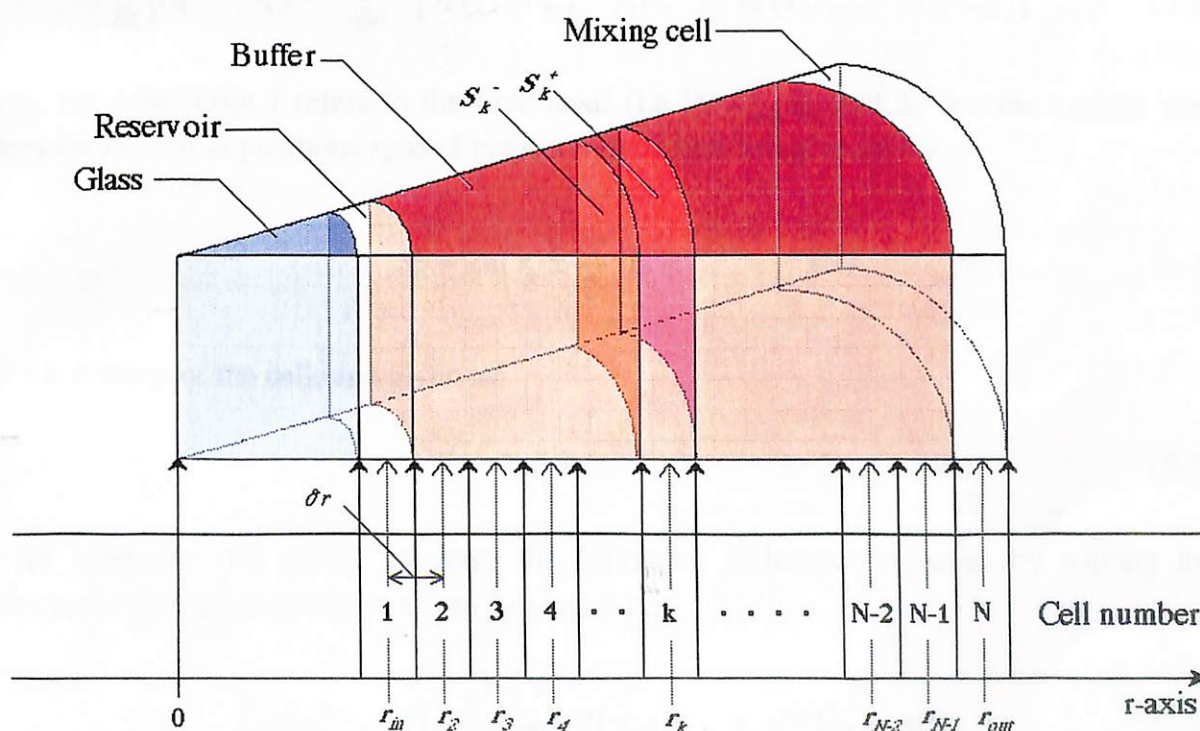


Figure 3-1 Spatial grid in the radial coordinate of the buffer material

In addition a cell for the total amount of each nuclide in the glass is included, and can be conceptually thought of as cell number zero in the above scheme.

In considering the discretisation of the governing equation, we need to numerically separate the processes of nuclide transport and decay in order to achieve sufficiently fast run times for long-term analysis more than 100 million years. This separation allows the decay part of the governing equation (2-11) to be handled analytically. So in each time stepping, the decay amount is calculated analytically in each cell, then the total amount of nuclide including the effect of decay is given to the differential equation relating to nuclide migration without decay (see equation (3-3)). The redistribution of total amount of nuclide in each cell to concentration of dissolved nuclides, concentration of sorbed nuclides and concentration of precipitate are calculated using  $\gamma$  factor which represents the ratio of concentration of dissolved nuclides to total amount of nuclide (see equation (2-19)). This procedure gives MESHNOTE an efficient time stepping scheme, and we don't need to set the extreme short time stepping to solve the problem with short half lives.

With this discretisation, we rewrite the governing equation (2-11) based on the finite difference method, and the following difference equation for each cell except  $k=1$  and  $N$  is given (see Appendix A):

$$\frac{V_k}{\delta t} (A_k^{l+1} - A_k^l) = \frac{\epsilon^B D_p^B}{\delta r} \left[ S_k^- (\gamma_{k-1} A_{k-1}^{l+1} - \gamma_k A_k^{l+1}) - S_k^+ (\gamma_k A_k^{l+1} - \gamma_{k+1} A_{k+1}^{l+1}) \right] \quad (3-3)$$

where, the superscript  $l$  refers to the time level (i.e.  $\delta t = t_{l+1} - t_l$ ), and  $S_k^\pm$  are the surface area factors for the cell at positions  $r_k \pm \delta r/2$  respectively. These are given by:

$$S_k^\pm = 2\pi \left( r_k \pm \frac{\delta r}{2} \right) L. \quad k=1, \dots, N. \quad (3-4)$$

$V_k$  is the volume of the cell, and given as:

$$V_k = 2\pi r_k \delta r L. \quad k=2, \dots, N-1. \quad (3-5)$$

For the reservoir cell ( $k=1$ ), we have the following difference equation by solving the equation (2-16) with discretisation (see Appendix A):

$$\frac{V^R}{\delta t} (A_1^{l+1} - A_1^l) = \frac{\epsilon^B D_p^B}{\delta r} \left[ S_1^+ (\gamma_2 A_2^{l+1} - \gamma_1 A_1^{l+1}) \right] + g_{SI} M_G^{l+1}, \quad (3-6)$$

where  $V^R$  is the volume of the reservoir and  $M_G$  is the amount of nuclide in the glass. Similarly, for mixing cell ( $k=N$ ) we have the following difference equation by solving the equation (2-



17) with discretisation(see Appendix A):

$$\frac{V^M}{\delta t}(A_N^{l+1} - A_N^l) = -Q\gamma_N A_N^{l+1} - \frac{\varepsilon^B D_p^B}{\delta r} [S_N(\gamma_N A_N^{l+1} - \gamma_{N-1} A_{N-1}^{l+1})] \quad (3-7)$$

where  $V^M$  is the volume of the mixing cell. The equation for the amount of nuclide in the glass is simply:

$$\frac{1}{\delta t}(M_G^{l+1} - M_G^l) = -g_S M_G^{l+1}. \quad (3-8)$$

### 3.2 Solution algorithm

The finite difference equations (3-3), (3-6), (3-7) and (3-8) form the tridiagonal matrix for the total amount of each nuclide ( $A_{ij}$ ). Due to the separation of the process of nuclide migration and the process of nuclide decay, this tridiagonal system is solved with each timestep without need for extreme short timestep. Constant factors in the matrix are calculated once at the onset of the code and stored for use at each timestep. At each timestep the tridiagonal system is solved after the radioactive decay has been dealt with. Any partitioning of obtained total amount is taken into account by the  $\gamma$  factors (see 2.3.2).

In the MESHNOTE code, the setting of the timestep is controlled by considering the solutions at  $(t+\delta t)$ . This method represents the two solutions ( $f_{ij}^1, f_{ij}^2$ ) obtained from taking a length of timestep  $\delta t$  and length of two timesteps  $\delta t/2$  (see Figure 3-2).

At first, the  $\gamma$  factors and the decay amount for a certain time period of  $t \sim t+\delta t$  are calculated, then the tridiagonal matrix is solved with timestep  $\delta t$ . In order to check the accuracy for the current step, setting the timestep  $\delta t/2$ , the  $\gamma$  factors, the decay amount and the tridiagonal matrix are solved for time period  $t \sim t+\delta t/2$  and then similar calculation is carried out for  $t+\delta t/2 \sim t+\delta t$ . Finally, the maximum error,  $E_{max}$ , which is derived from  $f_{ij}^1$  and  $f_{ij}^2$  is compared with tolerance ( $TOL$ ).

$E_{max}$  is defined as:

$$E_{max}(t+\delta t) = \max_{(i,j),r} \frac{|f_{ij}^1(r, t+\delta t) - f_{ij}^2(r, t+\delta t)|}{|f_{ij}^1(r, t+\delta t) + f_{ij}^2(r, t+\delta t)| + \varepsilon}, \quad (3-9)$$

where  $\varepsilon$  is a small number close to machine precision and introduced to avoid numerical instability. Here the parameter  $f_{ij}^1$  and  $f_{ij}^2$  represent the amount of isotope  $j$  of element  $i$  at the end of the timestep, obtained by the full and two half-step routes.

The next timestep is set to a factor times the current step. This factor is given by:

$$\eta = \max(0.5, \min(1.5, 0.9 \sqrt{\frac{TOL}{E_{max}}}), \quad (3-10)$$

Clearly, if  $E_{max}$  exceeds  $TOL$ , then  $\eta$  is less than unity, and vice versa. The factor of 0.9, and the constraints of 0.5 and 1.5 in equation (3-10) are inserted for caution. Such a timestep scheme is similar to second order Runge-Kutta or Modified midpoint rule timesteps.

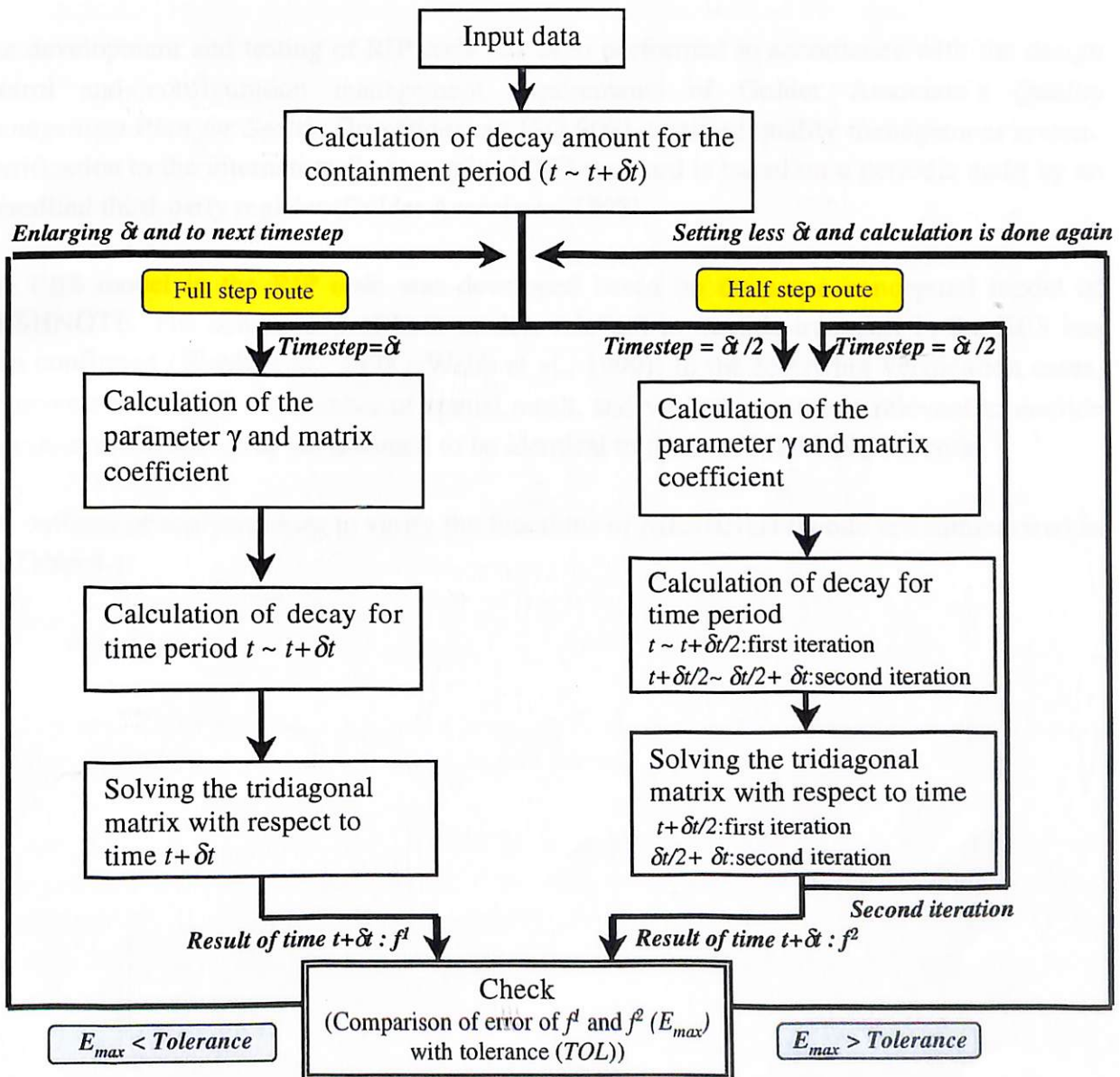


Figure 3-2 Solution algorithm

#### 4 Verification

We considered the following analysis cases to verify the fundamental function of MESHNOTE code. In these cases, the results from MESHNOTE are compared with the analytical solution or the result calculated by RIP code (Golder Associates, 1998). The RIP code, which can probabilistically simulate the release, transport, and contaminants within complex engineered and/or natural environmental system, was developed by Golder Associates. RIP code can combine a basic structure of cells, pipes and various 1-dimension pathways using advective or diffusive connections with a model to explicitly represent various source release mechanisms along with containers and other near-field engineered structures.

The development and testing of RIP code has been performed in accordance with the design control and configuration management requirements of Golder Associate's *Quality Management Plan for Seattle Operations*, an ISO 9001-certified quality management system. Certification to the internationally recognized ISO standard is based on a periodic audit by an accredited third-party register (Golder Associates, 1998).

The EBS model in the RIP code was developed based on the same conceptual model of MESHNOTE. The consistency of both models relevant to nuclide transport in the EBS has been confirmed (Webb et al., 1998 ; Webb et al., 1999). In the following verification cases, the geometry of EBS, the number of spatial mesh, and various parameter relevant to nuclide migration in the RIP code are assumed to be identical to those of MESHNOTE code.

The outlines of analysis cases to verify the functions of MESHNOTE code are summarized in the Table 4-1.

**Table 4-1 Summary of verification analysis**

| <i>Section</i>                   | <i>Verification contents</i>                      |
|----------------------------------|---|
| 4.1<br>Fundamental functions     | Single nuclide migration                          |
|                                  | Depletion of nuclide inventory                    |
|                                  | Non-linear sorption<br>(Langmuir isotherm )       |
| 4.2<br>Decay chain               | Single chain decay                                |
|                                  | Multiple chains decay                             |
|                                  | Branching and rejoining chains decay              |
| 4.3<br>Glass dissolution model   | First-order reaction model                        |
|                                  | Hydration reaction model                          |
| 4.4<br>Time dependent parameter  | Solubility  |
|                                  | Sorption constant                                 |
|                                  | Diffusion coefficient                             |
|                                  | Volume flow rate of water through the mixing cell |
| 4.5<br>Space dependent parameter | Solubility  |
|                                  | Sorption constant                                 |
|                                  | Diffusion coefficient                             |

## 4.1 Fundamental functions

### 4.1.1 Single nuclide migration

#### (1) Objective

A simple calculation considering the migration of a single nuclide accounting to fundamental migration processes (decay, linear sorption, diffusion and solubility limit) in the EBS is performed. The result is compared with the steady-state analytical solutions and the results of RIP.

#### (2) Analysis condition

In order to simplify the analysis condition, zero concentration at the outer boundary of the buffer and the constant glass dissolution model are assumed and the nuclide migration of Tc-99 in the buffer including the fundamental migration process is evaluated. The primary input parameters for the MESHNOTE code for this case are presented below:

|                                     |   |   |
|-------------------------------------|---|---|
| Nuclide                             | : | Tc-99   |
| Half life                           | : | $2.13 \times 10^5$ [y]                            |
| Inventory                           | : | $1.00 \times 10^{20}$ [mol]                       |
| Inner radius of the buffer material | : | 0.41 [m]  |
| Outer radius of the buffer material | : | 1.11 [m]  |
| Length of the buffer material       | : | 2.14 [m]  |
| Number of spatial mesh              | : | 40 [-]  |
| Diffusion coefficient in porewater  | : | $3 \times 10^{-2}$ [ $\text{m}^2 \text{y}^{-1}$ ] |
| Porosity                            | : | 0.41 [-]  |
| Dry density at the buffer material  | : | $1.6 \times 10^5$ [ $\text{kg m}^{-3}$ ]          |
| Distribution coefficient            | : | 0.1 [ $\text{m}^3 \text{kg}^{-1}$ ]               |
| Solubility                          | : | $4 \times 10^{-5}$ [ $\text{mol m}^{-3}$ ]        |

The zero concentration boundary condition is represented by the volume flow rate of water through the mixing cell, which is provided extremely large ( $1.0 \times 10^{10}$ ).

The effect of hydration and diffusion/dissipation of soluble Silicon are ignored and dissolution of the vitrified waste with simple constant glass dissolution model is considered. The constant glass dissolution rate can represent by initial dissolution rate when hydration rate and Solubility of Silicon are assumed zero and extremely large ( $1.0 \times 10^{10}$ ) respectively.

The parameters relevant to the outer boundary condition of the buffer and glass dissolution are presented as below:

|                          |   |  |
|--------------------------|---|--|
| Initial dissolution rate | : | $3.7 \times 10^{-1}$ [ $\text{g m}^{-2} \text{y}^{-1}$ ] |
| Hydration rate           | : | 0 [ $\text{g m}^{-2} \text{y}^{-1}$ ]                    |

|  |   |                      |                                    |
|--|---|----------------------|------------------------------------|
| Initial inventory of Silicon                         | : | 3090                 | [mol]                              |
| Distribution coefficient of Silicon<br>in porewater  | : | 0                    | [m <sup>3</sup> kg <sup>-1</sup> ] |
| Solubility of Silicon                                | : | 1.0×10 <sup>10</sup> | [mol m <sup>-3</sup> ]             |
| Surface area of vitrified waste                      | : | 17                   | [m <sup>2</sup> ]                  |
| Volume of vitrified waste                            | : | 0.15                 | [m <sup>3</sup> ]                  |
| Density of vitrified waste                           | : | 2.75×10 <sup>6</sup> | [m <sup>3</sup> g <sup>-1</sup> ]  |
| Volume flow rate of water through<br>the mixing cell | : | 1.0×10 <sup>10</sup> | [m <sup>3</sup> y <sup>-1</sup> ]  |

The glass life time is approximately 70,000 years in the above condition. This data sets relevant to glass dissolution is used in all verification cases, except for case for verification of glass dissolution model (see Section 4.3).

The above input parameters are basic conditions in the following all verification cases.

The results from MESHNOTE are compared with a steady-state analytical solution and the result of RIP with respect to the release rate from the EBS and the concentration profile in the buffer materials. The analytical solution of release rate from the EBS and the concentration profile in the EBS under the steady-state conditions are described below.

● **Analytical solution for the release rate from the EBS under steady-state conditions**

Assuming one-dimensional migration, cylindrical co-ordinates same as MESHNOTE, the release rate of element  $i$  from the EBS is given by equation (4-1):

$$f_i^{Buffer \rightarrow Hostrock} = 2\pi L \varepsilon^B D p_i C_i^* \frac{1}{\ln(r_{out}/r_{in})}, \quad (4-1)$$

where this solution is based on the following assumptions:

- the radionuclide decay is ignored;
- the nuclide concentration at the inner boundary of the buffer is limited by solubility;
- the nuclide concentration at the outer boundary of the buffer is zero (zero concentration boundary condition).

● **Analytical solution for the concentration profile in the EBS under steady-state conditions**

The analytical solution of concentration profile in the EBS under steady-state is given by equation (4-2), assuming the same conditions as above:

$$C_i(r) = \frac{\ln(r/r_{out})}{\ln(r_{in}/r_{out})} C_i^*. \quad (4-2)$$

**(3) Result**

The release rate of Tc-99 calculated by MESHNOTE, the steady-state analytical solution of release rate (see equation (4-1)), and the release rate of Tc-99 calculated by RIP are shown in Figure 4-1.

The following observations are made regarding the time-dependence release rate of Tc-99 from the EBS:

- During the period of 5,000 years, the release rate of Tc-99 from the EBS does not reach steady-state due to the effect of diffusion and retardation in the buffer;
- The release rate between 5,000 and  $1 \times 10^7$  years doesn't change with time and equals to the steady-state analytical solution of release rate;
- The release rate calculated by MESHNOTE and calculated by RIP are quite consistent throughout the period of assessment.

The concentration profile in the buffer material under steady-state conditions calculated by MESHNOTE is shown in Figure 4-2 with the steady-state analytical solution of concentration profile (see equation (4-2)). The concentration profile from MESHNOTE is calculated for time of  $1 \times 10^6$  years, when the release rate from the EBS reaches steady-state. This figure shows that the concentration in the buffer material estimated by MESHNOTE and by the analytical solution are quite consistent.

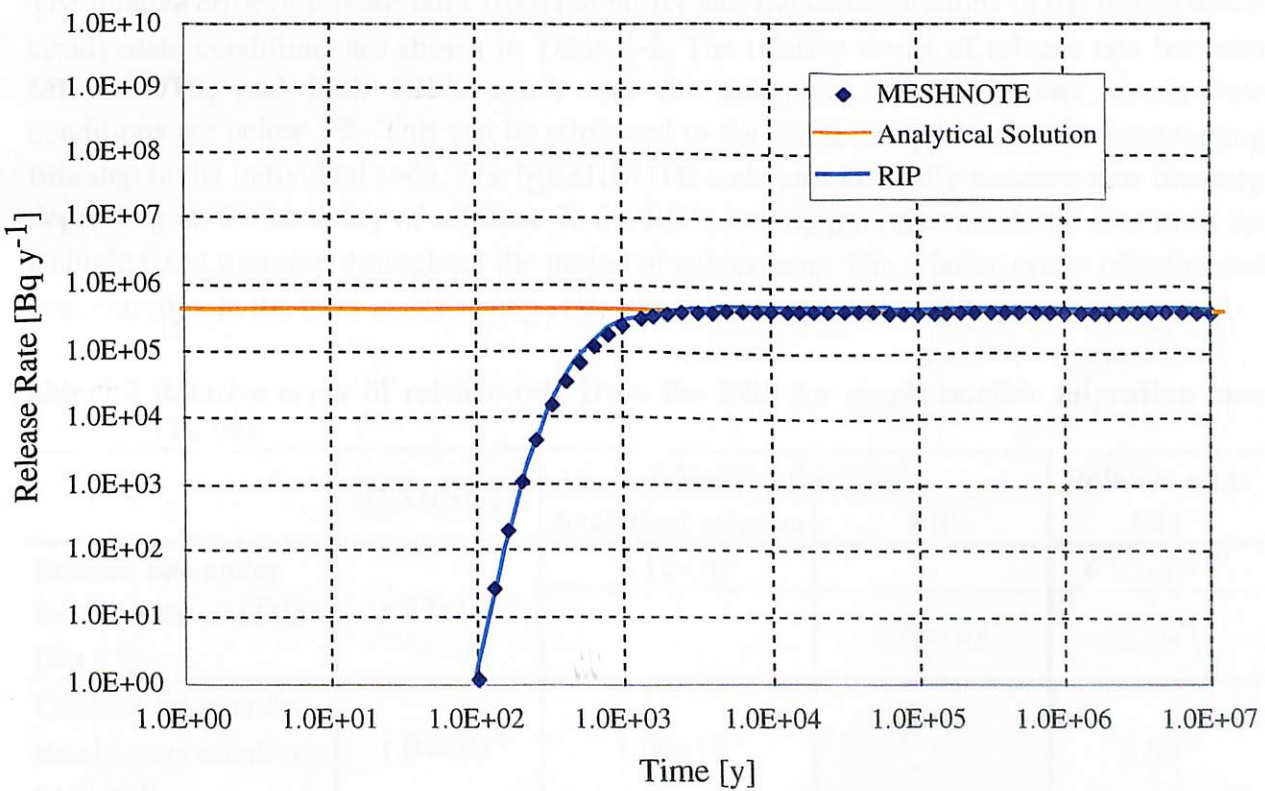


**Figure 4-1 Comparison of release rate from the EBS for single nuclide migration (Tc-99)**



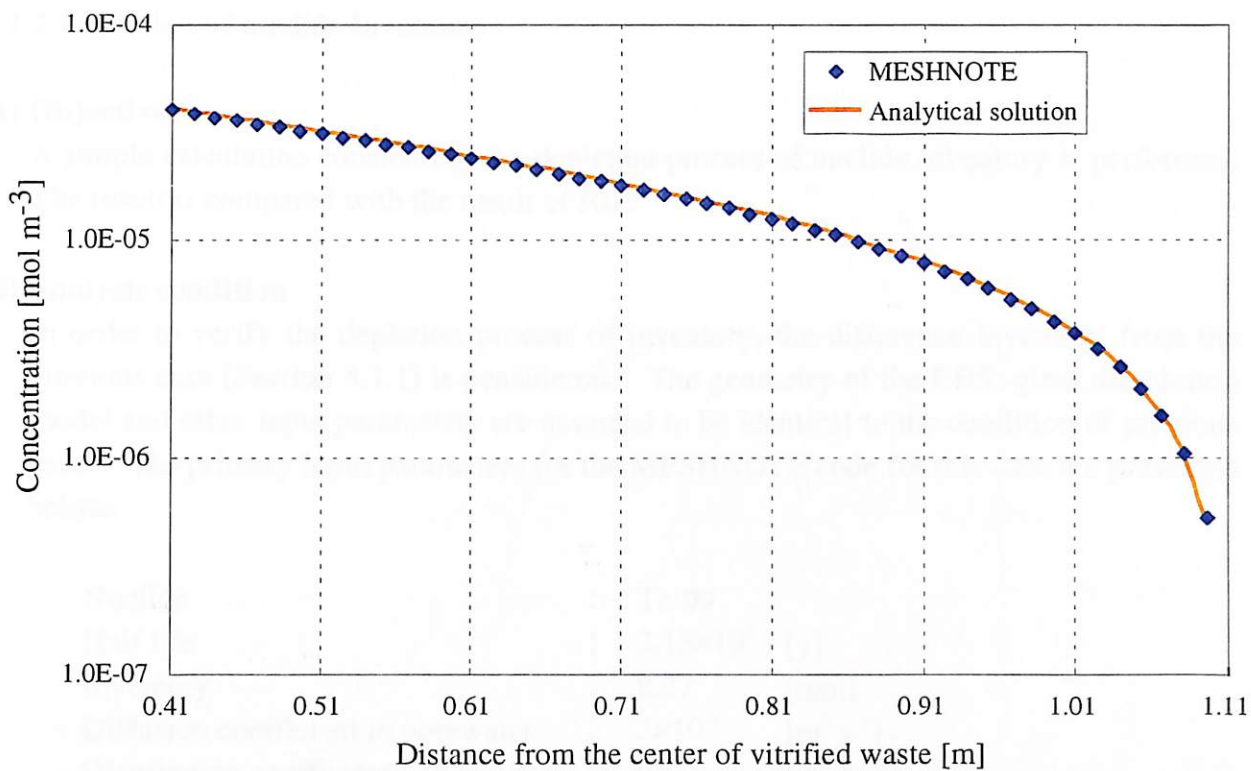


**Figure 4-2 Comparison of concentration profile in the buffer materials for single nuclide migration (Tc-99) (this concentration profile estimated by MESHNOTE is at  $1 \times 10^6$  years.)**

The relative error of release rates from the buffer and the concentrations in the buffer under steady-state conditions are shown in Table 4-2. The relative errors of release rate between MESHNOTE, and both RIP's result and the analytical solution under steady-state conditions are below 3%. This can be attributed to the different approaches for establishing timestep in the individual code. The MESHNOTE code automatically makes a new timestep depending on the accuracy of solution. In the RIP code, on the other hand, the user must set a single fixed timestep throughout the period of assessment. The relative errors of estimated concentration in the EBS under steady-state condition is also below 3%.

**Table 4-2 Relative error of release rate from the EBS for single nuclide migration case (Tc-99)**

|   | MESHNOTE              | Verification tools    |                      | Relative error [%]       |
|---|-----------------------|-----------------------|----------------------|--------------------------|
|   |                       | Analytical solution   | RIP                  |                          |
| Release rate under steady-state condition [Bq y <sup>-1</sup> ]   | 4.15×10 <sup>5</sup>  | 4.12×10 <sup>5</sup>  | -                    | 6.85×10 <sup>-1</sup> *1 |
|   |                       | -                     | 4.26×10 <sup>5</sup> | 2.69*1                   |
| Concentration under steady-state condition [mol m <sup>-3</sup> ] | 1.04×10 <sup>-6</sup> | 1.06×10 <sup>-6</sup> | -                    | 2.66*2                   |

\*1 Relative error for analytical solution = |MESHNOTE - analytical solution| / analytical solution × 100

Relative error for RIP = |MESHNOTE - RIP| / RIP × 100

\*2 The maximum relative error of concentration profile in the buffer materials is selected.



### 4.1.2 Depletion of nuclide inventory

#### (1) Objective

A simple calculation considering the depletion process of nuclide inventory is performed. The result is compared with the result of RIP.

#### (2) Analysis condition

In order to verify the depletion process of inventory, the difference inventory from the previous case (Section 4.1.1) is considered. The geometry of the EBS, glass dissolution model and other input parameters are assumed to be identical to the condition of previous case. The primary input parameters for the MESHNOTE code for this case are presented below:

|   |   |   |
|---|---|---|
| Nuclide   | : | Tc-99   |
| Half life   | : | $2.13 \times 10^5$ [y]                              |
| Inventory   | : | 8.27 [mol]  |
| Diffusion coefficient in porewater                | : | $3 \times 10^{-2}$ [ $\text{m}^2 \text{y}^{-1}$ ]   |
| Distribution coefficient                          | : | 0.1 [ $\text{m}^3 \text{kg}^{-1}$ ]                 |
| Solubility  | : | $4 \times 10^{-5}$ [ $\text{mol m}^{-3}$ ]          |
| Volume flow rate of water through the mixing cell | : | $1.0 \times 10^{10}$ [ $\text{m}^3 \text{y}^{-1}$ ] |

#### (3) Result

The release rate of Tc-99 calculated by MESHNOTE and the release rate calculated by RIP are shown in Figure 4-3.

The following observations are made regarding the time-dependence release rate of Tc-99 from the EBS:

- The release rates calculated by MESHNOTE and RIP between 5,000 and  $5 \times 10^5$  years don't change with time (steady-state);
- After  $5 \times 10^5$  years, the release rates of Tc-99 calculated by MESHNOTE and RIP decrease sharply due to complete migration of the inventory of Tc-99 to outside of buffer materials until this time.

The maximum release rates from the EBS and the depletion time are shown in Table 4-3. The relative error of the depletion time between estimates by MESHNOTE and RIP's is approximately 11%. As described in Section 4.1.1 (3), the constant timestep is used in the RIP code throughout the period of calculation (100 years is used in this case), but in MESHNOTE code, the timestep which is defined automatically taking into account the accuracy of solution is used. So the depletion time by RIP might have a relatively large difference from one by MESHNOTE.

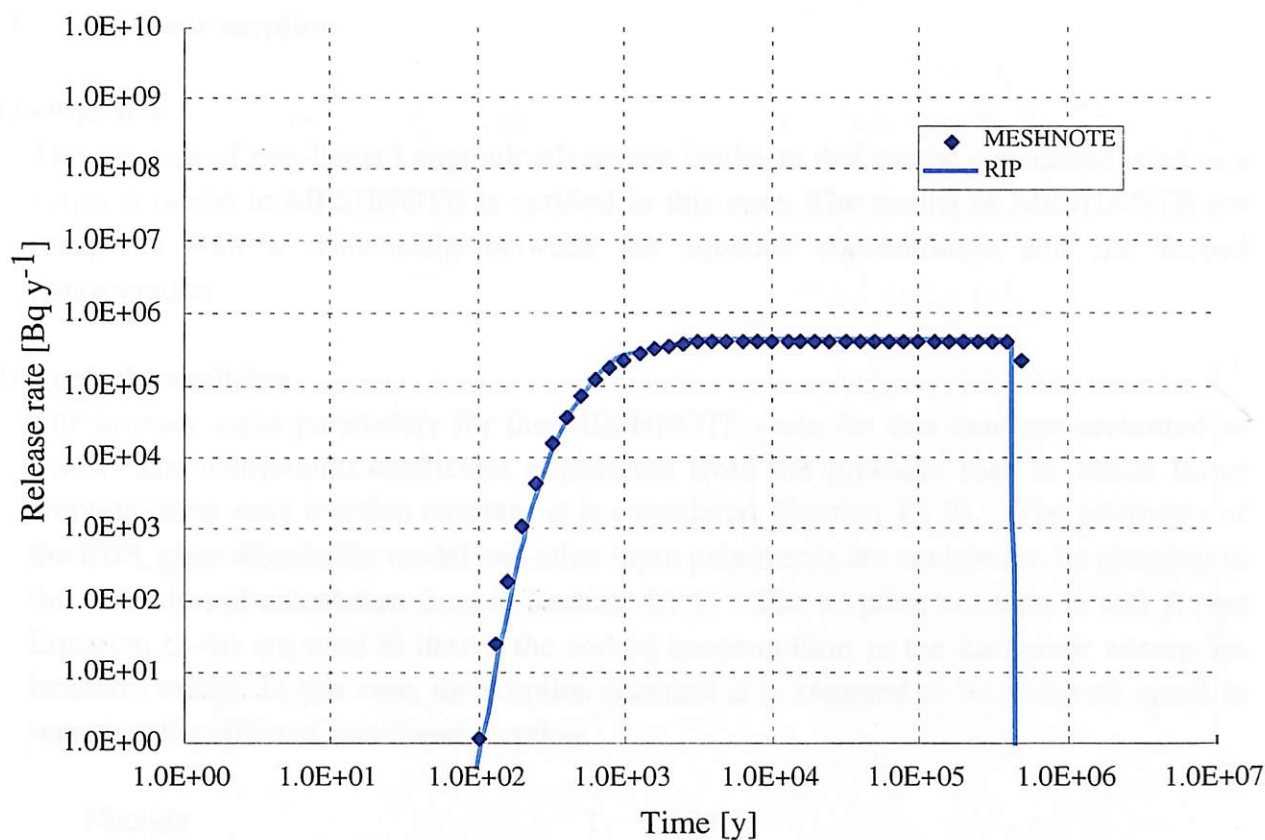


Figure 4-3 Comparison of release rate from the EBS for the depletion process of nuclide inventory (Tc-99)

Table 4-3 Relative error of release rate from the EBS for the effect of depletion of nuclide (Tc-99) inventory

|  | MESHNOTE             | Verification tools   | Relative error [%] <sup>*1</sup> |
|--|----------------------|----------------------|----------------------------------|
|  |                      | RIP                  |                                  |
| Maximum Release rate [Bq y <sup>-1</sup> ] | 4.15×10 <sup>5</sup> | 4.26×10 <sup>5</sup> | 2.69                             |
| Depletion time of inventory [y]            | 5.00×10 <sup>5</sup> | 4.50×10 <sup>5</sup> | 11.1                             |

<sup>\*1</sup> Relative error for RIP = |MESHNOTE - RIP| / RIP × 100

### 4.1.3 Non-linear sorption

#### (1) Objective

The function of non-linear Langmuir adsorption isotherm that can be considered used as a sorption model in MESHNOTE is verified in this case. The results of MESHNOTE are compared with a relationship between the aqueous concentration and the sorbed concentration.

#### (2) Analysis condition

The primary input parameters for the MESHNOTE code for this case are presented as below. The distribution coefficient is different from the previous case in which linear sorption using only sorption constant  $\alpha$  is considered (Section 4.1.2). The geometry of the EBS, glass dissolution model and other input parameters are assumed to be identical to the condition of calculation case in Section 4.1.1. The sorption constant  $\alpha$  and  $\beta$  (see Equation (2-4)) are used to derive the sorbed concentration in the Langmuir adsorption isotherm model. In this case, the sorption constant  $\alpha$  is assumed to be relatively small to represent the effect of non-linear sorption.

|   |   |   |
|---|---|---|
| Nuclide   | : | Tc-99   |
| Half life   | : | $2.13 \times 10^5$ [y]                              |
| Inventory   | : | 8.27 [mol]  |
| Diffusion coefficient in porewater                | : | $3 \times 10^{-2}$ [ $\text{m}^2 \text{y}^{-1}$ ]   |
| Sorption constant $\alpha$                        | : | 2.7 [-]   |
| Sorption constant $\beta$                         | : | $1 \times 10^5$ [-]                                 |
| Solubility  | : | $4 \times 10^{-5}$ [ $\text{mol m}^{-3}$ ]          |
| Volume flow rate of water through the mixing cell | : | $1.0 \times 10^{10}$ [ $\text{m}^3 \text{y}^{-1}$ ] |

To verify the function of the Langmuir adsorption isotherm model, the relationship between the concentration of dissolved nuclide and the concentration of sorbed nuclide calculated by MESHNOTE (i.e. the relationship of concentration in the buffer at one time) is compared with an equation of relationship between the dissolved concentration and sorbed concentration, which represents a non-linear Langmuir adsorption isotherm. This relation is given by equation (4-3),

$$S_i(C_i) = \frac{\alpha_i C_i}{1 + \beta_i C_i}. \quad (4-3)$$

#### (3) Result

The relationship between the concentration of dissolved nuclide and the concentration of sorbed nuclide calculated by MESHNOTE and the analytical solution are shown in Figure 4-4. The following observations are made regarding these relations:

- The concentration of sorbed nuclide increases quickly until the concentration of the

dissolved nuclide reaches  $1 \times 10^{-5} [\text{mol m}^{-3}]$ ;

- After the concentration of dissolved nuclide exceed  $1 \times 10^{-5} [\text{mol m}^{-3}]$ , the increase in the concentration of sorbed nuclide reaches an upper limit due to the limit of sorbed capacity;
- The results of MESHNOTE and analysis solution are quite consistent.

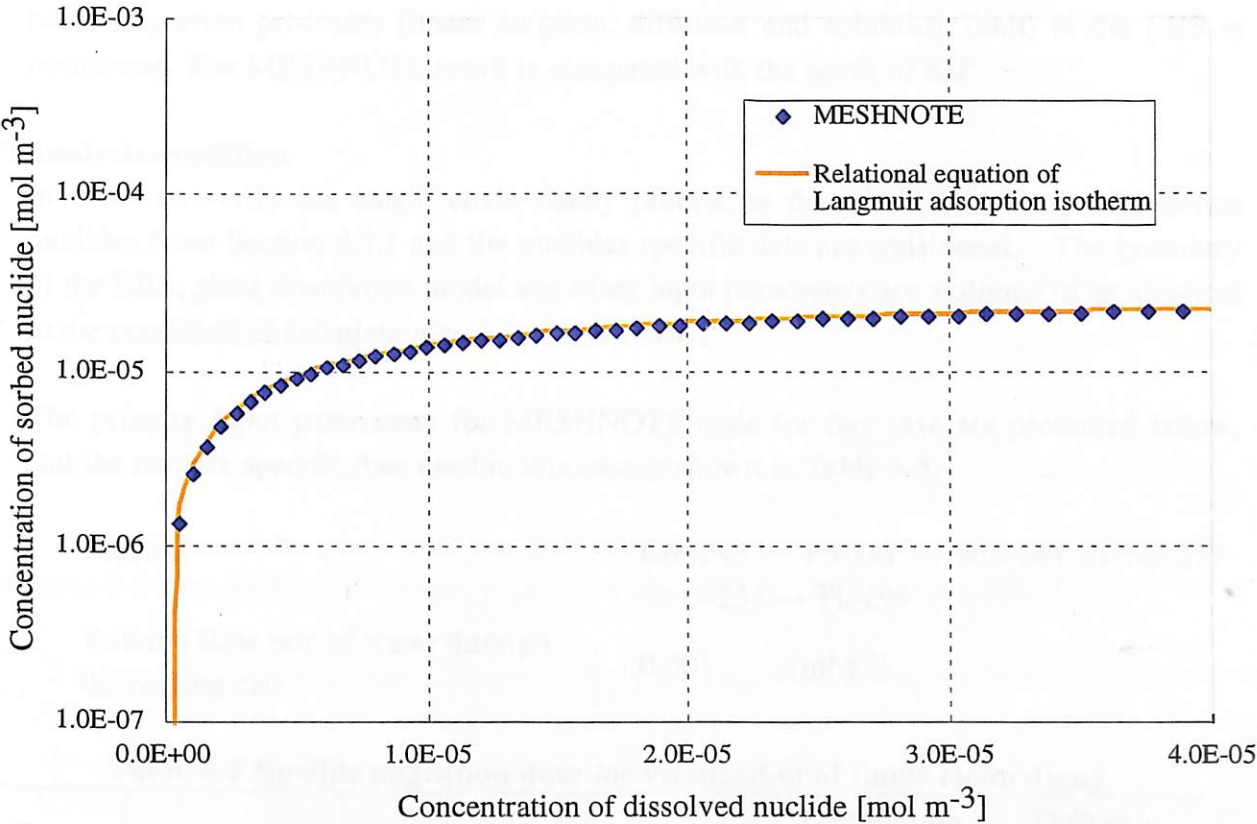


**Figure 4-4 Comparison of the relation between the concentration of dissolved nuclide and the concentration of sorbed nuclide for the non-linear sorption model (Tc-99) (these concentration are at 1,000 years, when the release rate from the EBS is steady-state)**

The concentrations of sorbed nuclide for MESHNOTE and for the analytical solution under steady-state conditions (at 1,000 years) are shown in Table 4-4 with those relative errors. The maximum relative error is extremely small.

**Table 4-4 Relative error of the concentration of sorbed nuclide (Tc-99)**

|   | MESHNOTE              | Verification tool     | Maximum relative error [%] <sup>*1</sup> |
|---|-----------------------|-----------------------|--|
|   |                       | Analytical solution   |  |
| Concentration of sorbed nuclide [ $\text{mol m}^{-3}$ ] | $1.20 \times 10^{-5}$ | $1.20 \times 10^{-5}$ | $4.78 \times 10^{-2}$                    |

<sup>\*1</sup> Relative error for analytical solution =  $|\text{MESHNOTE} - \text{analytical solution}| / \text{analytical solution} \times 100$

## 4.2 Decay chain

### 4.2.1 Single chain decay

#### (1) Objective

A calculation considering the migration of nuclides with single chain decay accounting to basic migration processes (linear sorption, diffusion and solubility limit) in the EBS is performed. The MESHNOTE result is compared with the result of RIP.

#### (2) Analysis condition

In order to verify the single chain decay process in the MESHNOTE, the difference nuclides from Section 4.1.1 and the nuclides specific data are considered. The geometry of the EBS, glass dissolution model and other input parameters are assumed to be identical to the condition of calculation case in Section 4.1.1.

The primary input parameters for MESHNOTE code for this case are presented below, and the nuclide specific data used in this case is shown in Table 4-5:

Nuclide : Cm-245 → Pu-241 → Am-241 → Np-237  
→ U-233 → Th-299

Volume flow rate of water through the mixing cell : 0.001 [m<sup>3</sup> y<sup>-1</sup>]

**Table 4-5 Nuclide migration data for verification of single chain decay**

|        | Half life [y]      | Inventory [mol]       | Solubility [mol m <sup>-3</sup> ] | Distribution coefficient [m <sup>3</sup> kg <sup>-1</sup> ] | Diffusion coefficient [m <sup>2</sup> y <sup>-1</sup> ] |
|--------|--------------------|-----------------------|-----------------------------------|---|---|
| Cm-245 | $8.50 \times 10^3$ | $7.26 \times 10^{-3}$ | $2 \times 10^{-4}$                | 10  | $3 \times 10^{-2}$                                      |
| Pu-241 | $1.44 \times 10^1$ | $1.23 \times 10^{-5}$ | $3 \times 10^{-5}$                | 10  | $3 \times 10^{-2}$                                      |
| Am-241 | $4.32 \times 10^2$ | $1.88 \times 10^{-1}$ | $2 \times 10^{-4}$                | 10  | $3 \times 10^{-2}$                                      |
| Np-237 | $2.14 \times 10^6$ | 3.74                  | $2 \times 10^{-5}$                | 1   | $3 \times 10^{-2}$                                      |
| U-233  | $1.59 \times 10^5$ | $1.17 \times 10^{-3}$ | $8 \times 10^{-6}$                | 1   | $3 \times 10^{-2}$                                      |
| Th-229 | $7.34 \times 10^3$ | $2.51 \times 10^{-6}$ | $5 \times 10^{-3}$                | 1   | $3 \times 10^{-2}$                                      |

The result of MESHNOTE is compared to the result from RIP with respect to the release rate from the EBS.

#### (3) Result

The release rates of single chain decay calculated by MESHNOTE and calculated by RIP are shown in Figure 4-5. Both results are well consistent, but the release rate of Np-237, U-233 and Th-229 until  $5.0 \times 10^3$  years have small difference between MESHNOTE and RIP. This difference can be attributed to method of time stepping used in the individual code.



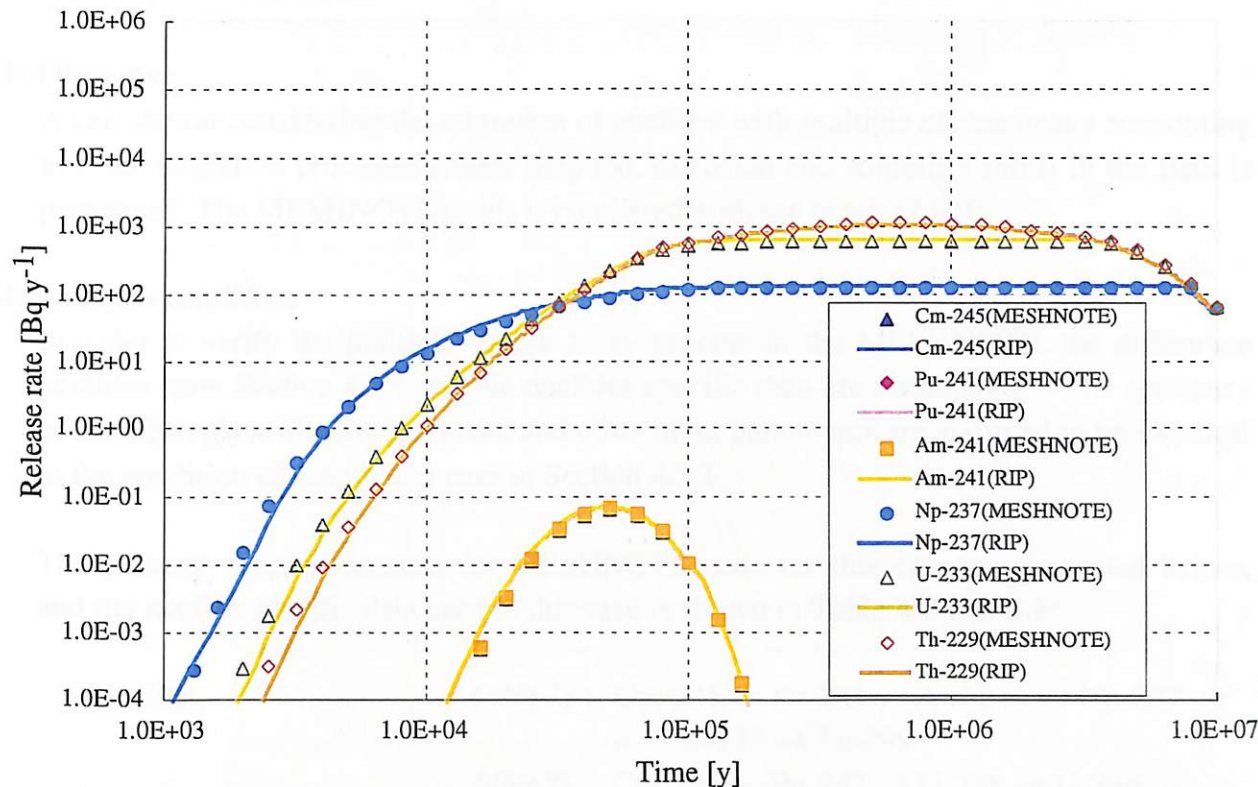


Figure 4-5 Comparison of release rate from the EBS in verification of single chain decay

The maximum release rates from the EBS and their relative error are shown in Table 4-6. The relative errors of maximum release rate are below 3% except for Th-229. As described above, the calculation in the RIP is carried out using a specified timestep throughout the period of calculation. The relative error of Th-229 may depend on the difference of specified timestep.

Table 4-6 Relative error of the maximum release rate in verification of single chain decay

|        | MESHNOTE              | Verification tool     | Relative error [%]*   |
|--------|-----------------------|-----------------------|-----------------------|
|        |                       | RIP                   |                       |
| Cm-245 | $6.54 \times 10^{-2}$ | $6.60 \times 10^{-2}$ | 1.00                  |
| Pu-241 | $6.55 \times 10^{-2}$ | $6.61 \times 10^{-2}$ | 1.00                  |
| Am-241 | $6.90 \times 10^{-2}$ | $6.97 \times 10^{-2}$ | 1.01                  |
| Np-237 | $1.21 \times 10^2$    | $1.21 \times 10^2$    | $1.10 \times 10^{-1}$ |
| U-233  | $5.75 \times 10^2$    | $5.91 \times 10^2$    | 2.75                  |
| Th-229 | $1.13 \times 10^3$    | $9.78 \times 10^2$    | 15.2                  |

\* Relative error for RIP =  $|\text{MESHNOTE} - \text{RIP}| / \text{RIP} \times 100$

## 4.2.2 Multiple chains decay

### (1) Objective

A calculation considering the migration of nuclides with multiple chains decay accounting to basic migration processes (linear sorption, diffusion and solubility limit) in the EBS is performed. The MESHNOTE result is compared with the result of RIP.

### (2) Analysis condition

In order to verify the multiple chains decay process in the MESHNOTE, the difference nuclides from Section 4.1.1 and the nuclides specific data are considered. The geometry of the EBS, glass dissolution model and other input parameters are assumed to be identical to the condition of calculation case in Section 4.1.1.

The primary input parameters for MESHNOTE code for this case are presented below, and the nuclide specific data used in this case is shown in Table 4-7 and 4-8:

|  |  |
|--|--|
| Nuclide  | (4N+1) : Cm-245 → Pu-241 → Am-241 → Np-237 →<br>U-233 → Th-299         |
|  | (4N+2) : Cm-246 → Pu-242 → U-238 → U-234 →<br>Th-230 → Ra-226 → Pb-210 |
|  | (4N+3) : Am-243 → Pu-239 → U-235 → Pa-231 →<br>Ac-227                  |
|  | (4N) : Pu-240 → U-236 → Th-232   |
| Diffusion coefficient in porewater<br>(all nuclides) | : $3 \times 10^{-2}$ [m <sup>2</sup> y <sup>-1</sup> ]                 |
| Volume flow rate of water through<br>the mixing cell | : 0.001 [m <sup>3</sup> y <sup>-1</sup> ]                              |

The results from MESHNOTE are compared to the results of RIP with respect to the release rate from the EBS.

**Table 4-7 Half lives and inventories of nuclides in verification of multiple chains decay**

|             | Half life [y]         | Inventory [mol]       |
|-------------|-----------------------|-----------------------|
| <b>4N+1</b> |                       |                       |
| Cm-245      | $8.50 \times 10^3$    | $7.26 \times 10^{-3}$ |
| Pu-241      | $1.44 \times 10^1$    | $1.23 \times 10^{-5}$ |
| Am-241      | $4.32 \times 10^2$    | $1.88 \times 10^{-1}$ |
| Np-237      | $2.14 \times 10^6$    | 3.74                  |
| U-233       | $1.59 \times 10^5$    | $1.17 \times 10^{-3}$ |
| Th-229      | $7.34 \times 10^3$    | $2.51 \times 10^{-6}$ |
| <b>4N+2</b> |                       |                       |
| Cm-246      | $4.73 \times 10^3$    | $8.29 \times 10^{-4}$ |
| Pu-242      | $3.87 \times 10^5$    | $1.12 \times 10^{-2}$ |
| U-238       | $4.47 \times 10^9$    | $1.31 \times 10^1$    |
| U-234       | $2.45 \times 10^5$    | $1.50 \times 10^{-2}$ |
| Th-230      | $7.70 \times 10^4$    | $5.37 \times 10^{-5}$ |
| Ra-226      | $1.60 \times 10^3$    | $2.62 \times 10^{-7}$ |
| Pb-210      | $2.23 \times 10^1$    | $3.48 \times 10^{-9}$ |
| <b>4N+3</b> |                       |                       |
| Am-243      | $7.38 \times 10^3$    | $4.01 \times 10^{-1}$ |
| Pu-239      | $2.41 \times 10^4$    | $1.60 \times 10^{-1}$ |
| U-235       | $7.04 \times 10^8$    | $1.46 \times 10^{-1}$ |
| Pa-231      | $3.28 \times 10^4$    | $2.23 \times 10^{-6}$ |
| Ac-227      | $2.18 \times 10^1$    | $1.48 \times 10^{-9}$ |
| <b>4N</b>   |                       |                       |
| Pu-240      | $6.54 \times 10^3$    | $1.78 \times 10^{-1}$ |
| U-236       | $2.34 \times 10^7$    | $1.05 \times 10^{-1}$ |
| Th-232      | $1.41 \times 10^{10}$ | $6.50 \times 10^{-6}$ |



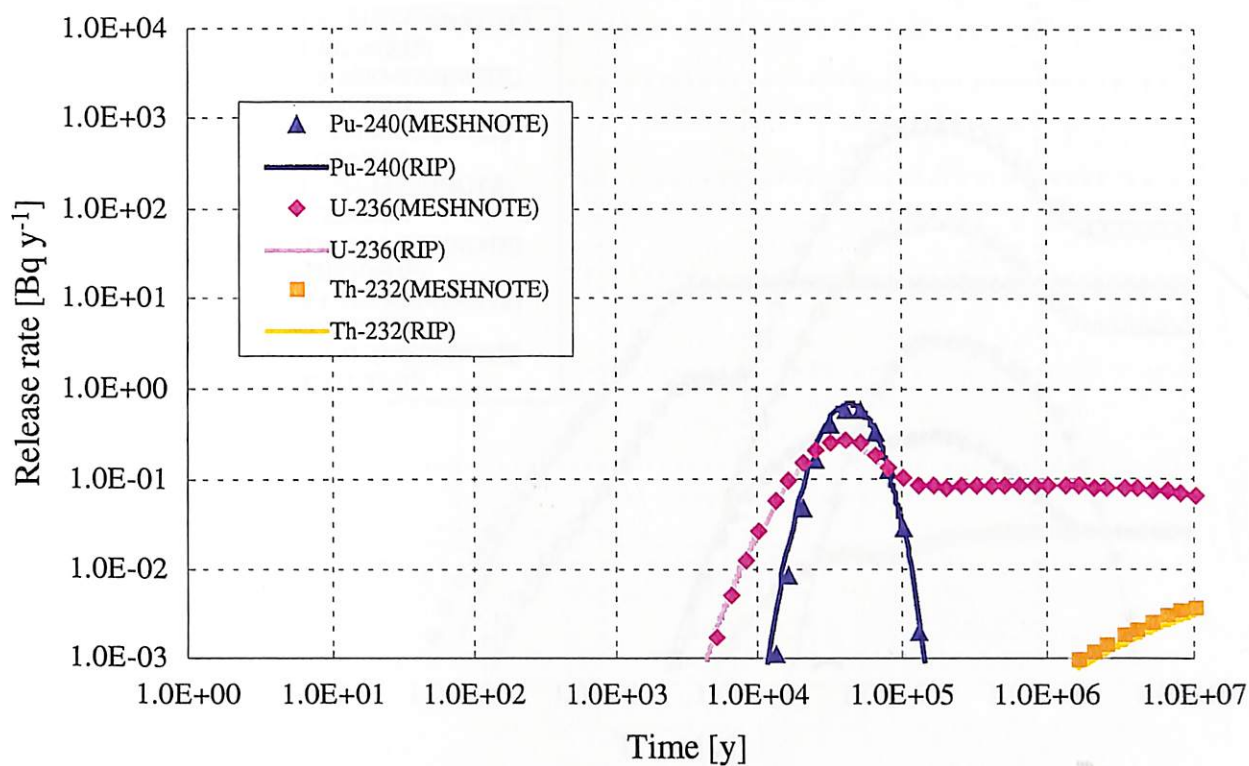
**Table 4-8 Solubilities and distribution coefficients in verification of multiple chains decay**

| Element | Solubility [mol m <sup>-3</sup> ] | Distribution coefficient [m <sup>3</sup> kg <sup>-1</sup> ] |
|---------|-----------------------------------|---|
| Pb      | $2 \times 10^{-3}$                | 0.1   |
| Ra      | $1 \times 10^{-9}$                | 0.01  |
| Ac      | $2 \times 10^{-4}$                | 1   |
| Th      | $5 \times 10^{-3}$                | 1   |
| Pa      | $2 \times 10^{-5}$                | 1   |
| U       | $8 \times 10^{-6}$                | 1   |
| Np      | $2 \times 10^{-5}$                | 1   |
| Pu      | $3 \times 10^{-5}$                | 10  |
| Am      | $2 \times 10^{-4}$                | 10  |
| Cm      | $2 \times 10^{-4}$                | 10  |

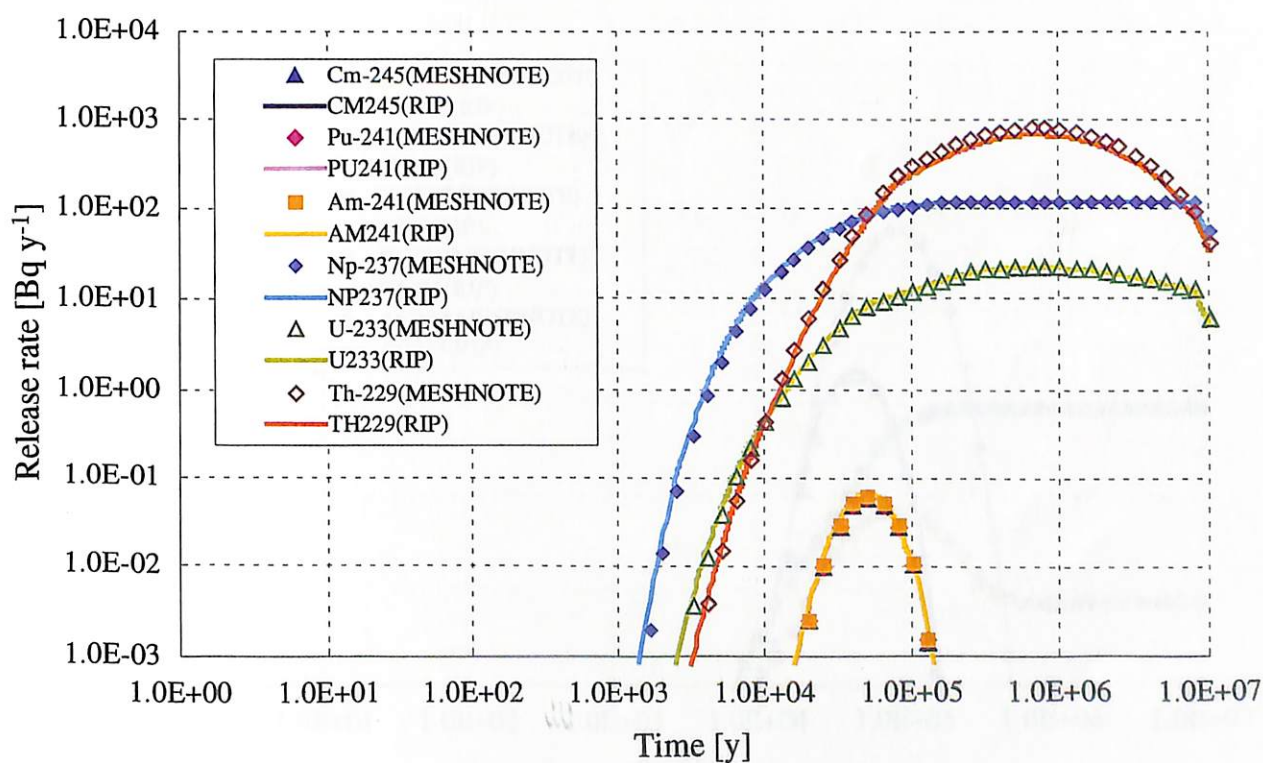
**(3) Result**

The release rates of nuclides in multiple decay chains calculated by MESHNOTE and calculated by RIP are shown in Figure 4-6. The both results are roughly consistent, but during the period of  $1.0 \times 10^3$  years, the release rate of Ra-226 and Pd-210 are common difference between MESHNOTE and RIP. This difference may depend on the difference of setting timestep in each code.

The maximum release rates from the EBS and their relative errors are shown in Table 4-9. The relative errors for some are over 10%. This difference can be attributed to the different approaches for establishing the timestep in the individual code as described above.

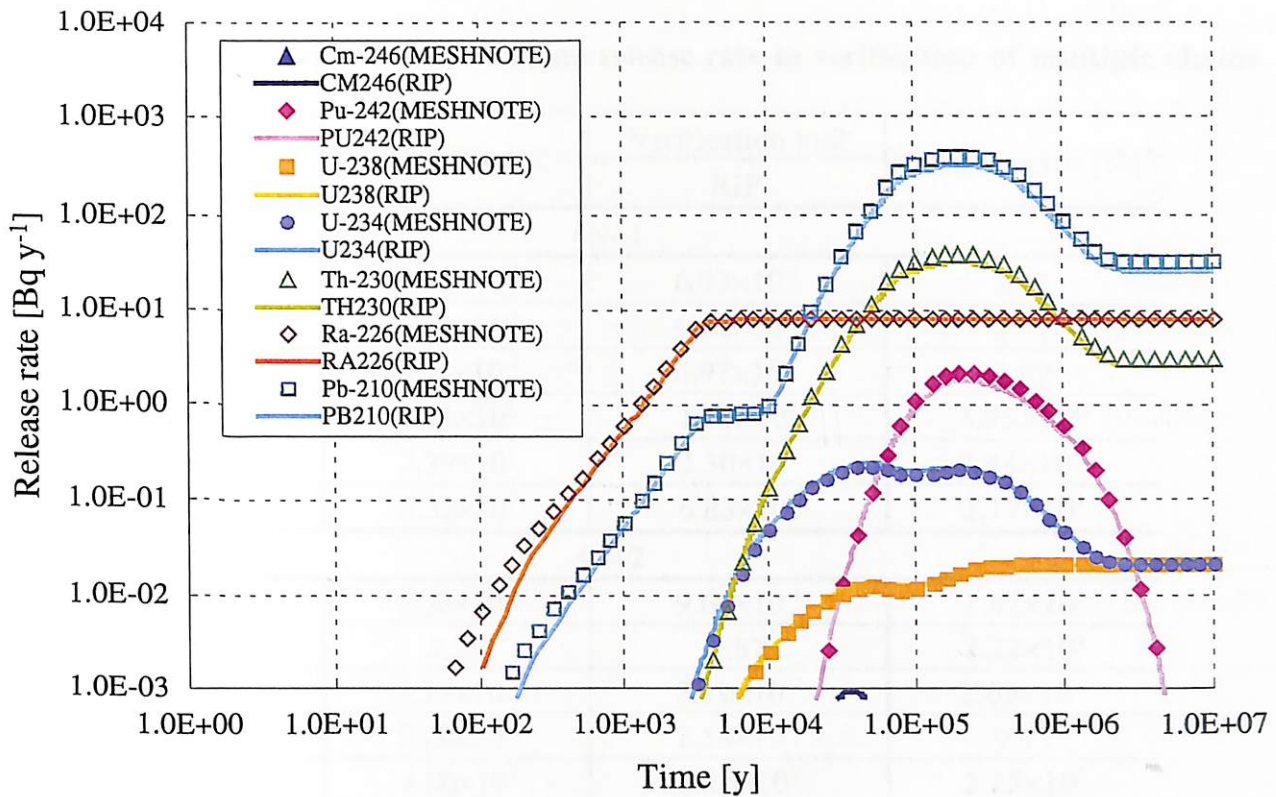


(a) 4N actinide chain

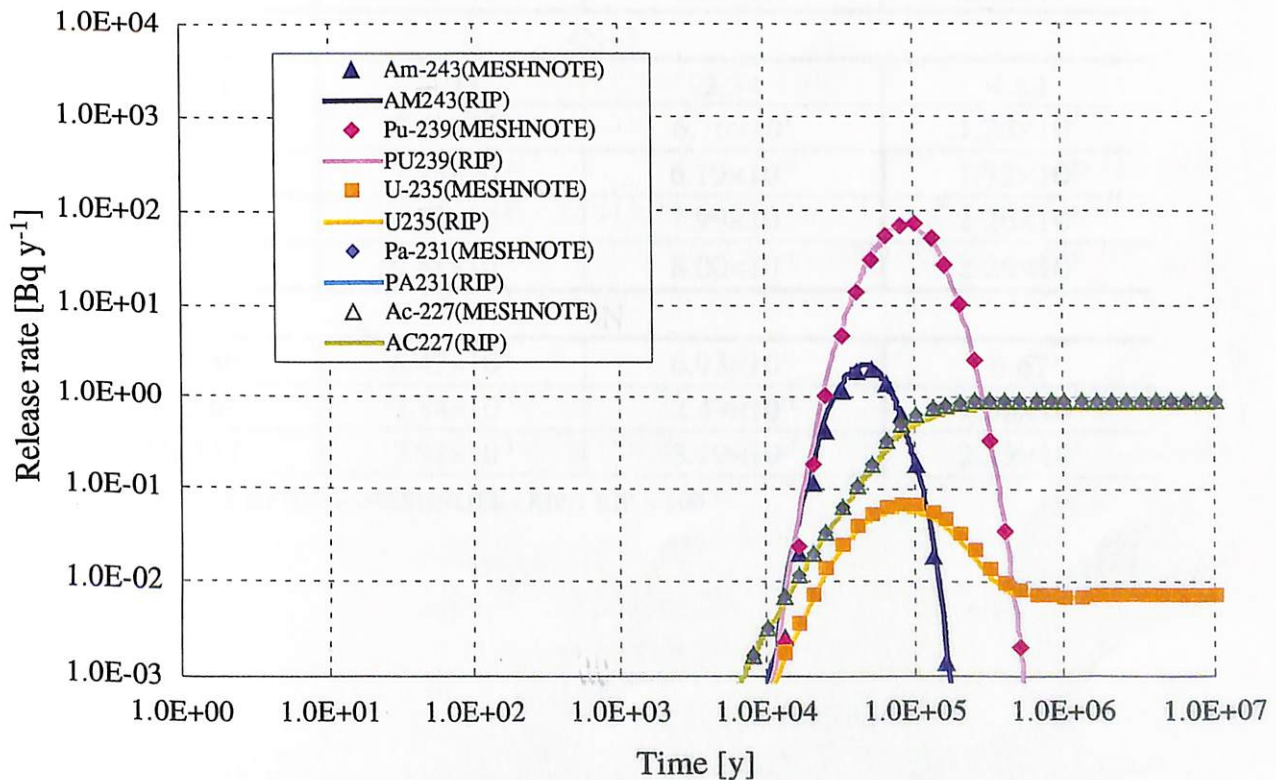


(b) 4N+1 actinide chain

**Figure 4-6 Comparison of release rate from the EBS in verification of multiple chains decay (1/2)**



(c) 4N+2 actinide chain



(d) 4N+3 actinide chain

Figure 4-6 Comparison of release rate from the EBS in verification of multiple chains decay (2/2)

**Table 4-9 Relative error of the maximum release rate in verification of multiple chains decay**

|        | MESHNOTE              | Verification tool     | Relative error [%]*   |
|--------|-----------------------|-----------------------|-----------------------|
|        |                       | RIP                   |                       |
| 4N+1   |                       |                       |                       |
| Cm-245 | $6.41 \times 10^{-2}$ | $6.93 \times 10^{-2}$ | 2.91                  |
| Pu-241 | $6.42 \times 10^{-2}$ | $6.61 \times 10^{-2}$ | 2.91                  |
| Am-241 | $6.77 \times 10^{-2}$ | $6.97 \times 10^{-2}$ | 2.92                  |
| Np-237 | $1.21 \times 10^2$    | $1.21 \times 10^2$    | $3.95 \times 10^{-2}$ |
| U-233  | $2.29 \times 10^1$    | $2.30 \times 10^1$    | $2.44 \times 10^{-1}$ |
| Th-229 | $8.32 \times 10^2$    | $6.83 \times 10^2$    | $2.17 \times 10^1$    |
| 4N+2   |                       |                       |                       |
| Cm-246 | $8.32 \times 10^{-4}$ | $9.69 \times 10^{-4}$ | $1.42 \times 10^1$    |
| Pu-242 | 2.29                  | 1.87                  | $2.22 \times 10^1$    |
| U-238  | $2.19 \times 10^{-2}$ | $2.19 \times 10^{-2}$ | $2.69 \times 10^{-2}$ |
| U-234  | $2.29 \times 10^{-1}$ | $2.54 \times 10^{-1}$ | 9.71                  |
| Th-230 | $4.00 \times 10^1$    | $3.26 \times 10^1$    | $2.25 \times 10^1$    |
| Ra-226 | 8.27                  | 8.26                  | $1.75 \times 10^{-1}$ |
| Pb-210 | $4.00 \times 10^2$    | $3.26 \times 10^2$    | $2.25 \times 10^1$    |
| 4N+3   |                       |                       |                       |
| Am-243 | 2.23                  | 2.34                  | 4.83                  |
| Pu-239 | $7.62 \times 10^1$    | $6.76 \times 10^1$    | $1.28 \times 10^1$    |
| U-235  | $7.25 \times 10^{-2}$ | $6.19 \times 10^{-2}$ | $1.72 \times 10^1$    |
| Pa-231 | $9.80 \times 10^{-1}$ | $7.99 \times 10^{-1}$ | $2.26 \times 10^1$    |
| Ac-227 | $9.81 \times 10^{-1}$ | $8.00 \times 10^{-1}$ | $2.26 \times 10^1$    |
| 4N     |                       |                       |                       |
| Pu-240 | $6.47 \times 10^{-1}$ | $6.93 \times 10^{-1}$ | 6.67                  |
| U-236  | $2.84 \times 10^{-1}$ | $2.49 \times 10^{-1}$ | $1.36 \times 10^1$    |
| Th-232 | $3.92 \times 10^{-3}$ | $3.19 \times 10^{-3}$ | $2.29 \times 10^1$    |

\* Relative error for RIP =  $|\text{MESHNOTE} - \text{RIP}| / \text{RIP} \times 100$

### 4.2.3 Branching and rejoining chains decay

#### (1) Objective

Calculations considering the decay from a single parent nuclide to plural daughter nuclides (branching) and the decay from plural parent nuclides to a single daughter nuclide (rejoining) are performed (see Figure 4-7). To focus on the function to treat branching and rejoining decay processes, we consider the EBS as a tank and calculate the amount of nuclide in the EBS, which is assume that migration is neglected numerically in order to control the release of nuclide from the EBS. The amount of nuclide in the EBS is compared with an analytical solution.

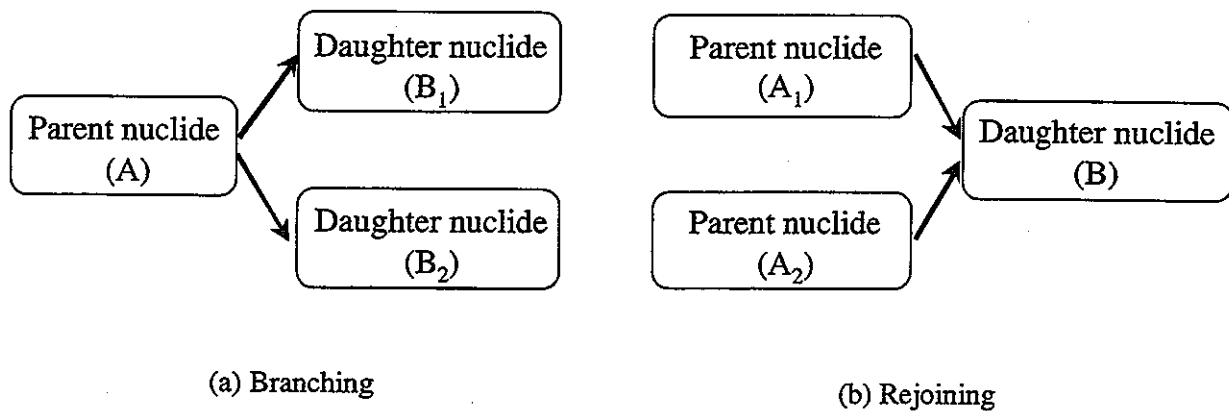


Figure 4-7 Branching and rejoining

#### (2) Analysis condition

We assume the decay from a parent nuclide to two daughter nuclides (branching) and the decay from two different parent nuclides to a daughter nuclide (rejoining). The half lives and inventories for this case are shown in Table 4-10 and 4-11.

Table 4-10 Half lives and inventories (branching)

|                 | Parent nuclide (A)   | Daughter nuclide (B <sub>1</sub> ) | Daughter nuclide (B <sub>2</sub> ) |
|-----------------|--|------------------------------------|------------------------------------|
| Half life [y]   | 1.0×10 <sup>5</sup> (A→B <sub>1</sub> )<br>1.0×10 <sup>6</sup> (A→B <sub>2</sub> ) | 1.0×10 <sup>4</sup>                | 1.0×10 <sup>4</sup>                |
| Inventory [mol] | 10   | 10                                 | 10                                 |

Table 4-11 Half lives and inventories (rejoining)

|                 | Parent nuclide (A <sub>1</sub> ) | Parent nuclide (A <sub>2</sub> ) | Daughter nuclide (B) |
|-----------------|----------------------------------|----------------------------------|----------------------|
| Half life [y]   | 1.0×10 <sup>5</sup>              | 1.0×10 <sup>4</sup>              | 1.0×10 <sup>6</sup>  |
| Inventory [mol] | 10                               | 10                               | 10                   |

To focus on the function to treat branching and rejoining decay behavior, we assume the

hypothetical system not released nuclides from the EBS. Diffusion coefficient in porewater is assumed to be extremely small value in order to control the migration in the EBS and volume flow rate of water through the mixing cell is assumed to be extremely small value in order to control the release from EBS to host rock. The geometry of the EBS, glass dissolution model and other input parameters are assumed to be identical to the condition of calculation case in Section 4.1.1.

The primary input parameters for MESHNOTE code for this case are presented below:

|   |   |                       |                               |
|---|---|-----------------------|-------------------------------|
| Diffusion coefficient in porewater (all nuclides) | : | $1 \times 10^{-10}$   | $[\text{m}^2 \text{y}^{-1}]$  |
| Porosity  | : | 0.41                  | $[-]$                         |
| True density at the buffer material               | : | $1.6 \times 10^5$     | $[\text{kg m}^{-3}]$          |
| Distribution coefficient (all nuclides)           | : | 0.1                   | $[\text{m}^3 \text{kg}^{-1}]$ |
| Solubility (all nuclides)                         | : | $1 \times 10^{10}$    | $[\text{mol m}^{-3}]$         |
| Volume flow rate of water through the mixing cell | : | $1.0 \times 10^{-10}$ | $[\text{m}^3 \text{y}^{-1}]$  |

To avoid the generation of precipitate in the EBS, solubility for all nuclides are assumed large value.

The amount of each nuclide in the buffer is compared with the analytical solution Beteman function given by equations (4-4) ~ (4-9).

### ● Branching

$$N_A = N_A^0 e^{-(\lambda_{AB_1} + \lambda_{AB_2})t} \quad (4-4)$$

$$N_{B_1} = \frac{\lambda_{AB_1}}{\lambda_{B_1} - (\lambda_{AB_1} + \lambda_{AB_2})} N_A^0 (e^{-(\lambda_{AB_1} + \lambda_{AB_2})t} - e^{-\lambda_{B_1}t}) + N_{B_1}^0 e^{-\lambda_{B_1}t} \quad (4-5)$$

$$N_{B_2} = \frac{\lambda_{AB_2}}{\lambda_{B_2} - (\lambda_{AB_1} + \lambda_{AB_2})} N_A^0 (e^{-(\lambda_{AB_1} + \lambda_{AB_2})t} - e^{-\lambda_{B_2}t}) + N_{B_2}^0 e^{-\lambda_{B_2}t} \quad (4-6)$$

|                  |   |                                  |                   |
|------------------|---|----------------------------------|-------------------|
| $N_A$            | : | Amount of parent nuclide A       | $[\text{mol}]$    |
| $N_{B_1}$        | : | Amount of daughter nuclide $B_1$ | $[\text{mol}]$    |
| $N_{B_2}$        | : | Amount of daughter nuclide $B_2$ | $[\text{mol}]$    |
| $N_A^0$          | : | Initial amount of nuclide A      | $[\text{mol}]$    |
| $N_{B_1}^0$      | : | Initial amount of nuclide $B_1$  | $[\text{mol}]$    |
| $N_{B_2}^0$      | : | Initial amount of nuclide $B_2$  | $[\text{mol}]$    |
| $\lambda_{AB_1}$ | : | Decay constant from A to $B_1$   | $[\text{y}^{-1}]$ |
| $\lambda_{AB_2}$ | : | Decay constant from A to $B_2$   | $[\text{y}^{-1}]$ |
| $\lambda_{B_1}$  | : | Decay constant of $B_1$          | $[\text{y}^{-1}]$ |
| $\lambda_{B_2}$  | : | Decay constant of $B_2$          | $[\text{y}^{-1}]$ |
| $t$              | : | Time                             | $[\text{y}]$      |



● Rejoining

$$N_{A_1} = N_{A_1}^0 e^{-\lambda_{A_1 B} t} \quad (4-7)$$

$$N_{A_2} = N_{A_2}^0 e^{-\lambda_{A_2 B} t} \quad (4-8)$$

$$N_B = \frac{\lambda_{A_1 B}}{\lambda_B - \lambda_{A_1 B}} N_{A_1}^0 (e^{-\lambda_{A_1 B} t} - e^{-\lambda_B t}) + \frac{\lambda_{A_2 B}}{\lambda_B - \lambda_{A_2 B}} N_{A_2}^0 (e^{-\lambda_{A_2 B} t} - e^{-\lambda_B t}) + N_B^0 e^{-\lambda_B t} \quad (4-9)$$

|                   |  |                    |
|-------------------|--|--------------------|
| $N_{A_1}$         | : Amount of parent nuclide A <sub>1</sub>  | [mol]              |
| $N_{A_2}$         | : Amount of parent nuclide A <sub>2</sub>  | [mol]              |
| $N_B$             | : Amount of daughter nuclide B             | [mol]              |
| $N_{A_1}^0$       | : Initial amount of nuclide A <sub>1</sub> | [mol]              |
| $N_{A_2}^0$       | : Initial amount of nuclide A <sub>2</sub> | [mol]              |
| $N_B^0$           | : Initial amount of nuclide B              | [mol]              |
| $\lambda_{A_1 B}$ | : Decay constant from A <sub>1</sub> to B  | [y <sup>-1</sup> ] |
| $\lambda_{A_2 B}$ | : Decay constant from A <sub>2</sub> to B  | [y <sup>-1</sup> ] |
| $\lambda_B$       | : Decay constant of B                      | [y <sup>-1</sup> ] |

### (3) Result

The amounts of nuclide in the EBS in the branching case and the rejoining case are shown in Figure 4-8 and 4-9 respectively.

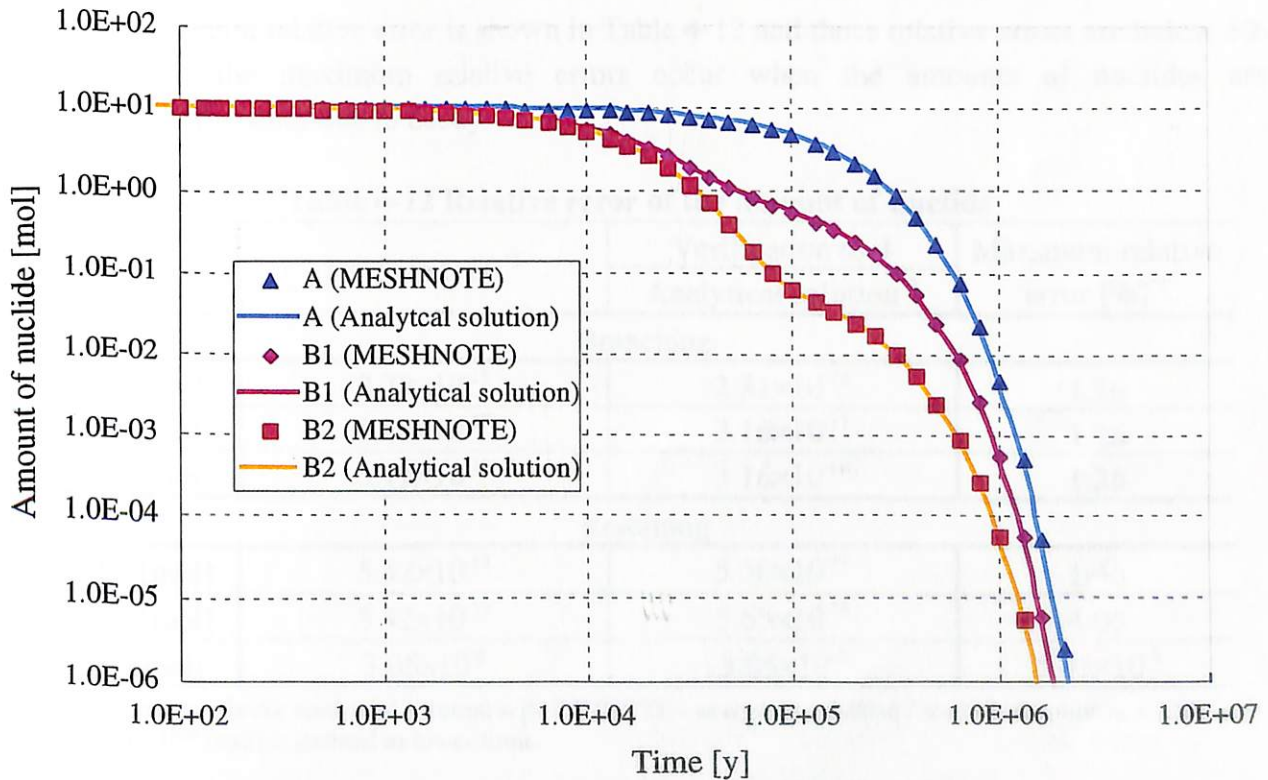


Figure 4-8 Comparison of nuclide amount in the EBS for the branching case

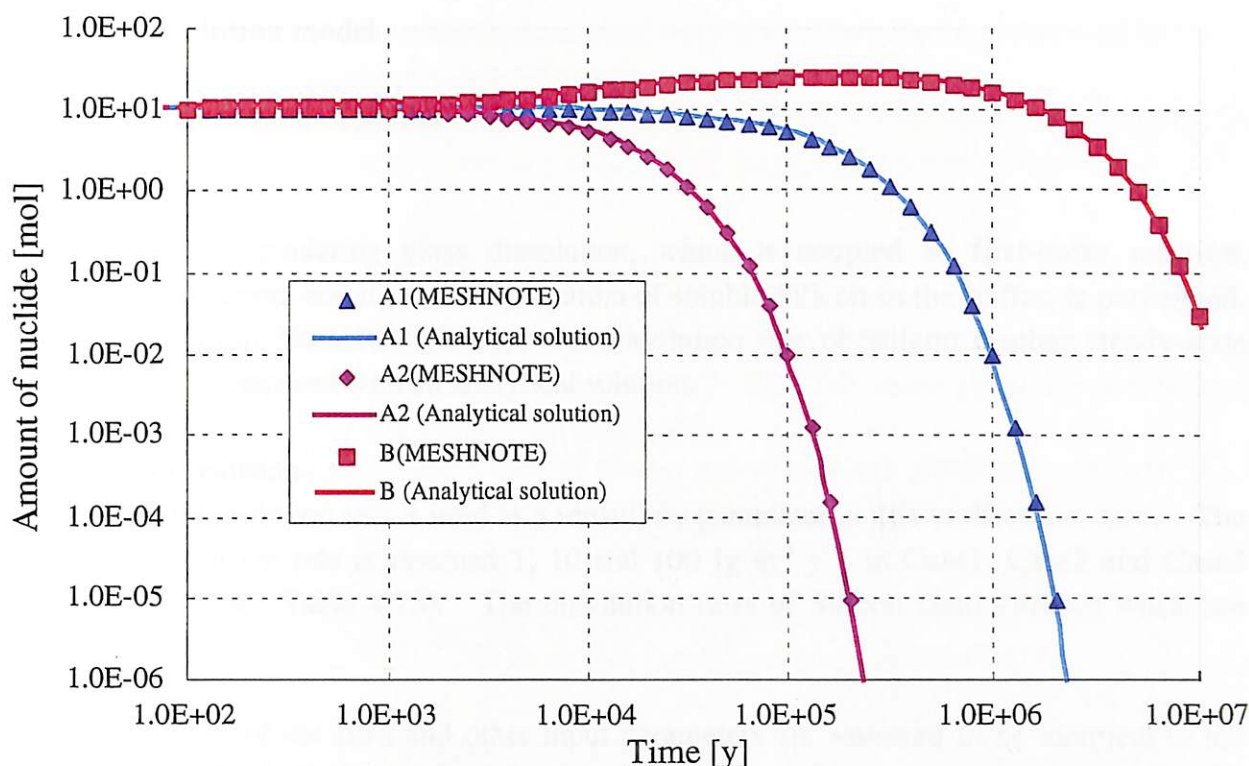


Figure 4-9 Comparison of nuclides amount in the EBS for the rejoining case

The amount of nuclides calculated by MESHNOTE and by the analytical solutions are quite consistent.

The maximum relative error is shown in Table 4-12 and these relative errors are below 5%. However, the maximum relative errors occur when the amounts of nuclides are significantly small due to decay.

Table 4-12 Relative error of the amount of nuclide

|           | MESHNOTE*2             | Verification tool      | Maximum relative error [%]*1 |
|-----------|------------------------|------------------------|------------------------------|
|           |                        | Analytical solution*2  |                              |
| Branching |                        |                        |                              |
| A [mol]   | 2.78×10 <sup>-16</sup> | 2.81×10 <sup>-16</sup> | 1.26                         |
| B1 [mol]  | 3.12×10 <sup>-17</sup> | 3.16×10 <sup>-17</sup> | 1.26                         |
| B2 [mol]  | 3.12×10 <sup>-18</sup> | 3.16×10 <sup>-18</sup> | 1.26                         |
| Rejoining |                        |                        |                              |
| A1 [mol]  | 5.42×10 <sup>-19</sup> | 5.50×10 <sup>-19</sup> | 1.46                         |
| A2 [mol]  | 5.42×10 <sup>-19</sup> | 5.65×10 <sup>-19</sup> | 4.05                         |
| B [mol]   | 3.05×10 <sup>-2</sup>  | 3.05×10 <sup>-2</sup>  | 5.05×10 <sup>-2</sup>        |

\*1 Relative error for analytical solution =  $|\text{MESHNOTE} - \text{analytical solution}| / \text{analytical solution} \times 100$

\*2  $1.0 \times 10^{-20}$  [mol] is defined as lower limit.



### 4.3 Glass dissolution model

#### 4.3.1 First-order reaction model

##### (1) Objective

Calculations considering glass dissolution, which is coupled to first-order reaction, hydration reaction, and diffusion/dissipation of soluble Silicon in the buffer, is performed. The result from MESHONTE when the dissolution rate of Silicon reaches steady-state condition is compared with an analytical solution.

##### (2) Analysis condition

The initial dissolution rate is used as a sensitivity parameter in this verification case. The initial dissolution rate is assumed 1, 10 and 100  $[\text{g m}^{-2} \text{y}^{-1}]$  in Case1, Case2 and Case3 respectively (see Table 4-13). The dissolution rates of Silicon from vitrified waste are calculated.

The geometry of the EBS and other input parameters are assumed to be identical to the conditions of calculation case of Section 4.1.1. The primary input parameters for the MESHNOTE code for this case are presented below:

|   |   |                      |                                   |
|---|---|----------------------|-----------------------------------|
| Hydration rate                                    | : | 1                    | $[\text{g m}^{-2} \text{y}^{-1}]$ |
| Initial inventory of Silicon                      | : | 3090                 | $[\text{mol}]$                    |
| Diffusion coefficient of Silicon                  | : | $3 \times 10^{-2}$   | $[\text{m}^2 \text{y}^{-1}]$      |
| Distribution coefficient of Silicon               | : | 0.01                 | $[\text{m}^3 \text{kg}^{-1}]$     |
| Solubility of Silicon                             | : | 10                   | $[\text{mol m}^{-3}]$             |
| Surface area of vitrified waste                   | : | 17                   | $[\text{m}^2]$                    |
| Volume of vitrified waste                         | : | 0.15                 | $[\text{m}^3]$                    |
| Density of vitrified waste                        | : | $2.75 \times 10^6$   | $[\text{g m}^{-3}]$               |
| Volume flow rate of water through the mixing cell | : | $1.0 \times 10^{10}$ | $[\text{m}^3 \text{y}^{-1}]$      |

**Table 4-13 Initial dissolution rate data**

|        | Initial dissolution rate $[\text{g m}^{-2} \text{y}^{-1}]$ |
|--------|--|
| Case 1 | 1  |
| Case 2 | 10   |
| Case 3 | 100  |

The dissolution rate of Silicon from the vitrified waste at steady state is compared to the steady-state analytical solution. The derivation of the analytical solution coupled of the migration of Silicon in the buffer and the glass dissolution under steady-state is described below.

● **The analytical solution of dissolution rate of Silicon under steady-state**

The release rate of Silicon from the EBS, when the glass dissolution rate is steady-state, is given by equation (4-10) applying to equation (4-1):

$$f_{Si}^{Buffer \rightarrow Hostrock} = 2\pi L \epsilon^B D p_{Si} C_{Si}^S \frac{1}{\ln(r_{out}/r_{in})}, \quad (4-10)$$

where  $C_{Si}^S$  is the concentration of dissolved Silicon at reservoir under the steady-state.

On the other hand, the dissolution rate of Silicon from vitrified waste to reservoir is given by equation (4-11) applying to equation (2-30):

$$f_{Si}^{Glass \rightarrow Buffer} = \left[ k^+ \left( 1 - \frac{C_{Si}^R}{C_{Si}^*} \right) + k_r \right] \frac{a^{Glass}}{\rho^{Glass} V^{Glass}} A_{Si}, \quad (4-11)$$

where  $A_{Si}$  represents the total amount of Silicon in the glass.

If the dissolution of Silicon from the vitrified waste and the migration of Silicon in the buffer are at steady-state,  $f_{Si}^{Buffer \rightarrow Hostrock}$  in the equation (4-10) is equal to  $f_{Si}^{Glass \rightarrow Buffer}$  in which allows substitution of  $C_{Si}^S$  for  $C_{Si}^R$ . Therefor we can solve the simultaneous equations (4-10) and (4-11) to derive  $C_{Si}^R$ , then the dissolution rate of Silicon from the vitrified waste (the steady-state dissolution rate :  $f_{Si}^S$ ) is given by:

$$f_{Si}^S = \frac{(k^+ + k_r) \psi}{\psi \frac{\rho^{Glass} V^{Glass}}{a^{Glass} A_{Si}} + \frac{k^+}{C_{Si}^*}}. \quad (4-12)$$

where  $\psi$  is defined as:

$$\psi = \frac{2\pi L \epsilon^B D p_{Si}}{\ln(r_{out}/r_{in})}. \quad (4-13)$$

### (3) Result

The dissolution rates of Silicon calculated by MESHNOTE and analytical solution of dissolution of Silicon are shown in Figure 4-10.

The following observations are made regarding the time-dependence dissolution rate of Silicon calculated by MESHNOTE.

- Until 100 years after start of dissolution, the dissolution rates of Silicon in the Case2 and Case3 are not in the steady-state. This reason is that the initial dissolution rate is dominant to glass dissolution rate during this period than the migration of Silicon.

The dissolution rates in these cases reach steady-state when the glass dissolution and migration of Silicon are balanced.

- On the other hand, the dissolution rate in Case1 reaches steady-state slowly, although the difference between the dissolution rate and steady-state are very small.

The dissolution rate of Silicon can be compared with the analytical solution when the dissolution rate of Silicon is equal to the release rate of Silicon from the buffer. The results from MESHNOTE and the analytical solution are quite consistent in Figure 4-10. The dissolution rates of Silicon calculated by MESHNOTE in all cases decrease sharply in order to completely dissolve the vitrified waste.

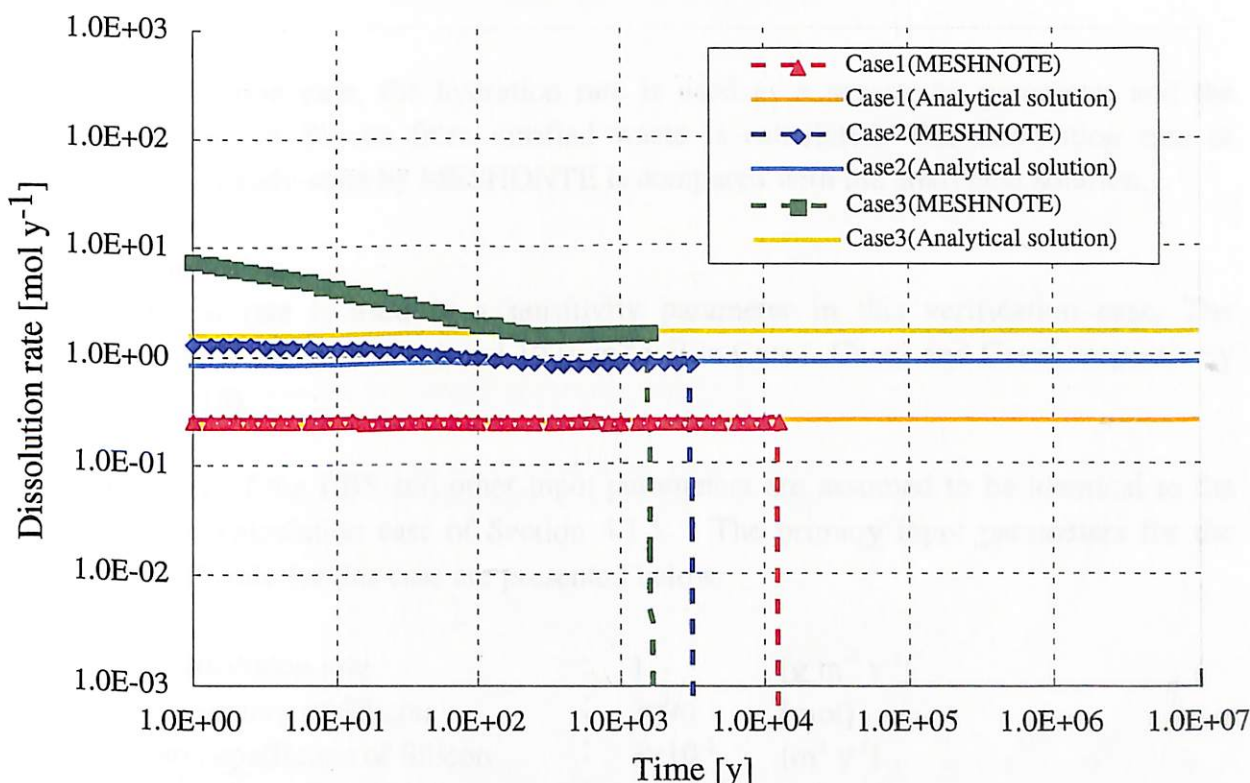


**Figure 4-10 Comparison of dissolution rate of Silicon from the vitrified waste (verification of initial dissolution rate)**

The relative errors between dissolution rate of Silicon calculated by MESHNOTE under steady-state and that by analytical solution are shown in Table 4-14. All relative errors are less than 1 %.

**Table 4-14 Relative error of the dissolution rate of Silicon**  
(verification of initial dissolution rate)

|                               | MESHNOTE              | Verification tool     | Relative error* %     |
|-------------------------------|-----------------------|-----------------------|-----------------------|
|                               |                       | Analytical solution   |                       |
| Case 1 [mol y <sup>-1</sup> ] | 2.37×10 <sup>-1</sup> | 2.37×10 <sup>-1</sup> | 1.85×10 <sup>-2</sup> |
| Case 2 [mol y <sup>-1</sup> ] | 7.96×10 <sup>-1</sup> | 7.96×10 <sup>-1</sup> | 3.82×10 <sup>-1</sup> |
| Case 3 [mol y <sup>-1</sup> ] | 1.50                  | 1.50                  | 7.97×10 <sup>-1</sup> |

\* Relative error = |MESHNOTE - analytical solution| / analytical solution × 100

### 4.3.2 Hydration reaction model

#### (1) Objective

In this verification case, the hydration rate is used as a sensitivity parameter and the dissolution rate of Silicon from vitrified waste is calculated. The dissolution rate of Silicon under steady-state by MESHONTE is compared with the analytical solution.

#### (2) Analysis condition

The hydration rate is used as a sensitivity parameter in this verification case. The hydration rate is assumed 0.1, 1 and 10 [g m<sup>-2</sup> y<sup>-1</sup>] in Case1, Case2 and Case3 respectively (see Table 4-15).

The geometry of the EBS and other input parameters are assumed to be identical to the conditions of calculation case of Section 4.1.1. The primary input parameters for the MESHNOTE code for this case are presented below:

|   |   |                      |                                      |
|---|---|----------------------|--------------------------------------|
| Initial dissolution rate                          | : | 1                    | [g m <sup>-2</sup> y <sup>-1</sup> ] |
| Initial inventory of Silicon                      | : | 3090                 | [mol]                                |
| Diffusion coefficient of Silicon                  | : | 3×10 <sup>-2</sup>   | [m <sup>2</sup> y <sup>-1</sup> ]    |
| Distribution coefficient of Silicon               | : | 0.01                 | [m <sup>3</sup> kg <sup>-1</sup> ]   |
| Solubility of Silicon                             | : | 10                   | [mol m <sup>-3</sup> ]               |
| Surface area of vitrified waste                   | : | 17                   | [m <sup>2</sup> ]                    |
| Volume of vitrified waste                         | : | 0.15                 | [m <sup>3</sup> ]                    |
| Density of vitrified waste                        | : | 2.75×10 <sup>6</sup> | [g m <sup>-3</sup> ]                 |
| Volume flow rate of water through the mixing cell | : | 1.0×10 <sup>10</sup> | [m <sup>3</sup> y <sup>-1</sup> ]    |

**Table 4-15 Hydration rate data**

|        | Hydration rate [g m <sup>-2</sup> y <sup>-1</sup> ] |
|--------|---|
| Case 1 | 0.1   |
| Case 2 | 1   |
| Case 3 | 10  |

The dissolution rate of Silicon from the vitrified waste under steady-state is compared to the steady-state analytical solution shown in equation (4-12).

### (3) Result

The dissolution rate of Silicon calculated by MESHNOTE and that by analytical solution are shown in Figure 4-11.

The dissolution rate of Silicon can be compared with the analytical solutions (equation (4-12)). The results from MESHNOTE and analytical solution are quite consistent in Figure 4-11. The dissolution rates of Silicon calculated by MESHNOTE in all cases decrease sharply in order to completely dissolve the vitrified waste.

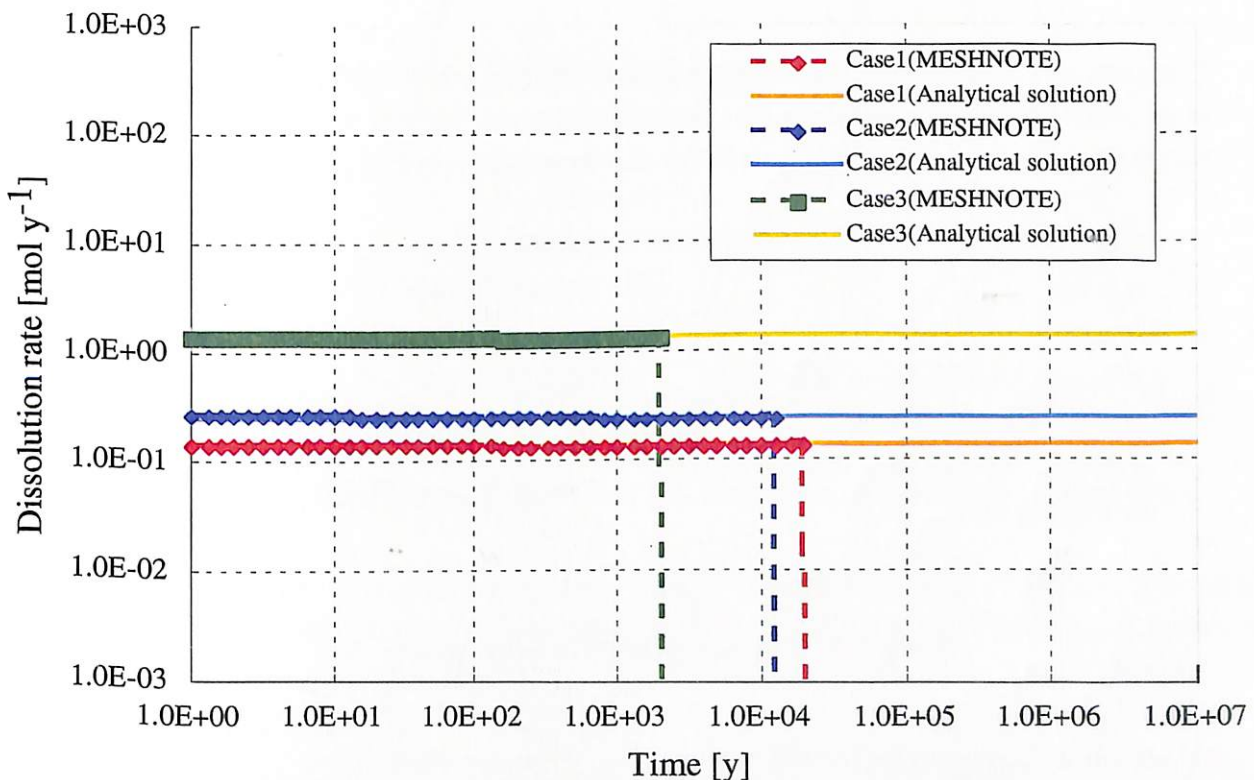


**Figure 4-11 Comparison of dissolution rate of Silicon from the vitrified waste (verification of hydration rate)**

The relative errors between dissolution rate of Silicon calculated by MESHNOTE under steady-state and that by analytical solution are shown in Table 4-16. All relative errors are less than 1 %.

**Table 4-16 Relative error of the dissolution rate of Silicon**  
**(verification of hydration rate)**

|                               | MESHNOTE              | Verification tool     | Relative error* %     |
|-------------------------------|-----------------------|-----------------------|-----------------------|
|                               |                       | Analytical solution   |                       |
| Case 1 [mol y <sup>-1</sup> ] | 1.30×10 <sup>-1</sup> | 1.30×10 <sup>-1</sup> | 1.47×10 <sup>-2</sup> |
| Case 2 [mol y <sup>-1</sup> ] | 2.37×10 <sup>-1</sup> | 2.37×10 <sup>-1</sup> | 1.85×10 <sup>-2</sup> |
| Case 3 [mol y <sup>-1</sup> ] | 1.30                  | 1.30                  | 1.47×10 <sup>-2</sup> |

\* Relative error = |MESHNOTE - analytical solution| / analytical solution × 100

#### 4.4 Time dependent parameter

##### 4.4.1 Solubility

###### (1) Objective

Calculations for the migration of nuclide with time-dependence solubility accounting to basic migration processes (decay, linear sorption, diffusion and solubility limit) in the EBS are performed. The MESHNOTE result is compared with the result of RIP.

###### (2) Analysis condition

The solubility is used as a sensitivity parameter in this verification case. The solubility of Tc is changed at 10,000 years from an initial value of  $4 \times 10^{-5}$  [mol m<sup>-3</sup>] to both a value of  $4 \times 10^{-4}$  [mol m<sup>-3</sup>] and  $4 \times 10^{-6}$  [mol m<sup>-3</sup>] (see Table 4-17).

The geometry of the EBS, glass dissolution model and other input parameters are assumed to be identical to the conditions of calculation case of Section 4.1.1. The primary input parameters for the MESHNOTE code for this case are presented below:

|   |   |  |
|---|---|--|
| Nuclide   | : | Tc-99  |
| Half life   | : | $2.13 \times 10^5$ [y]                                 |
| Inventory   | : | 8.27 [mol]   |
| Diffusion coefficient in porewater                | : | $3 \times 10^{-2}$ [m <sup>2</sup> y <sup>-1</sup> ]   |
| Distribution coefficient                          | : | 0.1 [m <sup>3</sup> kg <sup>-1</sup> ]                 |
| Volume flow rate of water through the mixing cell | : | $1.0 \times 10^{10}$ [m <sup>3</sup> y <sup>-1</sup> ] |

**Table 4-17 Time-dependence of solubility (Tc)**

|                             | Solubility of Tc [mol m <sup>-3</sup> ] |                                |
|-----------------------------|---|--------------------------------|
|                             | 0 ~ 10,000 [y]                          | 10,000 ~ $1.0 \times 10^7$ [y] |
| Case 1                      | $4 \times 10^{-5}$                      | $4 \times 10^{-4}$             |
| Case 2 (no time-dependence) | $4 \times 10^{-5}$                      | $4 \times 10^{-5}$             |
| Case 3                      | $4 \times 10^{-5}$                      | $4 \times 10^{-6}$             |

###### (3) Result

The release rates calculated by MESHNOTE, which is taken into account time-dependence solubility are shown in Figure 4-12. The release rate of Case1 increases sharply. Then its release rate is limited by a new solubility value, and the new steady-state condition is confirmed. The depletion time in the Case 1 is shorter than that of time Case 2 since the outflow amount from the EBS increases by the change of solubility.

The release rate of the Case3 decreases following the change of solubility and transition of



new steady-state condition is confirmed.

The release rates calculated by MESHNOTE can be compared with the RIP's results in the Figure 4-12. The results of MESHNOTE and RIP are consistent.

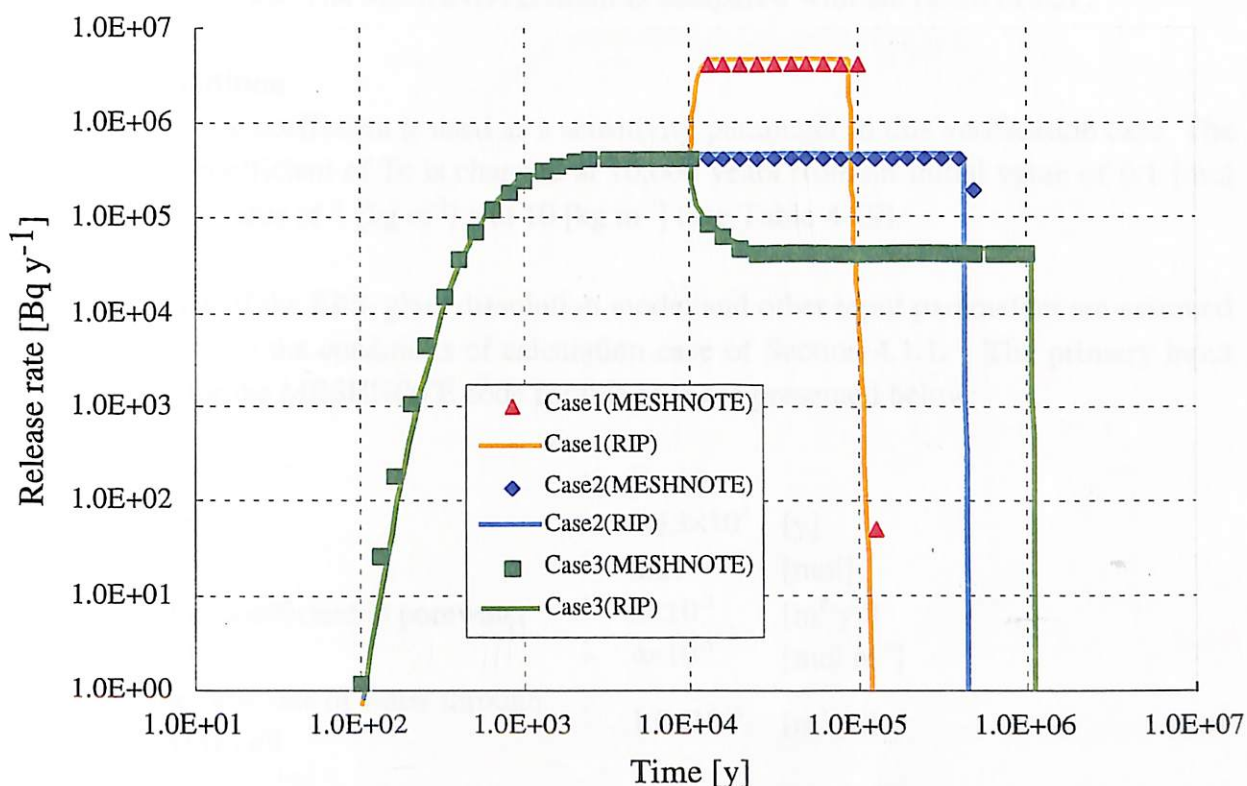


**Figure 4-12 Comparison of release rate from the EBS for time dependent solubility**

Release rates under new steady-state after change of solubility at 10,000 years, calculated by MESHNOTE are compared with those of RIP in Table 4-18. The relative errors of MESHNOTE to RIP are less than 3 %.

**Table 4-18 Relative error of the release rate from the EBS for time dependent solubility**

|                              | MESHNOTE <sup>*1</sup> | Verification tool <sup>*1</sup> | Relative error <sup>*2</sup> % |
|------------------------------|------------------------|---------------------------------|--------------------------------|
|                              |                        | RIP                             |                                |
| Case 1 [Bq y <sup>-1</sup> ] | 4.15×10 <sup>6</sup>   | 4.26×10 <sup>6</sup>            | 2.64                           |
| Case 2 [Bq y <sup>-1</sup> ] | 4.15×10 <sup>5</sup>   | 4.26×10 <sup>5</sup>            | 2.69                           |
| Case 3 [Bq y <sup>-1</sup> ] | 4.15×10 <sup>4</sup>   | 4.26×10 <sup>4</sup>            | 2.73                           |

<sup>\*1</sup> Release rates under the steady-state after change of solubility at 10,000 years

<sup>\*2</sup> Relative error for RIP =  $|\text{MESHNOTE} - \text{RIP}| / \text{RIP} \times 100$



#### 4.4.2 Sorption constant

##### (1) Objective

Calculations for the migration of nuclide with time-dependence sorption accounting to basic migration processes (decay, linear sorption, diffusion and solubility limit) in the EBS are performed. The MESHNOTE result is compared with the result of RIP.

##### (2) Analysis condition

The distribution coefficient is used as a sensitivity parameter in this verification case. The distribution coefficient of Tc is changed at 10,000 years from an initial value of 0.1 [ $\text{mol m}^{-3}$ ] to both a value of 1 [ $\text{kg m}^{-3}$ ] and 10 [ $\text{kg m}^{-3}$ ] (see Table 4-19).

The geometry of the EBS, glass dissolution model and other input parameters are assumed to be identical to the conditions of calculation case of Section 4.1.1. The primary input parameters for the MESHNOTE code for this case are presented below:

|   |   |   |
|---|---|---|
| Nuclide   | : | Tc-99   |
| Half life   | : | $2.13 \times 10^5$ [y]                              |
| Inventory   | : | 8.27 [mol]  |
| Diffusion coefficient in porewater                | : | $3 \times 10^{-2}$ [ $\text{m}^2 \text{y}^{-1}$ ]   |
| Solubility  | : | $4 \times 10^{-5}$ [ $\text{mol m}^{-3}$ ]          |
| Volume flow rate of water through the mixing cell | : | $1.0 \times 10^{10}$ [ $\text{m}^3 \text{y}^{-1}$ ] |

**Table 4-19 Time-dependence of distribution coefficient (Tc)**

|                            | Distribution coefficient of Tc [ $\text{kg m}^{-3}$ ] |                                |
|----------------------------|---|--------------------------------|
|                            | 0 ~ 10,000 [y]  | 10,000 ~ $1.0 \times 10^7$ [y] |
| Case 1(no time-dependence) | 0.1   | 0.1                            |
| Case 2                     | 0.1   | 1                              |
| Case 3                     | 0.1   | 10                             |

##### (3) Result

The release rates calculated by MESHNOTE taking into account time-dependence distribution coefficients are shown in Figure 4-13. Release rates decrease inversely proportional to their increase of distribution coefficients since the dissolved nuclide in the porewater of the buffer is sorbed on the buffer with increase of distribution coefficient.

In the case2, the release rate at 10,000 years decreases sharply once, but then recovers to steady-state. In the case3, the release rate after 10,000 years doesn't reach the steady-state.

The release rates calculated by MESHNOTE are compared with RIP's results in the

Figure 4-13. The results of MESHNOTE and RIP are consistent.

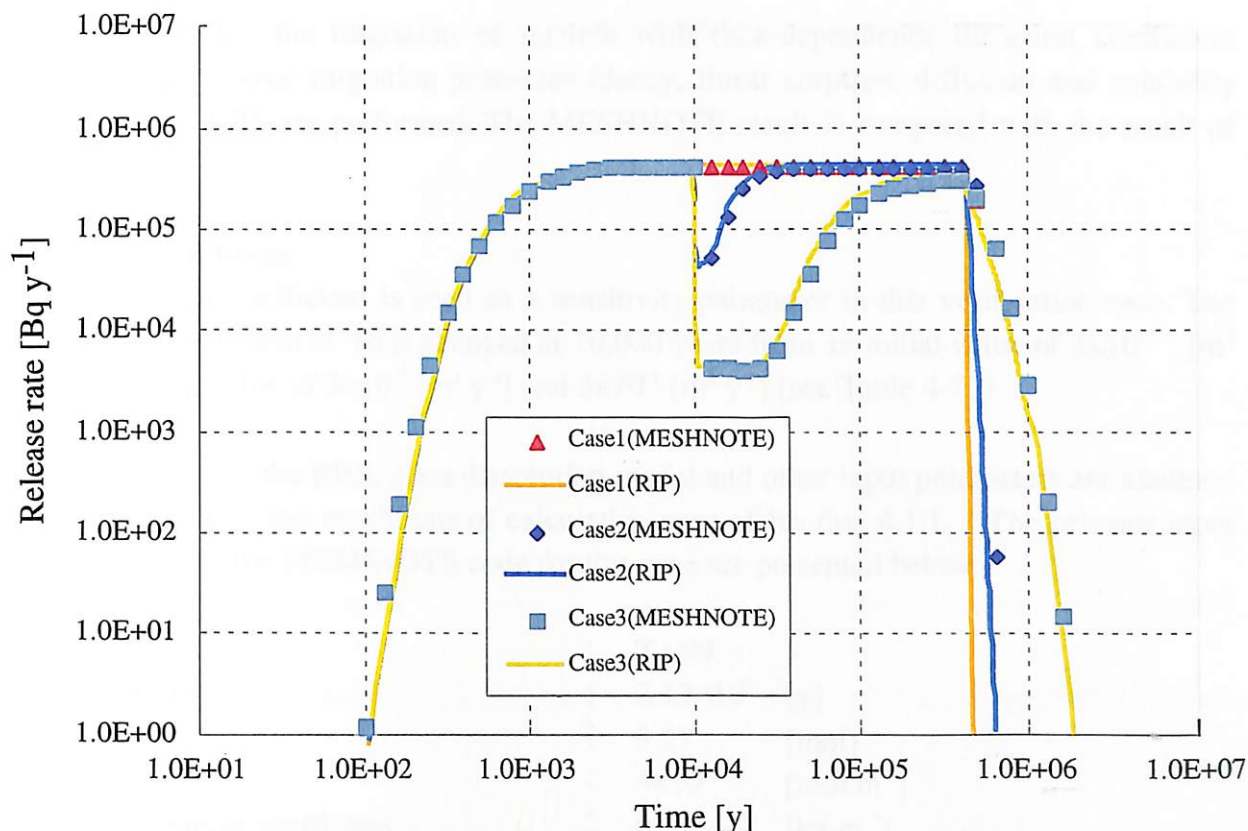


Figure 4-13 Comparison of release rate from the EBS for time dependent distribution coefficient

The maximum release rates after change of distribution coefficients at 10,000 years, that is calculated by MESHNOTE are compared with those of RIP in Table 4-20. The relative errors of MESHNOTE to RIP are less than 7 %.

Table 4-20 Relative error of the release rate from the EBS for time dependent distribution coefficient

|                              | MESHNOTE <sup>*1</sup> | Verification tool <sup>*1</sup> | Relative error <sup>*2</sup> % |
|------------------------------|------------------------|---------------------------------|--------------------------------|
|                              |                        | RIP                             |                                |
| Case 1 [Bq y <sup>-1</sup> ] | 4.15×10 <sup>5</sup>   | 4.26×10 <sup>5</sup>            | 2.71                           |
| Case 2 [Bq y <sup>-1</sup> ] | 4.02×10 <sup>5</sup>   | 4.14×10 <sup>5</sup>            | 2.90                           |
| Case 3 [Bq y <sup>-1</sup> ] | 2.93×10 <sup>5</sup>   | 3.12×10 <sup>5</sup>            | 6.09                           |

<sup>\*1</sup> Maximum release rates after change of distribution coefficients at 10,000 years.

<sup>\*2</sup> Relative error for RIP =  $|\text{MESHNOTE} - \text{RIP}| / \text{RIP} \times 100$

### 4.4.3 Diffusion coefficient

#### (1) Objective

Calculations for the migration of nuclide with time-dependence diffusion coefficient accounting to basic migration processes (decay, linear sorption, diffusion and solubility limit) in the EBS are performed. The MESHNOTE result is compared with the result of RIP.

#### (2) Analysis condition

The diffusion coefficient is used as a sensitivity parameter in this verification case. The diffusion coefficient of Tc is changed at 10,000 years from an initial value of  $3 \times 10^{-2}$  [ $\text{m}^2 \text{y}^{-1}$ ] to both a value of  $3 \times 10^{-3}$  [ $\text{m}^2 \text{y}^{-1}$ ] and  $3 \times 10^{-1}$  [ $\text{m}^2 \text{y}^{-1}$ ] (see Table 4-21).

The geometry of the EBS, glass dissolution model and other input parameters are assumed to be identical to the conditions of calculation case of Section 4.1.1. The primary input parameters for the MESHNOTE code for this case are presented below:

|   |   |   |
|---|---|---|
| Nuclide   | : | Tc-99   |
| Half life   | : | $2.13 \times 10^5$ [y]                              |
| Inventory   | : | 8.27 [mol]  |
| Solubility  | : | $4 \times 10^{-5}$ [ $\text{mol m}^{-3}$ ]          |
| Distribution coefficient                          | : | 0.1 [ $\text{kg m}^{-3}$ ]                          |
| Volume flow rate of water through the mixing cell | : | $1.0 \times 10^{10}$ [ $\text{m}^3 \text{y}^{-1}$ ] |

**Table 4-21 Time-dependence of diffusion coefficient (Tc)**

|                            | Diffusion coefficient of Tc [ $\text{m}^2 \text{y}^{-1}$ ] |                                |
|----------------------------|--|--------------------------------|
|                            | 0 ~ 10,000 [y]   | 10,000 ~ $1.0 \times 10^7$ [y] |
| Case 1                     | $3 \times 10^{-2}$   | $3 \times 10^{-3}$             |
| Case 2(no time-dependence) | $3 \times 10^{-2}$   | $3 \times 10^{-2}$             |
| Case 3                     | $3 \times 10^{-2}$   | $3 \times 10^{-1}$             |

#### (3) Result

The release rates calculated by MESHNOTE, which is taken into account time-dependence of diffusion coefficient, are shown in Figure 4-14. Release rates changed proportion to their diffusion coefficients since the steady-state release rate is proportion to the diffusion coefficient (see equation 4-1). Then their release rates after 10,000 years are reached new steady-state.

The release rates calculated by MESHNOTE are compared with RIP's results in the Figure 4-14. The results of MESHNOTE and RIP are consistent.

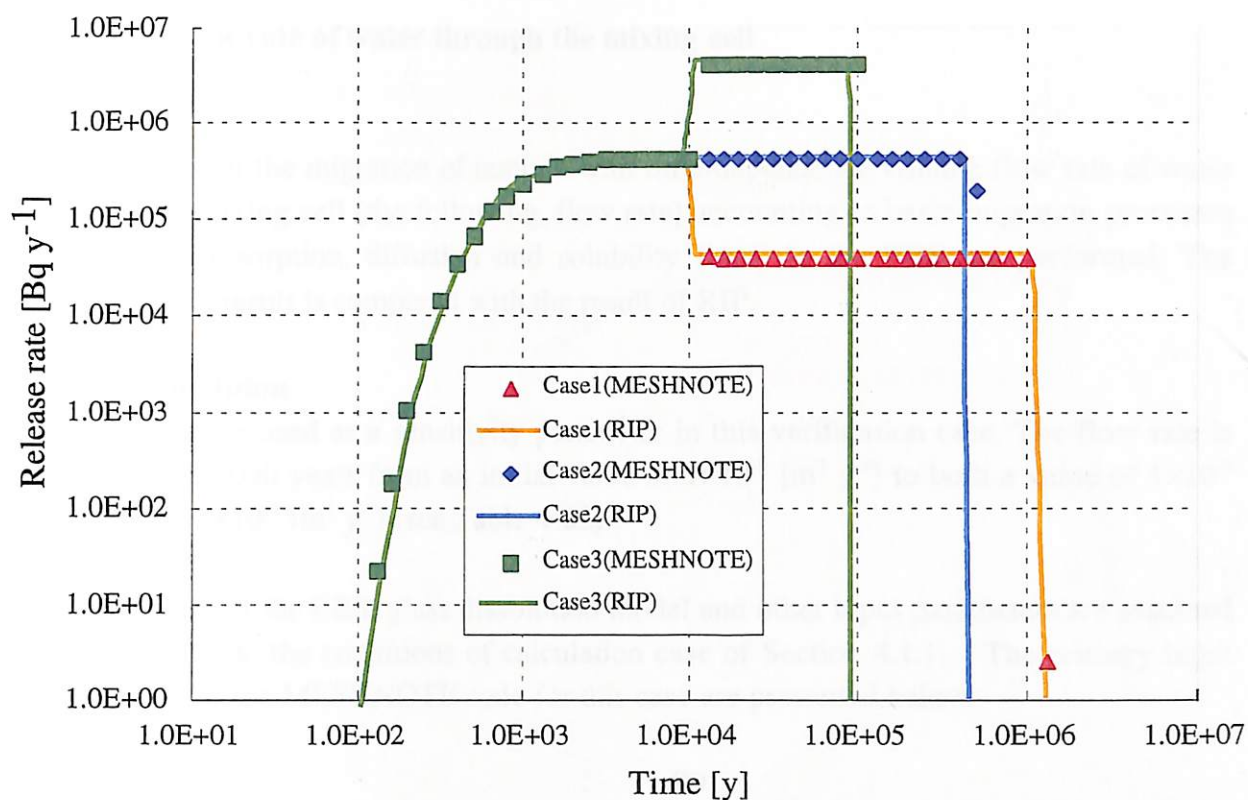


**Figure 4-14 Comparison of release rate from the EBS for time dependent diffusion coefficient**

The release rates under the new steady-state calculated by MESHNOTE after the change of diffusion coefficients at 10,000 years are compared with those of RIP in Table 4-22. The relative errors of MESHNOTE to RIP are less than 3 %.

**Table 4-22 Relative error of the release rate from the EBS for time dependent diffusion coefficient**

|                              | MESHNOTE* <sup>1</sup> | Verification tool* <sup>1</sup> | Relative error* <sup>2</sup> % |
|------------------------------|------------------------|---------------------------------|--------------------------------|
|                              |                        | RIP                             |                                |
| Case 1 [Bq y <sup>-1</sup> ] | 4.11×10 <sup>4</sup>   | 4.15×10 <sup>4</sup>            | 1.07                           |
| Case 2 [Bq y <sup>-1</sup> ] | 4.15×10 <sup>5</sup>   | 4.26×10 <sup>5</sup>            | 2.70                           |
| Case 3 [Bq y <sup>-1</sup> ] | 4.16×10 <sup>6</sup>   | 4.28×10 <sup>6</sup>            | 2.77                           |

\*1 Release rates under the steady-state after change of diffusion coefficient at 10,000 years

\*2 Relative error for RIP =  $|\text{MESHNOTE} - \text{RIP}| / \text{RIP} \times 100$

#### 4.4.4 Volume flow rate of water through the mixing cell

##### (1) Objective

Calculations for the migration of nuclide with time-dependence volume flow rate of water through the mixing cell (the following, flow rate) accounting to basic migration processes (decay, linear sorption, diffusion and solubility limit) in the EBS are performed. The MESHNOTE result is compared with the result of RIP.

##### (2) Analysis condition

The flow rate is used as a sensitivity parameter in this verification case. The flow rate is changed at 10,000 years from an initial value of  $1 \times 10^{-3} \text{ [m}^3 \text{ y}^{-1}\text{]}$  to both a value of  $1 \times 10^{-4} \text{ [m}^3 \text{ y}^{-1}\text{]}$  and  $1 \times 10^{-2} \text{ [m}^3 \text{ y}^{-1}\text{]}$  (see Table 4-23).

The geometry of the EBS, glass dissolution model and other input parameters are assumed to be identical to the conditions of calculation case of Section 4.1.1. The primary input parameters for the MESHNOTE code for this case are presented below:

|                          |   |  |
|--------------------------|---|--|
| Nuclide                  | : | Tc-99  |
| Half life                | : | $2.13 \times 10^5 \text{ [y]}$                         |
| Inventory                | : | 8.27 [mol]   |
| Solubility               | : | $4 \times 10^{-5} \text{ [mol m}^{-3}\text{]}$         |
| Distribution coefficient | : | 0.1 [kg m <sup>-3</sup> ]                              |
| Diffusion coefficient    | : | $3 \times 10^{-2} \text{ [m}^2 \text{ y}^{-1}\text{]}$ |

**Table 4-23 Time-dependence of volume flow rate of water through the mixing cell**

|                            | Volume flow rate of water through the mixing cell [m <sup>3</sup> y <sup>-1</sup> ] |                                |
|----------------------------|---|--------------------------------|
|                            | 0 ~ 10,000 [y]  | 10,000 ~ $1.0 \times 10^7$ [y] |
| Case 1                     | $1 \times 10^{-3}$  | $1 \times 10^{-4}$             |
| Case 2(no time-dependence) | $1 \times 10^{-3}$  | $1 \times 10^{-3}$             |
| Case 3                     | $1 \times 10^{-3}$  | $1 \times 10^{-2}$             |

##### (3) Result

The release rates calculated by MESHNOTE, which is taken into account time-dependence of flow rate, are shown in Figure 4-15. Release rates changed proportion to the flow rate since the release rate from the buffer into the host rock is depended on the flow rate (see equation 2-35).



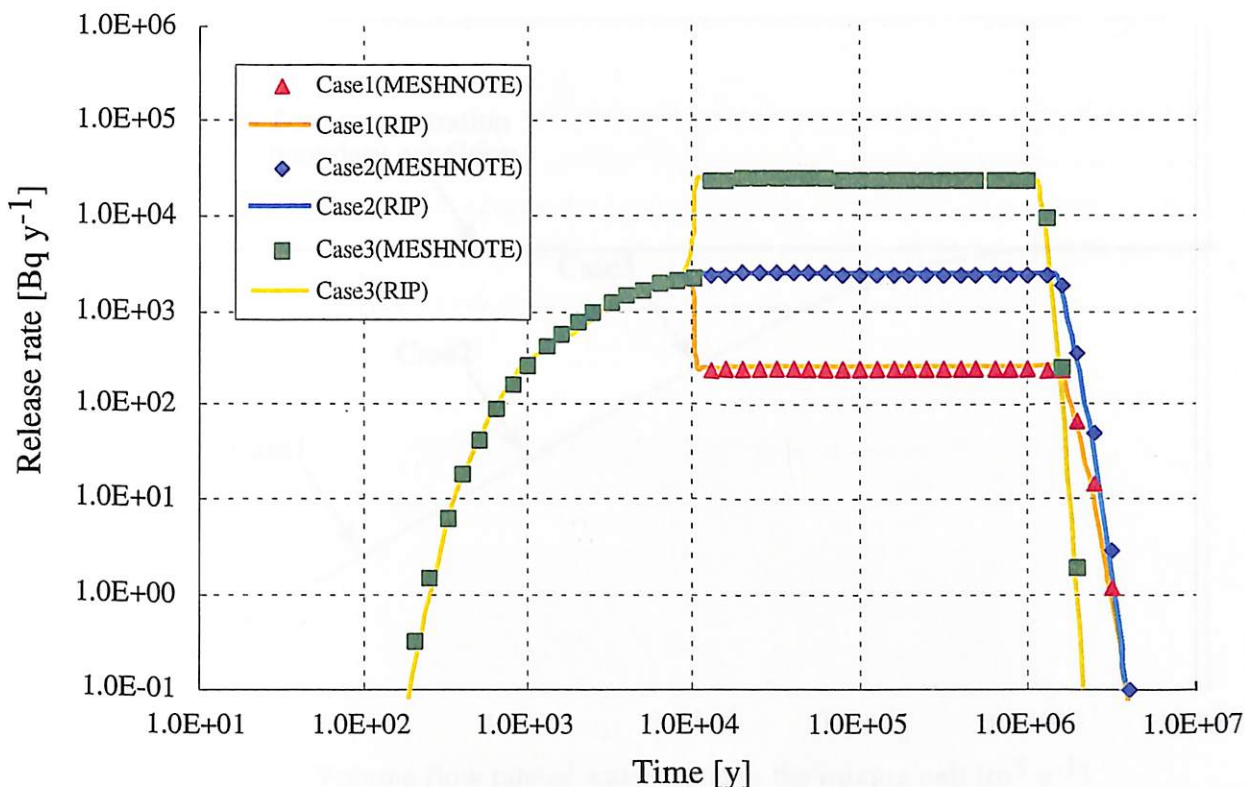


**Figure 4-15 Comparison of release rate from the EBS for time dependent volume flow rate of water through the mixing cell**

However, the increase in the release rate with increasing flow rate does reach an upper limit, as the nuclide concentration in the mixing cell tends to zero. The maximum release rates of Tc-99, calculated using a zero-concentration boundary condition are approximately two orders of magnitude greater than result of the Case2 (see Figure 4-16). Under the present model assumptions, the maximum release rate cannot exceed this upper limit, irrespective of the flow rate.

The release rates calculated by MESHNOTE can be compared with the RIP's results in the Figure 4-15. The results of MESHNOTE and RIP are consistent.

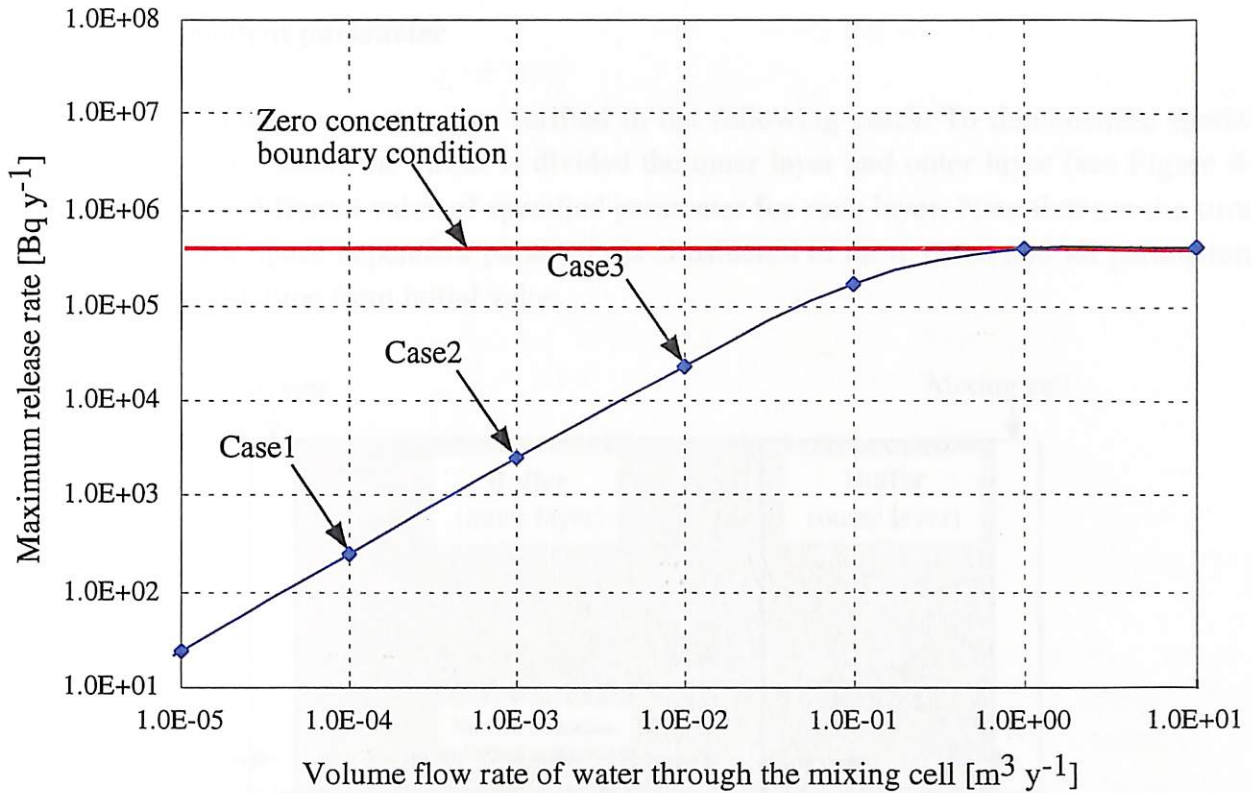


**Figure 4-16 Effect of volume flow rate of water through the mixing cell on release rate of Tc-99 from the EBS (the maximum release rates after 10,000 years when the flow rate changes)**

The release rates under the new steady-state calculated by MESHNOTE after the change of flow rate at 10,000 years are compared with those of RIP in Table 4-24. The relative errors of MESHNOTE to RIP are less than 2 %.

**Table 4-24 Relative error of the release rate from the EBS for time dependent volume flow rate of water through the mixing cell**

|                              | MESHNOTE <sup>*1</sup> | Verification tool <sup>*1</sup> | Relative error <sup>*2</sup> % |
|------------------------------|------------------------|---------------------------------|--------------------------------|
|                              |                        | RIP                             |                                |
| Case 1 [Bq y <sup>-1</sup> ] | 2.46×10 <sup>2</sup>   | 2.45×10 <sup>2</sup>            | 7.35×10 <sup>-1</sup>          |
| Case 2 [Bq y <sup>-1</sup> ] | 2.41×10 <sup>3</sup>   | 2.43×10 <sup>3</sup>            | 5.01×10 <sup>-1</sup>          |
| Case 3 [Bq y <sup>-1</sup> ] | 2.34×10 <sup>4</sup>   | 2.31×10 <sup>4</sup>            | 1.30                           |

<sup>\*1</sup> Release rates under the steady-state after change of volume flow rate of water through the mixing cell at 10,000 years

<sup>\*2</sup> Relative error for RIP =  $|\text{MESHNOTE} - \text{RIP}| / \text{RIP} \times 100$



## 4.5 Space dependent parameter

The space dependent parameters are verified in the following cases. To demonstrate spatial dependence of parameter, the buffer is divided the inner layer and outer layer (see Figure 4-17) and given the different value of specified parameter for each layer. Note that not the time dependent but the space dependent parameter is considered in these cases and all parameters do not change with time from initial value.

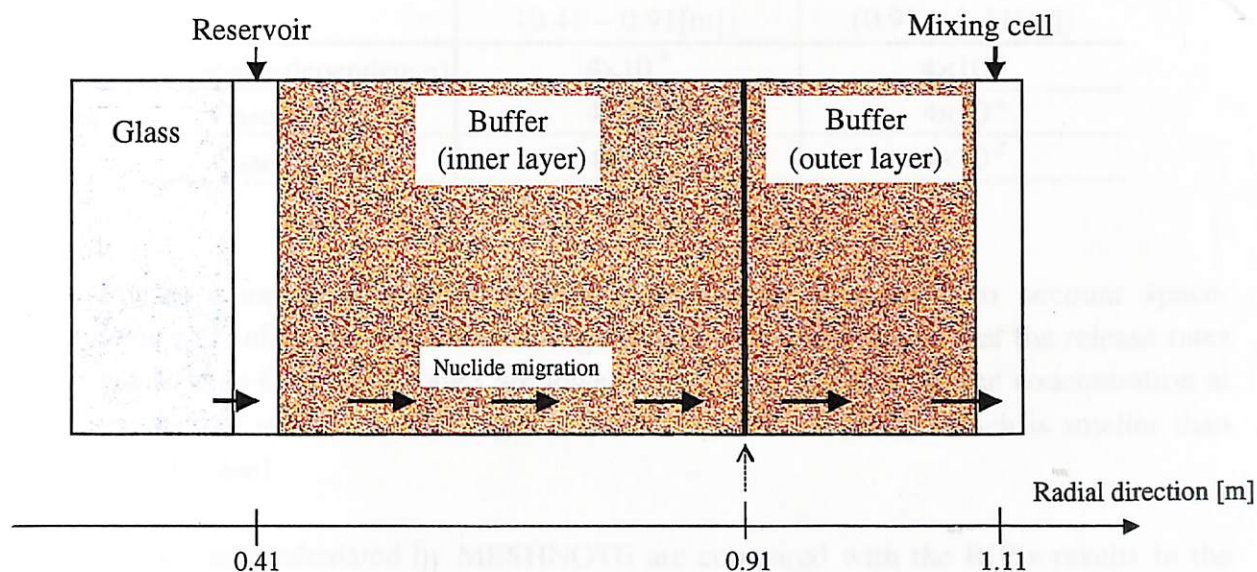


Figure 4-17 Geometry of the EBS for verification case of space dependent parameter

### 4.5.1 Solubility

#### (1) Objective

Calculations for the migration of nuclide with space-dependence of solubility accounting to basic migration processes (decay, linear sorption, diffusion and solubility limit) in the EBS are performed. The MESHNOTE result is compared with the result of RIP.

#### (2) Analysis condition

The difference solubility of Tc is given for an inner and outer layer of the buffer. (see Table 4-25).

The geometry of the EBS, glass dissolution model and other input parameters are assumed to be identical to the conditions of calculation case of Section 4.1.1. The primary input parameters for the MESHNOTE code for this case are presented below:

|                       |   |   |
|-----------------------|---|---|
| Nuclide               | : | Tc-99   |
| Half life             | : | $2.13 \times 10^5$ [y]                            |
| Inventory             | : | 8.27 [mol]  |
| Diffusion coefficient | : | $3 \times 10^{-2}$ [ $\text{m}^2 \text{y}^{-1}$ ] |



Distribution coefficient : 0.1 [m<sup>3</sup> kg<sup>-1</sup>]  
 Volume flow rate of water through the mixing cell : 1.0×10<sup>10</sup> [m<sup>3</sup> y<sup>-1</sup>]

Table 4-25 Space-dependence of solubility (Tc)

|                             | Solubility of Tc [mol m <sup>-3</sup> ] |                                 |
|-----------------------------|---|---------------------------------|
|                             | Inner layer<br>(0.41 ~ 0.91[m])         | Outer layer<br>(0.91 ~ 1.11[m]) |
| Case 1(no space-dependence) | 4×10 <sup>-5</sup>                      | 4×10 <sup>-5</sup>              |
| Case 2                      | 4×10 <sup>-5</sup>                      | 4×10 <sup>-6</sup>              |
| Case 3                      | 4×10 <sup>-5</sup>                      | 4×10 <sup>-7</sup>              |

### (3) Result

The release rates calculated by MESHNOTE, which is taken into account space-dependence of solubility, are shown in Figure 4-18. It is confirmed that the release rates from the EBS in Case2 and Case3 are lower than that of Case1 since the concentration at the boundary of inner and outer layer is limited by new solubility which is smaller than solubility in Case1.

The release rates calculated by MESHNOTE are compared with the RIP's results in the Figure 4-18. The results of MESHNOTE and RIP are consistent.

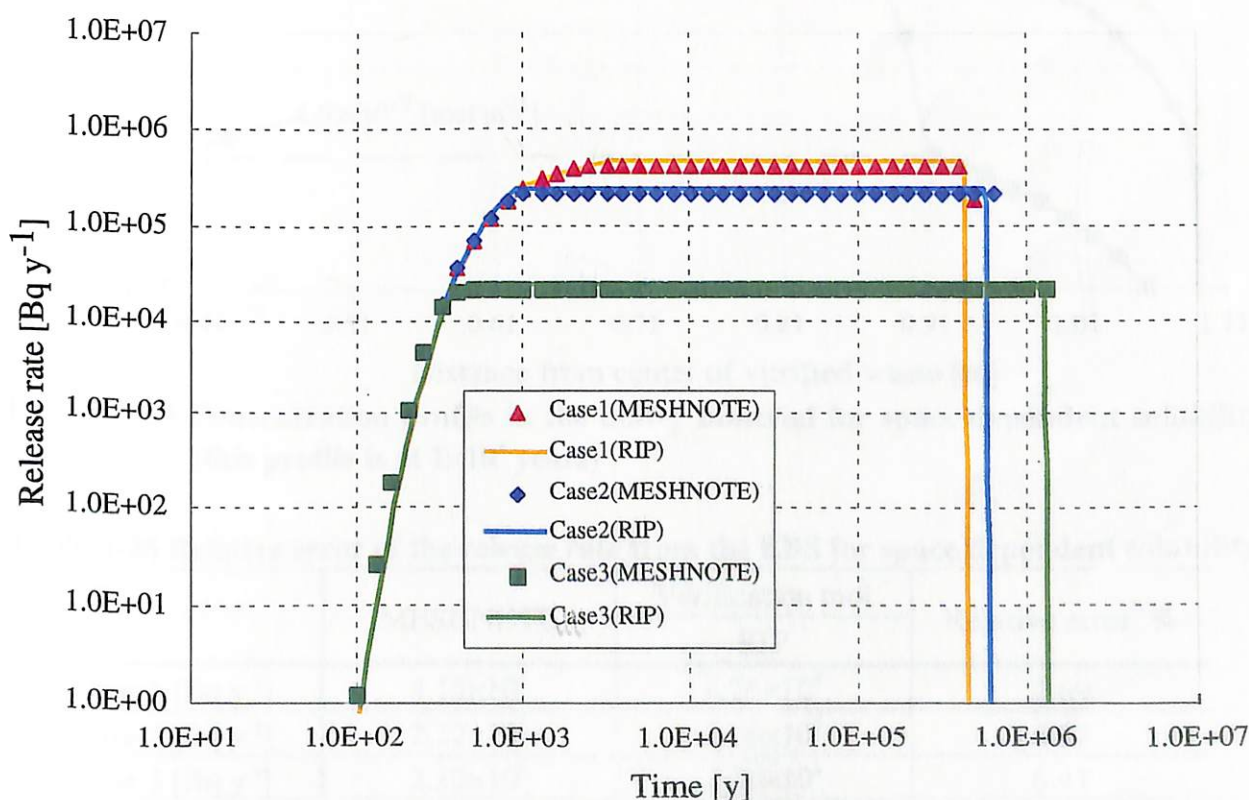


Figure 4-18 Comparison of release rate from the EBS for space dependent solubility

The concentration profile in buffer at  $1 \times 10^4$  years in each case, when the release rate from the EBS became the steady-state, is showed in the Figure 4-19. It is confirmed that the concentrations at the inner boundary of the buffer in the all cases are limited by inner solubility (same solubility in all cases) but the concentrations in the Case2 and Case3 have new profiles to match lower solubility limitation at the boundary of inner and outer layer. The concentration profile in the outer layer corresponds to the situation that the boundary of inner and outer layer gives new inner boundary condition with solubility limitation. This difference of concentration at the boundary of inner and outer layer causes the difference of release rate under steady-state (see Figure 4-18 and Figure 4-19).

The release rate under steady-state in each case that is calculated by MESHNOTE is compared with that of RIP in the Table 4-26. The relative errors of MESHNOTE to RIP are less than 7 %.

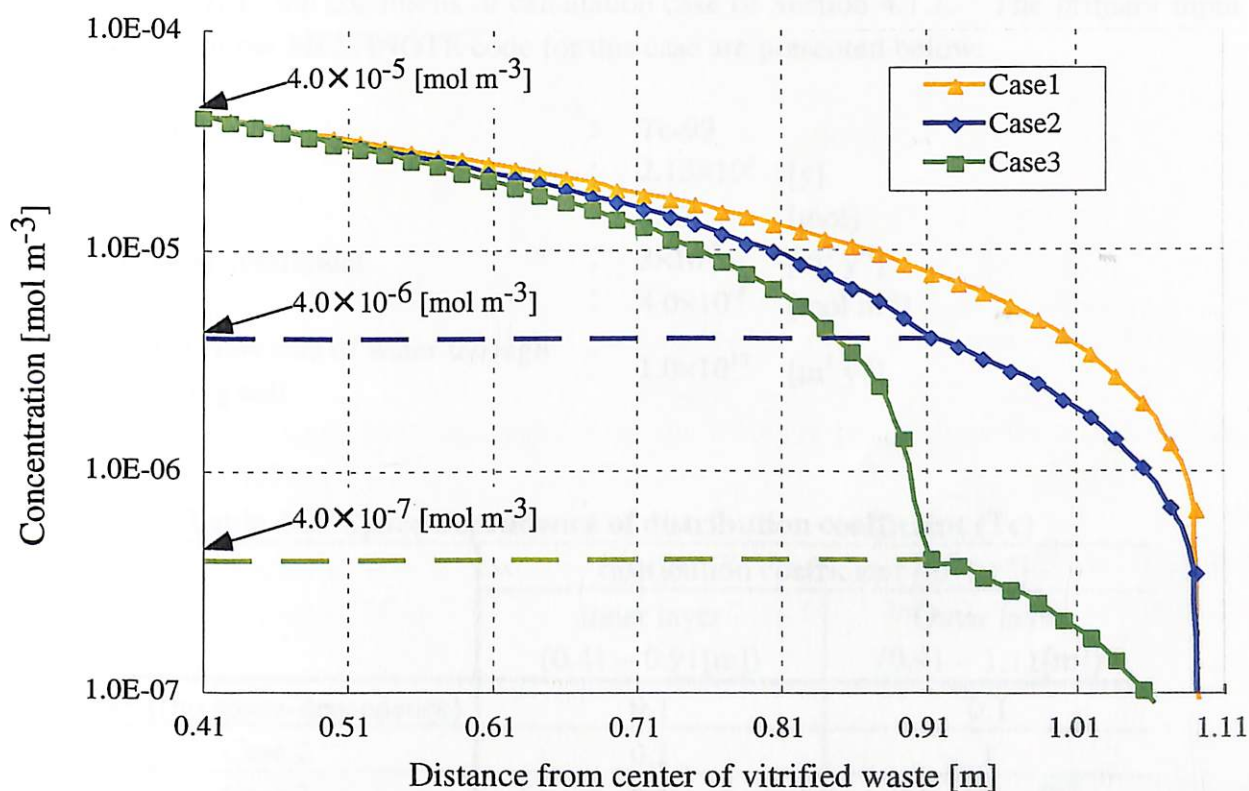


Figure 4-19 Concentration profile in the buffer material for space dependent solubility (this profile is at  $1 \times 10^4$  years)

Table 4-26 Relative error of the release rate from the EBS for space dependent solubility

|                              | MESHNOTE           | Verification tool  | Relative error* % |
|------------------------------|--------------------|--------------------|-------------------|
|                              |                    | RIP                |                   |
| Case 1 [Bq y <sup>-1</sup> ] | $4.15 \times 10^5$ | $4.26 \times 10^5$ | 2.69              |
| Case 2 [Bq y <sup>-1</sup> ] | $2.12 \times 10^5$ | $2.26 \times 10^5$ | 6.37              |
| Case 3 [Bq y <sup>-1</sup> ] | $2.12 \times 10^4$ | $2.26 \times 10^4$ | 6.41              |

\* Relative error for RIP =  $|\text{MESHNOTE} - \text{RIP}| / \text{RIP} \times 100$

### 4.5.2 Sorption constant

#### (1) Objective

Calculations for the migration of nuclide with space-dependence of sorption constant accounting to basic migration processes (decay, linear sorption, diffusion and solubility limit) in the EBS are performed. The MESHNOTE result is compared with the result of RIP.

#### (2) Analysis condition

The difference distribution coefficient of Tc is given for an inner and outer layer of the buffer. (see Table 4-27).

The geometry of the EBS, glass dissolution model and other input parameters are assumed to be identical to the conditions of calculation case of Section 4.1.1. The primary input parameters for the MESHNOTE code for this case are presented below:

|   |   |   |
|---|---|---|
| Nuclide   | : | Tc-99   |
| Half life   | : | $2.13 \times 10^5$ [y]                              |
| Inventory   | : | 8.27 [mol]  |
| Diffusion coefficient                             | : | $3 \times 10^{-2}$ [ $\text{m}^2 \text{y}^{-1}$ ]   |
| Solubility  | : | $4.0 \times 10^{-5}$ [ $\text{mol m}^{-3}$ ]        |
| Volume flow rate of water through the mixing cell | : | $1.0 \times 10^{10}$ [ $\text{m}^3 \text{y}^{-1}$ ] |

**Table 4-27 Space-dependence of distribution coefficient (Tc)**

|                             | distribution coefficient [ $\text{m}^3 \text{kg}^{-1}$ ] |                                 |
|-----------------------------|--|---------------------------------|
|                             | Inner layer<br>(0.41 ~ 0.91[m])                          | Outer layer<br>(0.91 ~ 1.11[m]) |
| Case 1(no space-dependence) | 0.1  | 0.1                             |
| Case 2                      | 0.1  | 1                               |
| Case 3                      | 0.1  | 10                              |

#### (3) Result

The release rates calculated by MESHNOTE, which is taken into account space-dependent of distribution coefficient, are shown in Figure 4-20. The difference of Case1 and both of Case2 and Case3 is only the time to reach the maximum release rate, and the both maximum release rates are consistent. This may be caused by the effect of higher retardation in the outer layer in Case2 and Case3.

The maximum release rates in the Case2 and Case3 are bit smaller than that of Case1. The reason may be that the depletion of nuclide inventory occurs before the release rate



reaches steady-state due to effect of higher sorption.

The release rates calculated by MESHNOTE are compared with the RIP's results in the Figure 4-20. The results of MESHNOTE and RIP are consistent.

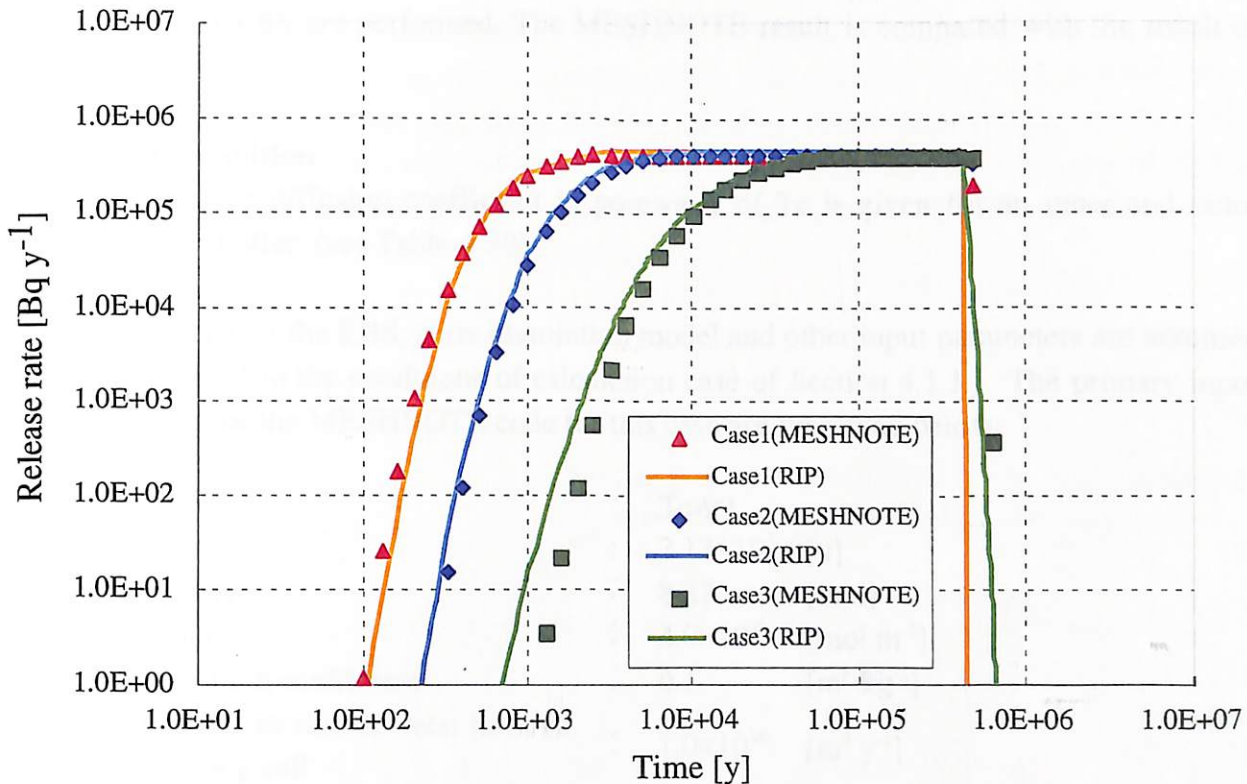


**Figure 4-20 Comparison of release rate from the EBS for space dependent distribution coefficient**

The maximum release rate in each case that is calculated by MESHNOTE is compared with that of RIP in the Table 4-28. The relative errors of MESHNOTE to RIP are less than 5 %.

**Table 4-28 Relative error of the release rate from the EBS for space dependent distribution coefficient**

|                              | MESHNOTE             | Verification tool    | Relative error* % |
|------------------------------|----------------------|----------------------|-------------------|
|                              |                      | RIP                  |                   |
| Case 1 [Bq y <sup>-1</sup> ] | 4.15×10 <sup>5</sup> | 4.26×10 <sup>5</sup> | 2.74              |
| Case 2 [Bq y <sup>-1</sup> ] | 4.12×10 <sup>5</sup> | 4.24×10 <sup>5</sup> | 2.84              |
| Case 3 [Bq y <sup>-1</sup> ] | 3.80×10 <sup>5</sup> | 3.98×10 <sup>4</sup> | 4.81              |

\* Relative error for RIP =  $|\text{MESHNOTE} - \text{RIP}| / \text{RIP} \times 100$

### 4.5.3 Diffusion coefficient

#### (1) Objective

Calculations for the migration of nuclide with space-dependence of diffusion coefficient accounting to basic migration processes (decay, linear sorption, diffusion and solubility limit) in the EBS are performed. The MESHNOTE result is compared with the result of RIP.

#### (2) Analysis condition

The difference diffusion coefficient in porewater of Tc is given for an inner and outer layer of the buffer. (see Table 4-29).

The geometry of the EBS, glass dissolution model and other input parameters are assumed to be identical to the conditions of calculation case of Section 4.1.1. The primary input parameters for the MESHNOTE code for this case are presented below:

|   |   |  |
|---|---|--|
| Nuclide   | : | Tc-99  |
| Half life   | : | $2.13 \times 10^5$ [y]                                 |
| Inventory   | : | 8.27 [mol]   |
| Solubility  | : | $4.0 \times 10^{-5}$ [mol m <sup>-3</sup> ]            |
| Distribution coefficient                          | : | 0.1 [m <sup>3</sup> kg <sup>-1</sup> ]                 |
| Volume flow rate of water through the mixing cell | : | $1.0 \times 10^{10}$ [m <sup>3</sup> y <sup>-1</sup> ] |

**Table 4-29 Space-dependence of diffusion coefficient in porewater (Tc)**

|                             | Diffusion coefficient in porewater [m <sup>2</sup> y <sup>-1</sup> ] |                                 |
|-----------------------------|--|---------------------------------|
|                             | Inner layer<br>(0.41 ~ 0.91[m])                                      | Outer layer<br>(0.91 ~ 1.11[m]) |
| Case 1(no space-dependence) | $3 \times 10^{-2}$   | $3 \times 10^{-2}$              |
| Case 2                      | $3 \times 10^{-2}$   | $3 \times 10^{-3}$              |
| Case 3                      | $3 \times 10^{-2}$   | $3 \times 10^{-4}$              |

#### (3) Result

The release rates calculated by MESHNOTE, which is taken into account space-dependent of diffusion coefficient, are shown in Figure 4-21. It is confirmed that the time to reach the maximum release rate in the Case2 and Case3 is later than that of Case1 and the maximum release rates in those cases are smaller.

The release rates calculated by MESHNOTE can be compared with the RIP's results in the Figure 4-21. The results of MESHNOTE and RIP are consistent.

The concentration profiles in buffer of MESHNOTE at  $1 \times 10^5$  years in each case, when the release rates from the EBS reaches the steady-state are showed in the Figure 4-22. It is

confirmed that the concentration in the inner layer in the Case3 is similar with solubility of Tc ( $4 \times 10^{-5} [\text{mol m}^{-3}]$ ). It may be that the leaching nuclide from the vitrified waste is accumulated in the inner layer since the outer layer with lower the diffusion coefficient than that of inner layer.

Comparing Figure 4-21 and Figure 4-22, it is confirmed that the release rate of Case3 is lowest (Figure 4-21) in the all cases although the concentration of Case3 in the buffer is highest when the release rate from the EBS reaches steady-state (Figure 4-22). This relationship is opposite to that of Section 4.5.1. This may be that the amount of nuclide released from the buffer in this verification case is smaller than that of Section 4.5.1. This relationship is confirmed by the equation (4-1).

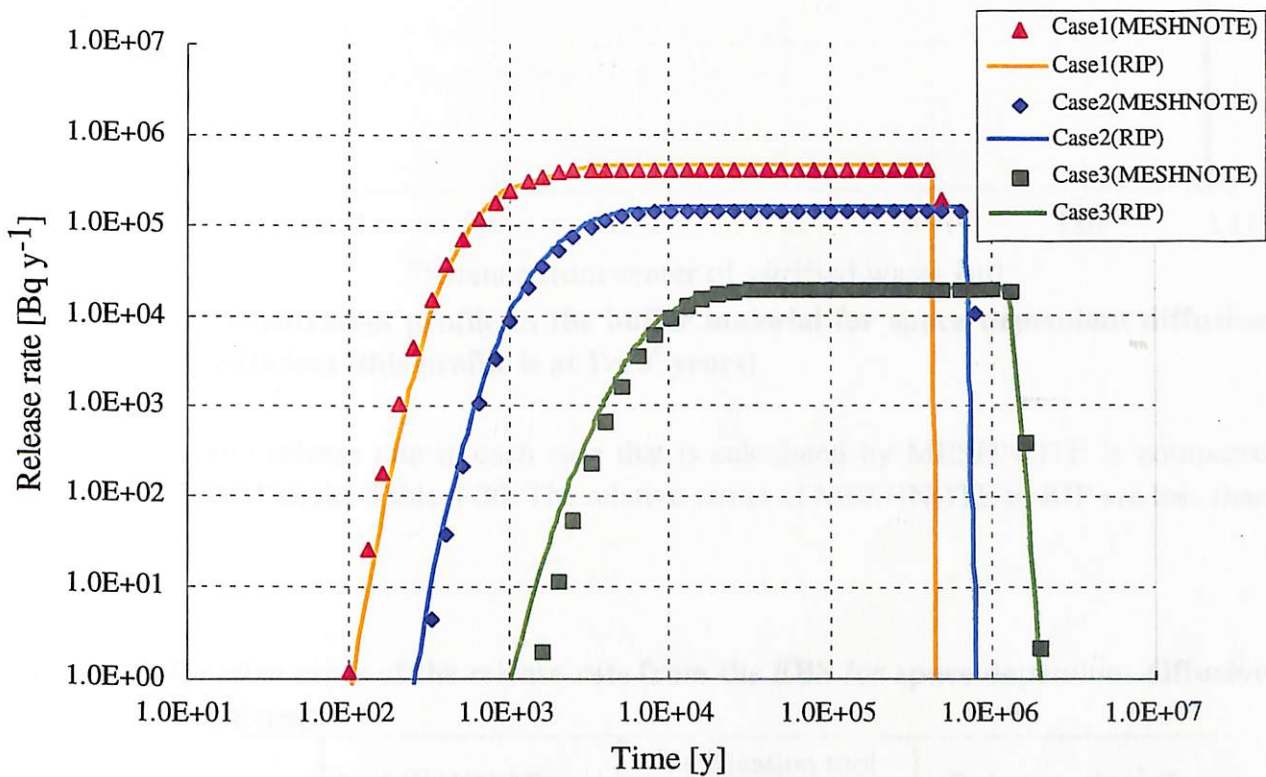


**Figure 4-21 Comparison of release rate from the EBS for space dependent diffusion coefficient**



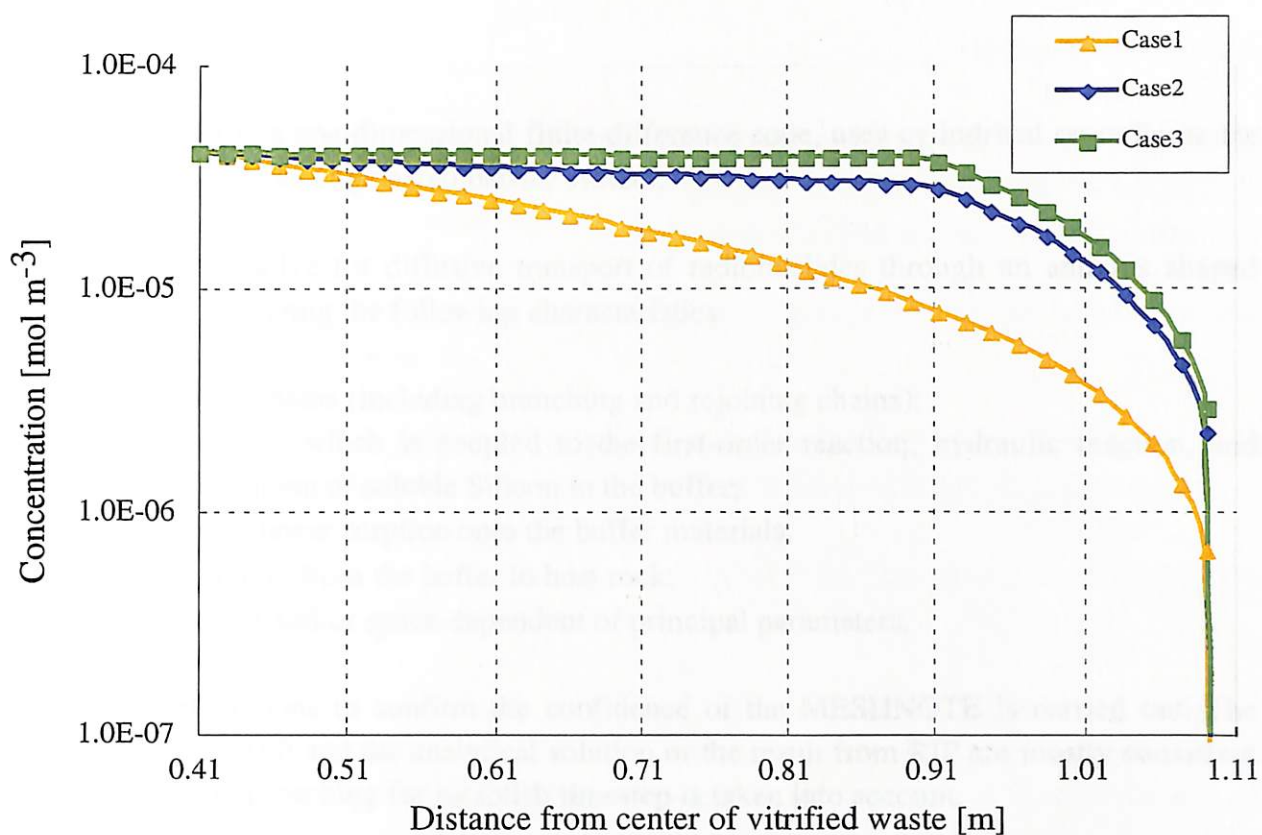


**Figure 4-22 Concentration profile in the buffer material for space dependent diffusion coefficient (this profile is at  $1 \times 10^5$  years)**

The maximum release rate in each case that is calculated by MESHNOTE is compared with that of RIP in the Table 4-30. The relative errors of MESHNOTE to RIP are less than 3 %.

**Table 4-30 Relative error of the release rate from the EBS for space dependent diffusion coefficient**

|                              | MESHNOTE           | Verification tool  | Relative error* % |
|------------------------------|--------------------|--------------------|-------------------|
|                              |                    | RIP                |                   |
| Case 1 [Bq y <sup>-1</sup> ] | $4.15 \times 10^5$ | $4.26 \times 10^5$ | 2.74              |
| Case 2 [Bq y <sup>-1</sup> ] | $1.44 \times 10^5$ | $1.46 \times 10^5$ | 1.63              |
| Case 3 [Bq y <sup>-1</sup> ] | $1.87 \times 10^5$ | $1.89 \times 10^4$ | 1.07              |

\* Relative error for RIP =  $|\text{MESHNOTE} - \text{RIP}| / \text{RIP} \times 100$



## 5 Conclusions

MESHNOTE code, a one-dimensional finite-difference code, uses cylindrical co-ordinate for nuclide migration in an engineered barrier system.

MESHNOTE can solve for diffusive transport of radionuclides through an annulus shaped buffer region considering the following characteristics:

- Multiple decay chains (including branching and rejoining chains);
- Glass dissolution, which is coupled to the first-order reaction, hydraulic reaction, and diffusion/dissipation of soluble Silicon in the buffer;
- Linear and non-linear sorption onto the buffer materials;
- Release of nuclide from the buffer to host rock;
- Time-dependent and/or space-dependent of principal parameters.

A series of calculations to confirm the confidence of the MESHNOTE is carried out. The result of MESHNOTE and the analytical solution or the result from RIP are mostly consistent if the difference approaching for establish timestep is taken into account.

## **6 Acknowledgements**

The authors are grateful to Dr. Webb, E. of Sandia National Laboratory for helpful calculations of RIP and English editing, and also grateful to Mr. Koo, S. of Nuclear Engineering System Inc. for helpful figures editing.

## 7 Reference

AEC (Advisory Committee on Nuclear Fuel Cycle Backend Policy of the Atomic Energy Commission) (1997) : Guidelines on Research and Development Relating to Geological Disposal of High-Level Radioactive Waste in Japan

Golder Associates (1998) : RIP Integrated Probabilistic Simulator for Environmental Systems, Theory Manual & User's Guide

Ohi, T., Miyahara, K. and Umeki, H. (1992) : RELEASE Code for Radionuclide Transport in Engineered Barrier System, PNC Technical Report, PNC TN8410 92-060 (in Japanese) .

Robinson, P. C., Williams, M. J. and Worgan, K. J. (1992) : A Description of MESHNOTE, Intera Report IM3479-1.

Webb, E.K., Wakasugi, K., Makino, H., Ishihara, Y., Ijiri, Y., Sawada, A., Baba, T., Ishiguro, K. and Umeki, H. (1998) : Performance Assessment Uncertainty Analysis for Japan's HLW Program Feasibility Study (H12), 1998 Annual Meeting of the Atomic Energy Society of Japan, M58

Webb, E.K., Wakasugi, K., Makino, H., Ishihara, Y., Ijiri, Y., Sawada, A., Baba, T., Ishiguro, K. and Umeki, H. (1999) : Performance Assessment Uncertainty Analysis for Japan's HLW Program Feasibility Study (H12), The 7th International Conference Proceedings on Radioactive Waste Management and Environmental Remediation (ICEM '99).

## Appendix A

### (1) Buffer region

The difference equation (3-3) relevant to the governing equation (2-11) is derived by finite difference method.

We consider mass balance in a small element volume (there after “control volume”) in the radial coordinate of the buffer region as shown in Figure A-1. Defining the total concentration, which is taken into account the dissolved nuclide, sorbed nuclide and precipitate nuclide, in the control volume (volume :  $V$ ), the quantity  $A$  as change of amount for timestep  $\delta t$  in the control volume is express by equation (A-1).

$$A^{t+\delta t}V - A^tV. \quad (\text{A-1})$$

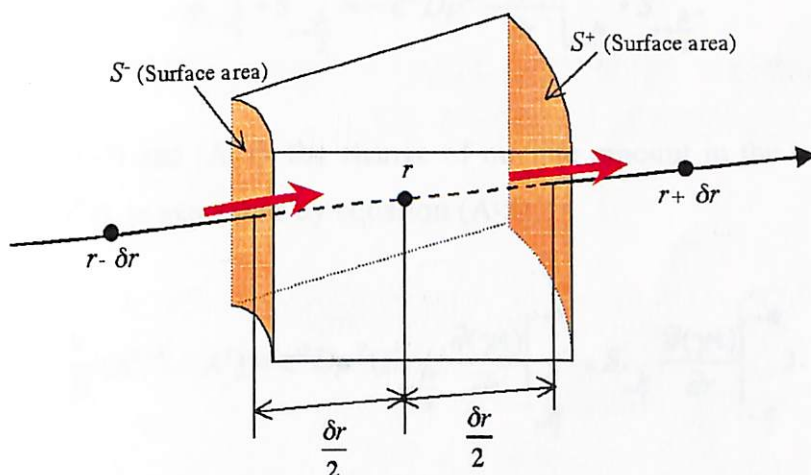


**Figure A-1 Control volume in the radial coordinate of the buffer region**

The inflow of into the control volume is occurred by diffusion and the flux (amount of nuclide per unit area and per unit time) is expressed as equation (A-2) by the Fick's first law:

$$q = -\varepsilon^B Dp^B \frac{\partial(\gamma A)}{\partial r}. \quad (\text{A-2})$$

- $q$  : Flux of dissolved nuclide [ $\text{mol m}^{-2} \text{y}^{-1}$ ]
- $\varepsilon^B$  : Porosity of the buffer [-]
- $Dp^B$  : Diffusion coefficient in porewater [ $\text{m}^2 \text{y}^{-1}$ ]
- $r$  : Distance from the center of vitrified waste [m]

- $A$  : Total concentration of nuclide in the unit volume of buffer  
 [mol m<sup>-3</sup>]  
 $\gamma$  : Factor to derive the concentration of dissolved nuclide from the  
 total concentration (see equation (2-19)) [-]

Applying the equation (A-2), the amount of inflow per unit time from the left side surface area is given by equation (A-3):

$$q\big|_{r-\frac{\delta r}{2}} \cdot S_{r-\frac{\delta r}{2}}^- = -\epsilon^B D p^B \frac{\partial(\gamma A)}{\partial r} \bigg|_{r-\frac{\delta r}{2}} \cdot S_{r-\frac{\delta r}{2}}^- \quad (\text{A-3})$$

On the other hand, the amount of outflow per unit time from right side surface area is given by equation (A-4):

$$q\big|_{r+\frac{\delta r}{2}} \cdot S_{r+\frac{\delta r}{2}}^+ = -\epsilon^B D p^B \frac{\partial(\gamma A)}{\partial r} \bigg|_{r+\frac{\delta r}{2}} \cdot S_{r+\frac{\delta r}{2}}^+ \quad (\text{A-4})$$

From equation (A-3) and (A-4), the change of nuclide amount in the control volume for unit time ( $t \sim t + \delta t$ ), is expressed by equation (A-5),

$$\frac{V}{\delta t} (A^{t+\delta t} - A^t) = \epsilon^B D p^B (S_{r+\frac{\delta r}{2}}^+ \frac{\partial(\gamma A)}{\partial r} \bigg|_{r+\frac{\delta r}{2}}^{t+\delta t} - S_{r-\frac{\delta r}{2}}^- \frac{\partial(\gamma A)}{\partial r} \bigg|_{r-\frac{\delta r}{2}}^{t+\delta t}). \quad (\text{A-5})$$

Introducing the difference method, the gradient terms in the equation (A-5) are expressed by equation (A-6) and (A-7):

$$\frac{\partial(\gamma A)}{\partial r} \bigg|_{r+\frac{\delta r}{2}}^{t+\delta t} = \frac{(\gamma A)_{r+\delta r}^{t+\delta t} - (\gamma A)_r^{t+\delta t}}{\delta r}, \quad (\text{A-6})$$

$$\frac{\partial(\gamma A)}{\partial r} \bigg|_{r-\frac{\delta r}{2}}^{t+\delta t} = \frac{(\gamma A)_r^{t+\delta t} - (\gamma A)_{r-\delta r}^{t+\delta t}}{\delta r}. \quad (\text{A-7})$$

From the equation (A-1), (A-5), (A-6) and (A-7), the equation (2-11) excepting the term relevant to radioactive decay is expressed by equation (A-8):

$$\frac{V}{\delta t}(A^{t+\delta} - A^t) = \frac{\varepsilon^B D p^B}{\delta r} \left[ S_{r+\frac{\delta r}{2}}^+ (\mathcal{A}_{r+\delta}^{t+\delta} - \mathcal{A}_r^{t+\delta}) - S_{r-\frac{\delta r}{2}}^- (\mathcal{A}_r^{t+\delta} - \mathcal{A}_{r-\delta}^{t+\delta}) \right]. \quad (\text{A-8})$$

The equation (A-8) is equal to equation (3-3).

## (2) Reservoir

For the reservoir cell shown in Figure 3-1, the equation (2-16) is derived by mass balance by taking into account the inflow from vitrified waste to reservoir and the outflow from reservoir to buffer.

Regarding the reservoir as a control volume, the change of amount for unit time ( $t \sim t + \delta t$ ) in the reservoir is expressed by equation (A-9):

$$A_{rin}^{t+\delta} V^R - A_{rin}^t V^R. \quad (\text{A-9})$$

- $r_{in}$  : Inner radius of buffer material [m]
- $A_{rin}$  : Total concentration of nuclide in the unit volume (reservoir) [mol m<sup>-3</sup>]
- $V^R$  : Volume of reservoir [m<sup>3</sup>]

Considering the leaching of nuclide with glass dissolution, the amount of inflow per unit time into the reservoir is defined by equation (A-10):

$$q|_{rin} \cdot S_{rin}^- = g_{Si} M. \quad (\text{A-10})$$

- $g_{Si}$  : Fractional rate of decrease of the glass volume [y<sup>-1</sup>]
- $M$  : Inventory of nuclide in the glass [mol]

On the other hand, the amount of outflow per unit time from reservoir to buffer is defined by equation (A-11):

$$q|_{r_{in}+\frac{\delta r}{2}} \cdot S^+_{r_{in}+\frac{\delta r}{2}} = -\epsilon^B D p^B \frac{\partial(\gamma A)}{\partial r} \Big|_{r_{in}+\frac{\delta r}{2}} \cdot S^+. \quad (A-11)$$

Introducing the difference method, the gradient term in the equation (A-11), then the equation (2-16) excepting the term relevant to radioactive decay are expressed by equation (A-12):

$$\frac{V^R}{\delta t} (A_{r_{in}}^{t+\delta t} - A_{r_{in}}^t) = \frac{\epsilon^B D p^B}{\delta r} \left[ S^+_{r_{in}+\frac{\delta r}{2}} (\gamma A_{r_{in}+\delta r}^{t+\delta t} - \gamma A_{r_{in}}^{t+\delta r}) \right] + g_{Si} M^{t+\delta t}. \quad (A-12)$$

The equation (A-12) is equal to equation (3-6).

### (3) Mixing cell

For the mixing cell shown in Figure 3-1, the equation (2-17) is derived by mass balance taking into account the inflow from buffer to mixing cell and the outflow from mixing cell to sink (outside of mixing cell).

Regarding the mixing cell as a control volume, the change of amount for unit time ( $t \sim t + \delta t$ ) in the mixing is expressed by equation (A-13):

$$A_{r_{out}}^{t+\delta t} V^M - A_{r_{out}}^t V^M. \quad (A-13)$$

- $r_{out}$  : Outer radius of buffer material [m]
- $A_{r_{out}}$  : Total concentration of nuclide in the unit volume (mixing cell) [mol m<sup>-3</sup>]
- $V^M$  : Volume of mixing cell [m<sup>3</sup>]

The amount of inflow per unit time from buffer to mixing cell is defined by equation (A-14):

$$q|_{r_{out}-\frac{\delta r}{2}} \cdot S^-_{r_{out}-\frac{\delta r}{2}} = -\epsilon^B D p^B \frac{\partial(\gamma A)}{\partial r} \Big|_{r_{out}-\frac{\delta r}{2}} \cdot S^-. \quad (A-14)$$

On the other hand, considering the migration by volume flow rate of water through the mixing cell ( $Q$ ), the amount of outflow per unit time into the mixing cell is defined by



equation (A-15):

$$q|_{r_{out}} \cdot S_{r_{out}}^* = Q\gamma A_{r_{out}}. \quad (\text{A-15})$$

Introducing the difference method, the gradient term in the equation (A-14) are expressed by equation (A-16) excepting the term relevant to radioactive decay is given by equation (2-17):

$$\frac{V^M}{\delta t} (A_{r_{out}}^{t+\delta t} - A_{r_{out}}^t) = -Q\gamma A_{r_{out}} + \frac{\varepsilon^B D p^B}{\delta r} \left[ S_{r_{out}}^- (\gamma A_{r_{out}-\delta r}^{t+\delta r} - \gamma A_{r_{out}}^{t+\delta t}) \right]. \quad (\text{A-16})$$

The equation (A-16) is equal to equation (3-7).

## **Appendix B**

### **Description of Input and Output Files**

## CONTENTS

|      |                            |      |
|------|----------------------------|------|
| 1    | Introduction               | B-3  |
| 2    | Input File                 | B-3  |
| 2.1  | Title Lines                | B-5  |
| 2.2  | DECAY                      | B-6  |
| 2.3  | INVENTORY                  | B-6  |
| 2.4  | PHYSICAL                   | B-6  |
| 2.5  | SOLUBILITY                 | B-8  |
| 2.6  | SORPTION                   | B-8  |
| 2.7  | TIMES                      | B-9  |
| 2.8  | GLASS                      | B-11 |
| 2.9  | DIFFUSION                  | B-13 |
| 2.10 | MIXING-CELL-FLUX           | B-13 |
| 2.11 | INNER-EXTENT               | B-14 |
| 2.12 | SWITCH-TIME                | B-14 |
| 3    | Output Files               | B-16 |
| 3.1  | Flux File                  | B-16 |
| 3.2  | Amount File                | B-17 |
| 3.3  | Concentration Profile File | B-17 |

## 1. Introduction

This document records the input and output file formats for MESHNOTE. The MESHNOTE input file is represented “\*.prb”. After making the appropriate input file, MESHNOTE is performed with tolerance parameter. MESHNOTE products the following four files at the end of calculation.

- \*.dbg (summary of debug file)
- \*.flx (change of release rates with time)
- \*.cnc (concentration profile of dissolved nuclides, sorbed nuclides and precipitate)
- \*.amt (total amounts of each nuclide in the reservoir)

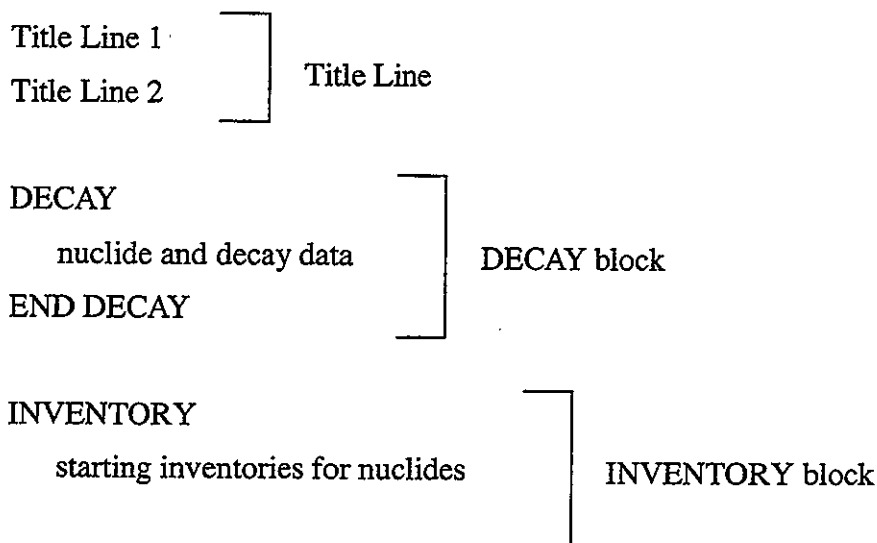
The input and output file formats are described below.

## 2. Input File

The MESHNOTE input file (\*.prb) has a keyword-based input format. The code allows some flexibility in the ordering of items in the file.

Comments can be included in the file, by using a # followed by the comment. Blank lines can be used to improve the layout (e.g. between input blocks).

The basic structure of the input file is as follows (each block is described in more detail in subsequent sub-sections):



END INVENTORY

PHYSICAL

physical properties of the system

END PHYSICAL

PHYSICAL block

SOLUBILITY

solubility data for elements

END SOLUBILITY

SOLUBILITY block  
(may be repeated, for different  
time-periods)

SORPTION

sorption isotherm data for elements

END SORPTION

SORPTION block  
(may be repeated, for different  
time-periods)

TIMES

output time specification

END TIMES

TIMES block

GLASS

physical and chemical properties of the glass

END GLASS

GLASS block  
(if GLASS block is omitted,  
instantaneous glass  
dissolution model are used.)

DIFFUSION

diffusion data for elements

END DIFFUSION

DIFFUSION block  
(may be repeated, for different  
time-periods)

MIXING-CELL-FLUX

physical data for mixing cell

END MIXING-CELL-FLUX

MIXING-CELL-FLUX block  
(may be repeated, for different  
time-periods)

INNER-EXTENT

diffusion data for elements

END INNER-EXTENT

INNER-EXTENT block  
(may be repeated, for different  
time-periods)

SWITCH-TIMES

time-period end times

SWITCH-TIMES block

## END SWITCH TIMES

### 2.1 Title Lines

The first *two lines* of the input file are taken as a title.

Additional comment lines, starting with a # may be added after these lines.

### 2.2 DECAY

The decay block consists of any number of lines, each describing a single decay. Two formats are allowed:

parent daughter half-life

or

parent half-life

The half-life is in years in each case. The second form is for use when the daughter is not of interest, because it does not appear as a parent (e.g. daughter is stable isotope).

Note that only those nuclides that appear as parents are included in the calculation. If a stable nuclide is to be included, then the half-life should be given as zero.

The names of nuclides must be one or two letters denoting the element name, followed by a dash, and any number of other characters denoting the isotope (e.g. U-238, Pu-238 and Am-242m).

The same parent may appear in more than one decay, in which case a branch is formed. The half-lives specified apply to the individual decays, and the total decay rates are computed from these. For example

A-1 B-1 200

A-1    C-1    600

creates a branch: 75% ( $=1/200/(1/200+1/600)$ ) of the decaying A-1 goes to B-1 and 25% ( $=1/600/(1/200+1/600)$ ) to C-1. The overall half-life for A-1 is 150 years ( $=1/(1/200+1/600)$ ). The fractions decaying each way are directly derived from the half-lives, i.e. (150/200) and (150/600). The debug file reports the total decay rate for the parent nuclide and the fraction decaying to each daughter.

## 2.3 INVENTORY

The inventory block consists of any number of lines, each giving the inventory of a single nuclide. If no inventory is given for a particular nuclide then it is given a zero inventory. Inventories can be given in TBq or moles. The format of each line is:

nuclide    TBq-val    0.0

or

nuclide    TBq-val

or

nuclide    0.0    mol-val

If two non-zero values are given, the first will be ignored and the second used as a value in moles.

## 2.4 PHYSICAL

The physical data block specifies the dimensions of the problem. It consists of three lines.

Line 1 has 4 values:



Containment-time [y]   Length [m]   Inner-radius [m]   Outer-radius [m]

The containment time indicates the start time of nuclide leaching from the glass. The length is that of the waste-package, and the inner- and outer-radius refer to the bentonite buffer.

Line 2 has 4 values:

Number-of-cells   Diffusion-coeff[m<sup>2</sup> y<sup>-1</sup>]   Reservoir-volume[m<sup>3</sup>]   Buffer-porosity

The number of cells is for discretisation of the system (including one cell for the reservoir and one for the mixing cell), typically 10-50 cells would be used. The Diffusion coefficient and porosity are for the bentonite. The reservoir volume is used in the code as the volume of water into which the glass dissolves. It should be less than the total volume of the waste package, but its precise value should not be very important in determining the results.

Note that the diffusion coefficient set here is used as a default value, and can be replaced by values specified in the DIFFUSION block.

Line 3 has 3 value:

Mixing-cell-volume [m<sup>3</sup>]   Mixing-cell-porosity   Mixing-cell-flow [m<sup>3</sup> yr<sup>-1</sup>]

These values control the outer boundary condition for the bentonite. For a zero-concentration outer boundary the flow can be set to be very large. Note that the mixing-cell-flow is used as a default value and can be replaced in the MIXING-CELL-FLUX block.

The physical data block must be given as three lines without any blank or comment lines, followed by the END line. Comments may be placed at the end of any of the lines.

## 2.5 SOLUBILITY

The solubility block, and some of the later blocks, can be repeated in order to specify values for different time-periods. Time-periods are numbered from 1 up to the number of time-switches plus one (see Section 2.12).

If the header line SOLUBILITY is used without any further data then the following block sets values for all time-periods. If an integer is given (e.g. SOLUBILITY 2) then the following block sets data for the specified time-period. The specific-time-period blocks must follow the all-time-period block.

Within the block there must be pairs of lines, giving data for particular elements. Each pair has the form

Element

inner-value [outer-value] [RES reservoir-value] [MIX mixing-cell-value]

All the values are in  $\text{mol m}^{-3}$ . The items in square brackets are optional. If no outer-value is given, the outer-value is equal to the inner-value. Inner and outer here refer to the splitting of the bentonite into inner and outer layer; the boundary between these layers is specified in the INNER-EXTENT block.

If no reservoir-value is given in a block for all time-periods, the inner-value is used; and if no mixing-cell value is given, the outer-value is used. If these values are not given for a specific time-period then the value set in the all-time-period block is used.

## 2.6 SORPTION

The sorption block can be repeated in order to specify values for different time-periods. Time-periods are numbered from 1 up to the number of time-switches plus one.

If the header line SORPTION is used without any further data then the following block

sets values for all time-periods. If an integer is given (e.g. SORPTION 2) then the following block sets data for the specified time-period. The specific-time-period blocks must follow the all-time-period block.

Within the block there must be groups of three lines, giving data for particular elements. Each group has the form

```

Element
inner-alpha inner-beta [outer-alpha outer-beta]
mixing-cell-alpha mixing-cell-beta

```

All the alpha values and beta-values are dimensionless. The items in square brackets are optional. If no outer-values are given, the outer-values are equal to the inner-values. Inner and outer here refer to the splitting of the bentonite into inner and outer layer; the boundary between these layers is specified in the INNER-EXTENT block.

If a linear sorption isotherm is required, then the alpha-value should be set to  $\rho Kd$  and the beta-value to zero.

## 2.7 TIMES

The times block has 3 lines, giving times for general output and for output of profiles.

The form is represented the following data:

```

Scheme-type Number-of-output-time Minimum [y] Maximum [y] Factor
Number-of-times-for-profile
[Time-for-profile1 Time-for-profile2 ..... Time-for-profile5]

```

Here scheme-type is a number specifying how the times will be set. The other data is used in a way that depends on this scheme-type.

If scheme-type is 1, then the times are uniformly distributed and the time-step of output time is derived from (Maximum - Minimum) / (Number-of-output-time - 1). Therefore if

adjoining the output times are assumed as  $T_i$  and  $T_{i+1}$ , the following equation are given:

$$T_{i+1} = T_i + \text{Factor} = T_i + (\text{Maximum} - \text{Minimum}) / (\text{Number-of-output-time} - 1)$$

If the scheme-type is 2 they are geometrically spaced and the time-step of output time is derived from  $(\log(\text{Maximum}) - \log(\text{Minimum})) / (\text{Number-of-output-time})$ . Therefor if adjoining the output times are assumed  $T_i$  and  $T_{i+1}$ , the following equation are given:

$$T_{i+1} = T_i + \text{Factor} = T_i + (\log(\text{Maximum}) - \log(\text{Minimum})) / (\text{Number-of-output-time})$$

In either case, three of the four following numbers must be give, with the other specified as zero. The zero value will be replaced by the value implied by the other items.

For example:

|   |    |       |        |     |
|---|----|-------|--------|-----|
| 1 | 10 | 100.0 | 1000.0 | 0.0 |
|---|----|-------|--------|-----|

gives times 100, 200, 300, ... 1000 [y].

|   |    |       |     |      |
|---|----|-------|-----|------|
| 1 | 10 | 100.0 | 0.0 | 50.0 |
|---|----|-------|-----|------|

gives times 100, 150, 200, ...550 [y].

|   |   |       |        |       |
|---|---|-------|--------|-------|
| 1 | 0 | 100.0 | 5000.0 | 300.0 |
|---|---|-------|--------|-------|

gives times 100, 400, 700, ...4900 [y].

If the scheme-type is 3, then the Number-of-output-time given is used as a number-per-decade, and a rounded set of time-values are generated. Recommended values for the Number-of-output-time are 1, 3, 5, 9 and 10. The following equation and table give the times that will be used within each decade.

$$T = \eta \times 10^5$$

| Number-of-output-time | Times used for each decade ( $\eta$ )  |
|-----------------------|--|
| 1                     | 1                                      |
| 3                     | 1, 2, 5                                |
| 5                     | 1, 1.6, 2.5, 4, 6.4                    |
| 9                     | 1, 2, 3, 4, 5, 6, 7, 8, 9              |
| 10                    | 1, 1.3, 1.6, 2, 2.5, 3.2, 4, 5, 6.4, 8 |

$\zeta$  is used an integer part of  $\log(\text{Minimum})$ , and Factor is not used if 3 of the Scheme-type is selected. For example:

3      5      10.0      1000.0      0.0

gives times

$$T_1 = 1.0 \times 10^1 = 10 \text{ [y]}$$

$$T_2 = 1.6 \times 10^1 = 16 \text{ [y]}$$

$$T_3 = 2.5 \times 10^1 = 25 \text{ [y]}$$

$$T_4 = 4.0 \times 10^1 = 40 \text{ [y]}$$

$$T_5 = 6.4 \times 10^1 = 64 \text{ [y]}$$

$$T_6 = 1.0 \times 10 \times 10^1 = 100 \text{ [y]}$$

$$T_7 = 1.6 \times 10 \times 10^1 = 160 \text{ [y]}$$

$$T_8 = 2.5 \times 10 \times 10^1 = 250 \text{ [y]}$$

•  
•  
•

Number-of-times-for-profile must be set less than or equal to 5. If Number-of-times-for-profile is assumed less than 0, the output times of concentration profile are identical to the output times of release rate and the items in square brackets are omitted

## 2.8 GLASS

The glass input block may be omitted if no glass dissolution model is used, in which case the inventory is placed directly in the reservoir volume.

The glass input block gives the physical and chemical properties of the glass and Si. It consists of 4 lines which must not be separated by blanks or comments.

Line 1 has 6 values:

Glass-volume   Glass -area   Glass -density    $k^+$     $k_r$     $u$

Here the Glass-volume [ $m^3$ ] and Glass -area [ $m^2$ ] are the initial values. The Glass-density is in [ $g\ m^{-3}$ ], and is used together with  $k^+$  [ $g\ m^{-2}\ y$ ] and  $k_r$  [ $g\ m^{-2}\ y$ ] to give the dissolution rate. The  $u$  parameter gives the dimensionality assumed for the area of the glass in relation to the volume as this is reduced. A value of 0.67 (2/3) gives a geometrically consistent behavior, but a value of zero can also be used.

Line 2 has 4 values

Si-buffer-alpha   Si-buffer-beta   Si-mixing-cell-alpha   Si-mixing-cell-beta

These are the non-linear isotherm values for the Si transport calculations. They have the same units as those specified in the SORPTION block for the other elements.

Line 3 has 2 values:

Si-solubility   Si-inventory

Si-solubility specifies solubility [ $mol\ m^{-3}$ ] of Si in the reservoir, buffer and mixing-cell. Initial inventory of Si can be given in moles.

Line 4 has 2 values:

Initial-Si-buffer,   Initial-Si-mixing-cell

These specify initial aqueous concentrations [ $mol\ m^{-3}$ ] of Si in the buffer and mixing-cell.



## 2.9 DIFFUSION

The diffusion block can be repeated in order to specify values for different time-periods. Time-periods are numbered from 1 up to the number of time-switches plus one. The block may be omitted completely, in which case the diffusion coefficient set in the preceding PHYSICAL block will be used throughout.

If the header line DIFFUSION is used without any further data then the following block sets values for all time-periods. If an integer is given (e.g. DIFFUSION 2) then the following block sets data for the specified time-period. The specific-time-period blocks must follow the all-time-period block.

Within the block, there must be pairs of lines, giving data for particular elements. Each pair has the form

Element

inner-value [outer-value]

All the values are in  $\text{m}^2 \text{y}^{-1}$ . The items in square brackets are optional. If no outer-value is given, the outer-value is equal to the inner-value. Inner and outer here refer to the splitting of the bentonite into inner and outer-layer; the boundary between these zones is specified in the INNER-EXTENT block.

## 2.10 MIXING-CELL-FLUX

The mixing-cell-flux block defines specified the volume flow rate of water through the mixing cell for different time-periods. Time-periods are numbered from 1 up to the number of time-switches plus one. The block may be omitted completely, in which case the flow-rate set in the PHYSICAL block will be used throughout.

If the header line MIXING-CELL-FLUX is used without any further data then the following block sets the value for all time-periods. If an integer is given (e.g. MIXING-CELL-FLUX 2) then the following block sets data for the specified time-period. The specific-time-period blocks must follow the all-time-period block.

Within the block, there must a single line giving the flow-rate [ $\text{m}^3 \text{y}^{-1}$ ].

## 2.11 INNER-EXTENT

The inner-extent block is used to specify the position of a boundary in the bentonite between the inner and outer-layer. Many of the properties can take different values in the two zones. Specifying a time-varying inner-extent allows modeling of changing geo-chemical conditions.

The inner-extent block can be repeated in order to specify values for different time-periods. Time-periods are numbered from 1 up to the number of time-switches plus one. The block may be omitted completely, in which case the whole bentonite will be use the outer-layer data throughout.

If the header line INNER-EXTENT is used without any further data then the following block sets the value for all time-periods. If an integer is given (e.g. INNER-EXTENT 2) then the following block sets data for the specified time-period. The specific-time-period blocks must follow the all-time-period block.

Within the block, there must a single line giving the position of the boundary between the inner and outer-layer in the bentonite. This is a radius [m]. If it is less than the inner-radius of the bentonite, then the bentonite is all in the outer-layer. If it is greater than the outer-radius of the bentonite, then the bentonite is all in the inner layer.

## 2.12 SWITCH-TIMES

The switch-times block is for setting the time-periods that are used in specifying much of the data for the problem. If the block is omitted then there is a single time period for the whole run.

The switch-times block consists of a sequence of input lines (one for each time-period end) followed by the END SWITCH-TIMES line. No comments or blank lines should

be added (although comments on each line after the value are allowed).

The block therefore takes the form

```
SWITCH-TIMES
time1
time2
...
timeN
END SWITCH-TIMES
```

The times must be in ascending order. Each gives the end-time for a time-period. The final time-period (N+1) continues to the end of the calculation.

### 3 Output Files

MESHNOTE produces four output files. These are:

- (1) Debug file (.dbg)
- (2) Flux file (.flx)
- (3) Amount file (.amt)
- (4) Concentration profile file (.cnc)

The debug file summaries data as it is read in, and has diagnostic information and error message written to it. It also has a summary of total released amounts and maximum fluxes.

The format of the other files is described below.

#### 3.1 Flux File

The flux file (\*.flx) gives fluxes from the mixing cell in  $\text{Bq y}^{-1}$  for each nuclide. If a glass dissolution calculation is being performed the two extra columns are added – the first column is the flux  $[\text{mol y}^{-1}]$  of Si leaving the glass, and the final column is the flux  $[\text{mol y}^{-1}]$  of Si leaving the mixing cell.

The first line is a header line giving the nuclide names and indicating that the first and last columns are for Si when appropriate.

The main part of the file is simply one line per output time, giving

time, [Si flux from glass], nuclide-release rate from mixing-cell, [Si from mixing-cell]

The items in square brackets are present only if a glass dissolution calculation is performed.

### 3.2 Amount File

The amount file (\*.amt) is only produced if a glass dissolution calculation is performed. It gives the total amounts [moles] of each nuclide in the reservoir at each profile output time.

The first line is a header line giving the nuclide.

The main part of the file is simply two lines per output time, giving

Time  
nuclide-amounts in reservoir

### 3.3 Concentration Profile file

The concentration profile file gives the aqueous, sorbed and precipitate concentrations for each nuclide in each cell (from the reservoir to the mixing cell). The output is written for each profile output time.

For each nuclide and each time, four output lines are generated. The first indicates the time and nuclide.

The second line gives the aqueous concentration ( $\text{mol m}^{-3}$  of water) in each cell (from reservoir to mixing cell).

The third line gives the sorbed concentration ( $\text{mol m}^{-3}$  of solid) in each cell.

The fourth line gives the precipitated concentration ( $\text{mol m}^{-3}$ ) in each cell.